S. Aaleti, S. Sritharan

Performance Verification of the PreWEC Concept and Development of Seismic Design Guidelines

ISU-CCEE Report 02/11
Submitted to the
Precast/Prestressed Concrete Institute

JULY 2011

Final

REPORT

IOWA STATE UNIVERSITY
OF SCIENCE AND TECHNOLOGY

Department of Civil, Construction and Environmental Engineering

Performance Verification of the PreWEC Concept and Development of Seismic Design Guidelines

by

Sriram Aaleti
Graduate Research Assistant

Sri Sritharan
Professor

ISU-CCEE Report 02/11

A Final Report to the Precast/Prestressed Concrete

Department of Civil, Construction and Environmental Engineering
Iowa State University
Ames, IA 50011

July 2011

Intentionally blank

ABSTRACT

This report was produced as part of a research project undertaken to improve the efficiency of the jointed wall system and make the precast systems more viable for seismic regions. A new innovative and cost-effective precast system, known as the PreWEC system, was developed. Proof testing of its lateral load resisting behavior was completed through a large-scale testing of a ½-scale precast wall system at the National Center for Research on Earthquake Engineering (NCREE), Taiwan. The PreWEC test specimen (PreWEC-1) was designed to match or exceed the moment resisting capacity of the cast-in-place reinforced concrete wall with continuous longitudinal reinforcement (RWN), tested in a PreNEESR project. As part of the PreWEC testing an innovative, economical mild steel connector was developed and its behavior under cyclic shear loading was characterized using experimental and analytical means. The PreWEC system performed exceptionally well with good energy dissipation, self-centering ability, and had 15% higher capacity compared to the traditional reinforced concrete wall.

A simplified analytical method was proposed to characterize the behavior and design of PreWEC systems. The method presented in this report makes similar approximation for neutral axis depth as the analytical procedure for the jointed wall systems. The simplified analysis captured an overall force-displacement response, connector displacements and wall contact length accurately.

Finally, a design methodology is introduced for PreWEC systems, which is also equally applicable to single precast walls that may be designed with unbonded post-tensioning. This design methodology is similar to the guidelines proposed by ITG 5.2 for jointed wall systems. The application of this design method is also demonstrated, using design examples

ACKNOWLEDGMENTS

The research described in this report was funded by the Precast/Prestressed Concrete Institute (PCI) to support performance verification and development of design guidelines for a novel precast wall system with unbonded post-tensioning known as the PreWEC system. The authors would like to thank Mr. Paul Johal and Mr. Jason J. Krohn of PCI for their contribution towards coordination of this project. The authors also would like to thank the National Science Foundation (NSF) and National Science Council (NSC) of Taiwan for providing financial assistance through the IREE program to conduct large-scale testing of the PreWEC system. Help from Professor KC Tsai, the former director of the NCREE laboratory in Taiwan and the laboratory staff to conduct the large-scale testing is greatly appreciated.

Conclusions, opinions and recommendations expressed in this report are those of the authors alone, and should not be constructed as being endorsed by the financial sponsors.

LIST OF FIGURES

TABLE OF CONTENTS

Chapter1
Introduction

1.1 Concrete Structural Walls

Concrete structural walls provide a cost effective way to resist lateral loads generated by wind and earthquakes; thus, they are frequently incorporated as the primary lateral load resisting system in buildings. Structural walls have a high in-plane stiffness, which helps decrease structural damage by limiting the inter-story drift during seismic events. The superior performance of the buildings consisted of structural walls as the primary lateral loading system is well documented in the literature. For example, during the 1985 Chilean earthquake buildings in which lateral force resistance was provided by structural walls showed excellent performance (Wood et al. 1987). Also, during the 1988 Armenia earthquake, poorly designed and constructed buildings that incorporated concrete walls as the main lateral force resisting system performed substantially better than buildings built with other structural systems (Wyllie 1989). Even during the most damaging earthquakes of recent times (e.g., 1994 Northridge earthquake in California, the 1995 Kobe earthquake in Japan, and the 1999 Kocaeli earthquake in Turkey), which altered the engineering community's view towards earthquake engineering, no building incorporating shear walls as a lateral load resisting system has collapsed. A detailed literature review on previous performance of shear walls is presented in references (Fintel 2002, Holden et al 2003, Thomas 2003).

Concrete walls can be constructed in different shapes, such as rectangular, T-, L- or C-shaped walls. However, rectangular walls are more prevalent compared to other shaped walls due to ease of construction and ease of placement of walls along the perimeter of a building. Traditionally, concrete structural walls are constructed with cast-in-place (CIP) reinforced concrete. Although the CIP concrete walls are more common, with the added benefits of prefabrication and recent developments in concrete technology, there has been an increased use of precast concrete walls designed to emulate behavior of cast-in-place concrete walls using the splicing provisions of ACI 318-05 building standard (ACI 318,

2005). With advances made over the past decade in utilizing precast concrete to improve seismic performance of structures, a new precast wall assembly has been developed, which are constructed by tying down precast walls to the foundation using unbonded post-tensioning tendons.

In seismic design of buildings, the life safety of the occupants is of vital importance. For loads representative of wind or small, frequent earthquakes, structural walls are typically designed to respond in an elastic manner. However, during larger, less frequent earthquakes, concrete walls in seismic regions are required to resist lateral loads while deforming in a ductile manner (i.e., allowing the wall to deform beyond its yield limit without experiencing any significant reduction in strength), thereby dissipating seismic energy imparted by an earthquake and preventing structural collapse. Reinforced concrete structural walls dissipate seismic energy by subjecting the longitudinal reinforcement in plastic hinge regions to large inelastic strains, thus leading to significant damage to the plastic hinge regions as well as large residual drifts and wide residual cracks (see Figure 1.1). Consequently, the repair cost of the structure should be expected to be high after a damaging seismic event. Excessive damage in the plastic hinge region and permanent deformation of reinforced concrete walls can be mitigated by uncoupling the energy dissipation mechanism from the structural force resisting mechanism and achieving energy dissipation through other means. Recent advancements in research of precast concrete structures have introduced such a concept and examples include the hybrid wall system (Holden et al. 2003), the jointed wall system (Priestley et al. 1999) and precast wall with end columns known as the PreWEC system (Aaleti and Sritharan 2007). These wall systems are considered superior to cast-in-place walls because they are capable of maintaining structural integrity as well as providing sufficient energy dissipation when subjected to seismic loads.

In precast wall systems, post-tensioning steel is typically designed to remain elastic until the design-level earthquake loading. As a result, this post-tension steel will provide the necessary restoring force for the wall system to recenter when the applied lateral load is removed, thus minimizing the residual displacements associated with earthquake input motion. The behavior of a fully post-tensioned precast wall system without any energy dissipaters can be idealized to bilinear elastic behavior. In these systems damage is restricted

to the bottom corners of the wall about which it rocks. By proper detailing, such damage can be minimized. The drawback with this system is that only a very small amount of seismic energy is dissipated by the system, which will lead the structure to experience a larger lateral displacement. The jointed wall and PreWEC systems address this concern by accommodating easily replaceable external energy dissipating elements.

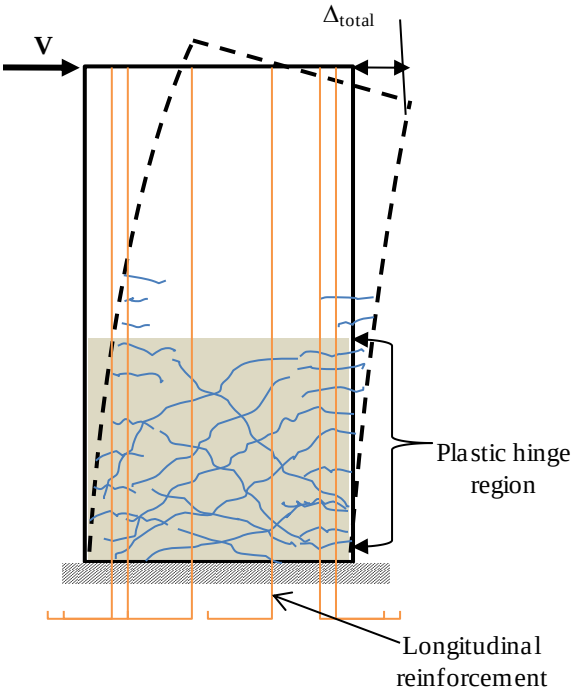

Figure 1.1 Plastic hinge region of a cast-in-place reinforced concrete wall

In a jointed wall system, two or more precast walls anchored individually to the foundation by unbonded post-tensioning are connected to each other horizontally along the height, by energy dissipating shear connectors, as shown in Figure 1.2. The post-tensioning steel in the wall may be distributed evenly along the wall length or concentrated at the center of each wall. The superior seismic performance of the jointed wall system has been experimentally demonstrated (Priestley et al. 1999) and further validated by analytical studies (Sritharan et al. 2007). Despite its successful establishment, this wall system has not been implemented in the field since the concept was proven 10 years ago for two reasons: 1) the moment resistance of the wall system is less than an equivalent cast-in-place wall, primarily due to the reduction in the lever arm associated with splitting of the wall; and 2) the UFP

connectors, which have performed satisfactorily, are expensive and their behavior, which is strain history dependent, is difficult to predict. The PreWEC system concept was developed by Aaleti and Sritharan (2007) by addressing the aforementioned problems.

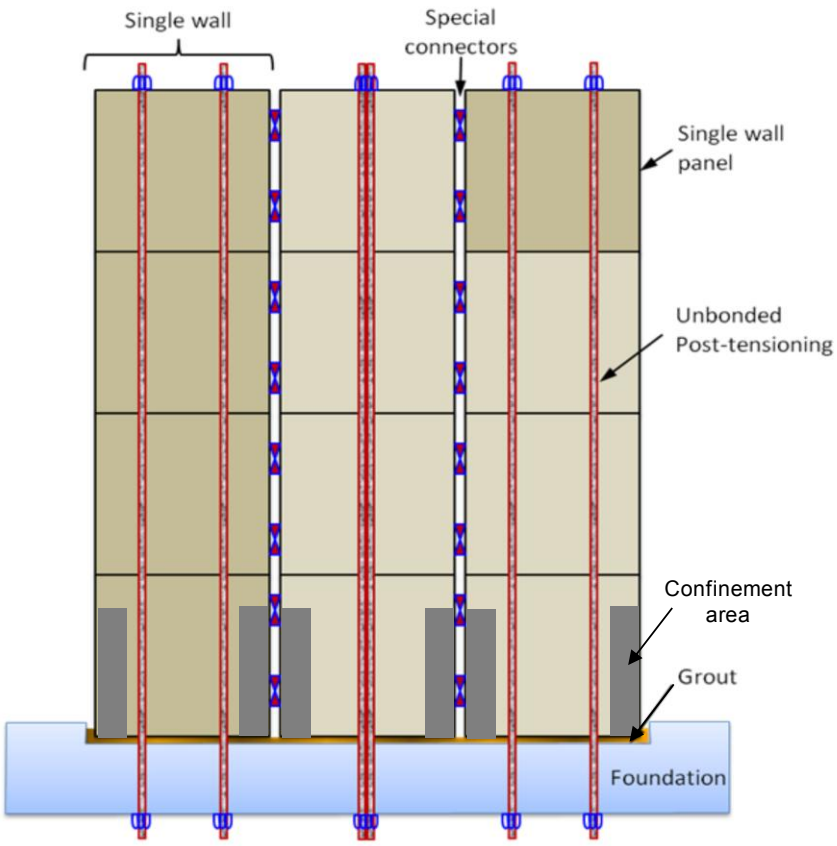

Figure 1.2 Typical details of a precast concrete jointed wall system

In a PreWEC system, a single precast wall is connected with two (steel or precast) end columns using special energy dissipating connectors, as shown in Figure 1.3. The wall and end columns are anchored to the foundation using unbonded post-tensioning. The post-tensioning steel in the wall may be distributed evenly along the wall length or concentrated at the center of the wall. The energy dissipating connectors are placed between the wall and end columns. More details of the PreWEC system is discussed in Chapter 2 of this document. To validate and code verify the PreWEC system performance under lateral loads, a large-scale test was conducted at the National Center for Research on Earthquake Engineering (NCREE) in Taiwan, in March 2008, as a part of an international collaboration project.

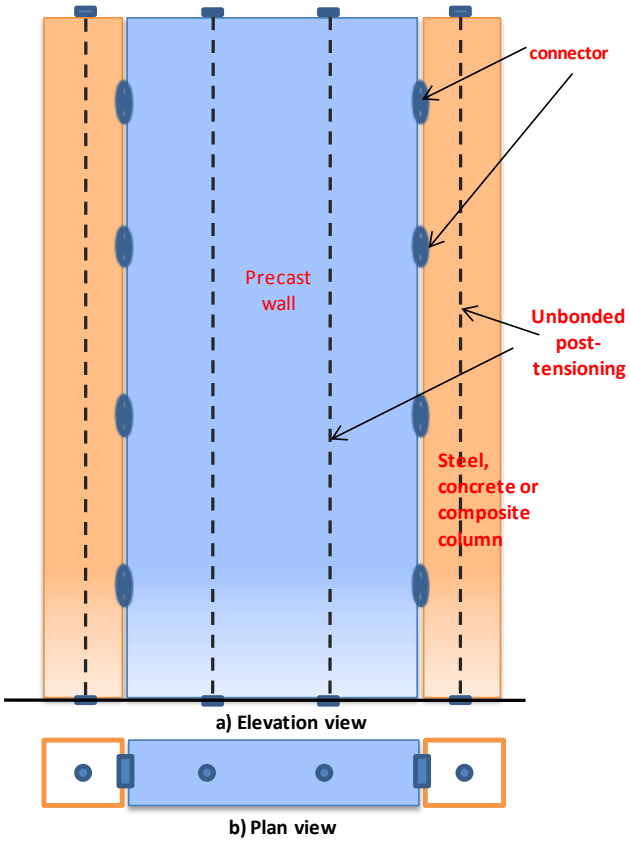

Figure 1.3 Typical details of a precast wall with end columns (PreWEC) system

1.2 Research Tasks

To prove the viability of the PreWEC system concept, with the help of a supplemental award from the National Science Foundation's International Research and Education in Engineering (IREE) program and the National Science Council of Taiwan, a PreWEC system was tested at the National Center for Research on Earthquake Engineering (NCREE) in Taiwan in March 2008. To supplement these efforts, the research project was further supported by the PCI through the Jenny Fellowship, to establish an innovative cost-effective system to enable the precast industry to market precast walls competitively in seismic regions while ensuring superior performance over comparable cast-in-place or steel solution. The different tasks of the research undertaken in this project are as follows:

Task 1: Complete data reduction

The PreWEC test unit was extensively instrumented with strain gauges, displacement transducers, and rotation devices. In addition, a photogrammetric measurement was also attempted. This task will complete the data reduction of the test unit and produce results to show the wall system has satisfied the ITG 5.1 (2007) requirement.

Task 2: Establish design guidelines

Using the recently published design guidelines for the jointed wall system as the basis (Sritharan et. al. 2007), seismic design guidelines for PreWEC will be developed. It is noted the design guidelines developed for the jointed wall by Sritharan et al. (2007) have been integrated into ITG 5.2 (ACI Innovation Task Group 5 2007b).

Task 3: Develop design examples

Design examples demonstrating application of PreWEC will be developed. The performance of these walls under monotonic loading will be compared to the response of equivalent cast-in-place walls.

1.3 Report Layout

This report consists of five chapters, including the general introduction presented in this chapter. The following chapter discusses the design and experimental testing of the PreWEC system and its components along with the code validation of the PreWEC system response. A simplified analytical procedure and its validation with the experimental data are presented in Chapter 3. Chapter 4 presents a design procedure for the PreWEC system. Chapter 5 presents conclusions from this study and recommendations for future research.

Chapter 2
Experimental Investigation of the PreWEC System and Its Components

Over the past decade, researchers have demonstrated experimentally the viability of using precast structures combined with unbonded post-tensioning (UPT) in seismic regions. During this period, several precast moment resisting frame and wall systems were developed. The UPT precast wall systems developed to date include single wall, hybrid wall, and jointed wall systems. The precast frame systems have been successfully implemented in buildings in seismic regions, but the adoption of precast wall systems has been limited.

The unbonded post-tensioned single precast walls do not have adequate capability to dissipate the energy imparted to the building during a seismic event. Consequently, the walls will experience large seismic displacements, leading to damage to non-structural elements. The jointed wall system uses special connectors to increase the energy dissipation capacity of the system. But, it has considerably less moment resisting capacity (about 30%) than an equivalent traditional reinforced concrete wall, affecting the cost-effectiveness of the system. These disadvantages have significantly compromised their practical applications, despite their proven superior performance in terms of self-centering capability and minimum structural damage during a seismic event. By addressing these concerns, a new cost-effective precast wall system, known as the Precast Wall with End Columns (PreWEC) system, has been introduced by Aaleti and Sritharan (2007). Lateral load behavior of this system has been previously investigated analytically (Aaleti and Sritharan 2007), pending an experimental validation to confirm its performance. Also, the use of the PreWEC system for real world applications in seismic regions requires experimental validation of the system's performance under lateral loads and satisfying the requirements set forth by ACI 318 (ACI 318, 2005). Chapter 21 of ACI 318 (ACI 318, 2008) specifies that "a reinforced concrete structural system not satisfying the requirements of this chapter shall be permitted if it is demonstrated by experimental evidence and analysis that the proposed system will have strength and

toughness equal to or exceeding those provided by a comparable monolithic reinforced concrete structure satisfying this chapter."

The minimum experimental evidence needed to achieve the code-validation of the PreWEC system is specified in ACI ITG-5.1 (2007) for "special" reinforced concrete (RC) shear walls. As part of the study presented in this report, a large-scale test of a PreWEC system and its associated components was conducted at the National Center for Research on Earthquake Engineering (NCREE) in Taiwan. This was part of a collaborative research project between the United States, Taiwan, and New Zealand, with support from the National Science Foundation in the U.S, the National Science Council of Taiwan and the Tertiary Education Commission in New Zealand. A PreWEC test specimen was subjected to in-plane cyclic displacements to validate its performance under cyclic lateral loads. The design and experimental testing of the PreWEC system and its components are discussed in this chapter.

2.1 PreWEC System Concept

The precast wall with end column (PreWEC) system, as shown in Figure 2.1, consists of a single precast concrete wall and two end columns constructed from steel, concrete or a composite material (e.g. concrete filled tubes). The wall and columns in this system are anchored to the foundation using unbonded post-tensioning and joined together using special energy dissipating connectors. The post-tensioning tendons can be distributed along the length of the wall or concentrated at the center. By leaving the tendons unbonded, the tendons develop constant strain along the length of the tendon, eliminating the development of large localized strains. This approach allows the wall system to undergo large lateral displacements without the prestressing tendons exceeding their yield strain and/or premature fracture of strands. Leaving the tendons unbonded also eliminates the development of large bond stresses in surrounding concrete and the associated local damage to concrete. When the PreWEC system is subjected to a lateral load, the wall and end columns rock individually with the opening of mainly a single crack at the base of the wall and columns. The post-tensioned steel in the system is designed to remain elastic when subjected to events up to design-level earthquakes. As a result, post-tensioning steel provides the necessary restoring force to recenter the PreWEC system when the applied lateral force is removed, minimizing

the residual displacements. When subjected to lateral loads, special, replaceable connectors placed between the wall and end columns experience relative vertical displacements due to the gap opening at the base of the wall system. This results in connectors enduring large inelastic deformations and providing the necessary energy dissipation for the system.

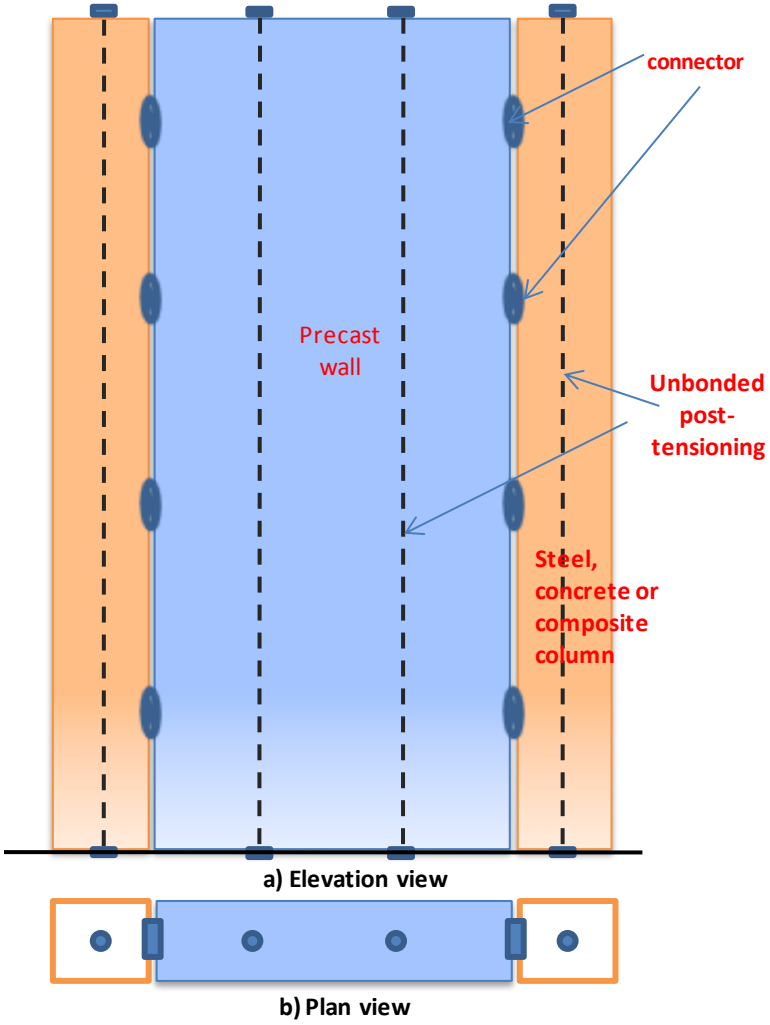

Figure 2.1 Sketch of the PreWEC concept

2.2 Test Unit

A PreWEC system for testing was designed following the basic guidelines in ACI ITG-5.2 (2009) and ACI 318 (2008) (ACI 318 2008). It was designed to match or exceed the moment resisting capacity of the cast-in-place reinforced concrete wall with continuous longitudinal reinforcement (RWN), tested as part of the PreNEESR project (Aaleti, 2009).

RWN was designed to comply with the current design practices and included Grade 50 (f_y =60 ksi) mild steel longitudinal reinforcement continuing from the foundation to the wall top without any splices. The cross-section details of the RWN and its performance under lateral loads are presented in Figure 2.2. The prototype design of the PreWEC system involves the following tasks.

- Arriving at the required post-tensioning steel area to anchor the precast wall and columns to the foundation;
- Development of a low-cost connector;
- Designing the confinement reinforcement boundary elements to sustain large compressive strains;
- Designing the required shear reinforcement to resist the design base shear; and
- Quantification of the number of connectors required to provide energy dissipation without affecting the self-centering nature of the system.

The post-tensioning steel was designed to yield between 2 to 2.5% lateral drift in accordance with ITG 5.2 guidelines (ACI ITG 5.2, 2009). The amounts of post-tensioning steel and the number of connectors were designed so the PreWEC specimen would match the lateral load capacity of RWN in #6 bars in tension direction. Confinement reinforcement was designed to sustain a maximum expected compressive strain based on an equation proposed by Aaleti and Sritharan (2009).

To design a cost effective and easily replaceable connector for the wall system, an extensive analytical investigation was conducted before the final design was validated through experimental testing. Based upon an analytical investigation, an oval shaped connector, or O-connector, made from grade A50 steel was found to provide the most efficient design (Henry et al. 2009). The designed O-connector can provide the necessary energy dissipation by primarily experiencing inelastic strains in the connector leg regions (Figure 2.3b).

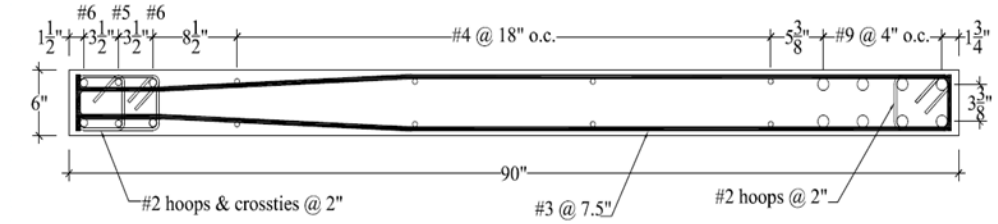

a) Cross section of RWN

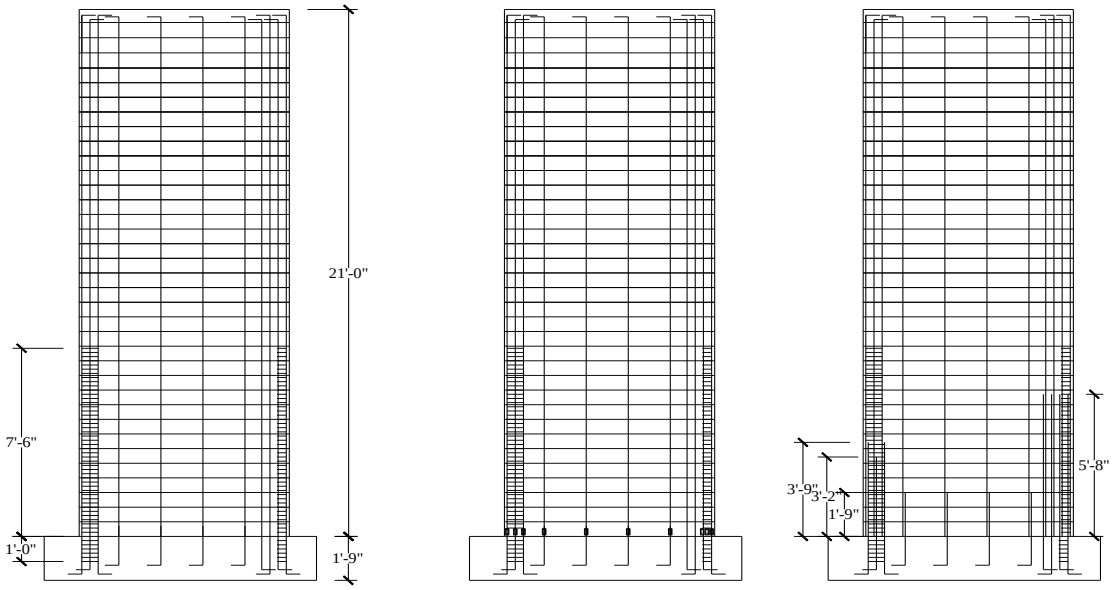

b) Reinforcement details of RWN

c) Cyclic response of RWN

Figure 2.2 Reinforcement details and cyclic behavior of the cast-in-place reinforced concrete wall, RWN tested as part of a PreNEESR project (Aaleti, 2009).

The cross-section of the PreWEC system at the base are shown in Figure 2.4, while the cross section and reinforcement details of the precast wall panel are depicted in Figure 2.5 and Figure 2.6, respectively. The PreWEC system was designed with a 72 in. (1828.8 mm) long, 6 in. (152.4 mm) thick precast wall, connected to a pair of 8 in. by 6 in. (203.2 mm by 152.4 mm) concrete filled steel tube (CFT) end columns as shown in **Error! Reference source not found.**. The thickness of the steel tube was 0.25 in. (6.5 mm). The total PreWEC system length was kept to 90 inches so it would match the length of RWN. The PreWEC system height was 258 in. (6.553 m), same as that for RWN. Since the prestressing tendons contribute towards the base moment resistance of the PreWEC system,

the longitudinal reinforcement in the wall panel was designed to satisfy the ACI 318 (ACI 318, 2005) minimum longitudinal steel ratio requirements. The longitudinal reinforcement was terminated within the wall panel, as seen in Figure 2.5. The boundary elements, or confinement regions, were provided in the bottom corners of the precast wall by means of Grade 40 (f_y = 40 ksi), #3 (d_b=9.5 mm) hoops spaced at 2 in. (50.8 mm) over the bottom 72 in. (1828.8 mm) height of the wall. Although there are no specific guidelines available for determining the height of the boundary elements in the literature, it was decided to follow the ACI design code provisions recommended for reinforced concrete walls for detailing the precast wall. The single crack opening at the base of the wall causes the concentration of the curvatures at the wall-foundation interface leading to a decrease in the length of the plastic hinge region. In addition to the confinement reinforcement, a 2-ft (0.61 m) long, 0.25 in. (6.4 mm) thick steel channel was attached to the bottom of the wall near the toe regions to minimize the spalling of the concrete in these regions (see Figure 2.5). The precast wall and each end column were designed to be anchored to the foundation using 12, 0.6 in.(15.2 mm) diameter post-tensioning strands with a total area of 2.604 in^2(1680 mm^2) and 3, 0.6 in.(15.2 mm) diameter post-tensioning strands with a total area of 0.651 in^2 (420 mm^2), respectively. In accordance with shear design provisions of ACI 318-05, shear reinforcement in the wall panel was provided with #3 (d_b=9.53 mm) bars at 7.5 in. (190 mm c/c) spacing. However, due to the unavailability of grade 60 #3 reinforcement in Taiwan, grade 40 #3 bars at 6 in. (150 mm c/c) spacing were used as the shear reinforcement.

To design a suitable connector, a target force-displacement envelope was derived based on the dimensions and expected maximum lateral drift of the PreWEC system. This design envelope, shown in Figure 2.3a, was used to develop suitable dimensions for the O-connector, shown in Figure 2.3b. Subsequently, from this information, it was determined that six pairs of O-connectors at each end of the wall were required to connect the wall and the end columns. The connector also had the ability to undergo large relative displacements in excess of 2 in., before experiencing failure. The O-connectors were made by cutting an oval shaped plate from a standard Grade 50 (f_y =50 ksi) steel plate, making it very economical.

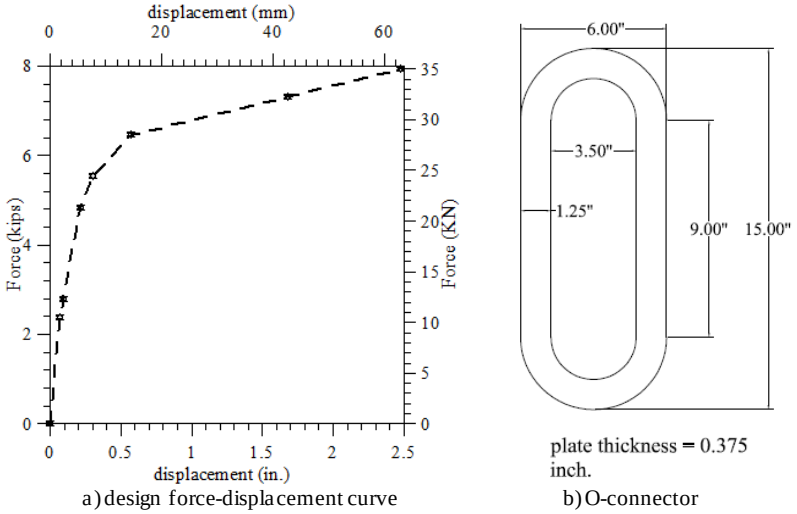

Figure 2.3 Target force-displacement envelope and the dimensions of the O-connector

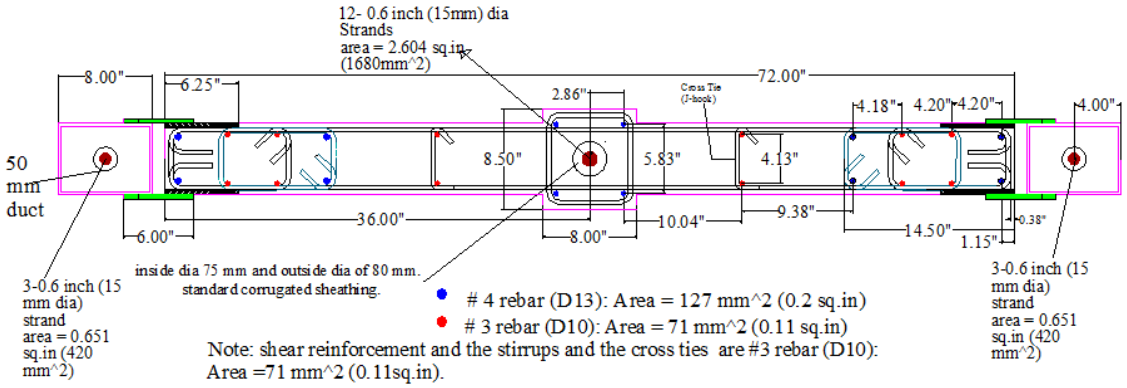

Figure 2.4 Cross section details of the PreWEC test specimen at the base

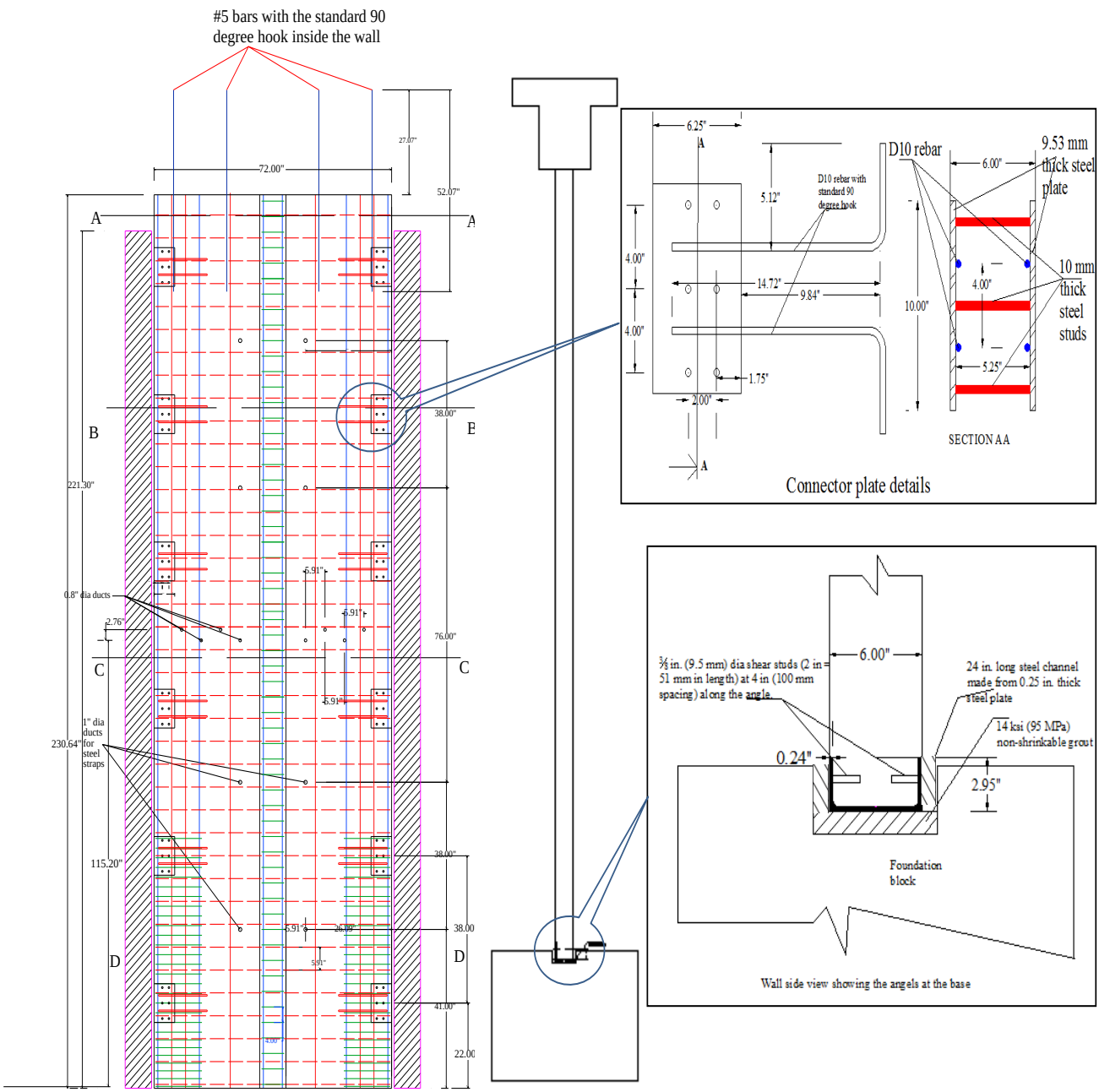

Figure 2.5 Reinforcement details of the PreWEC test specimen

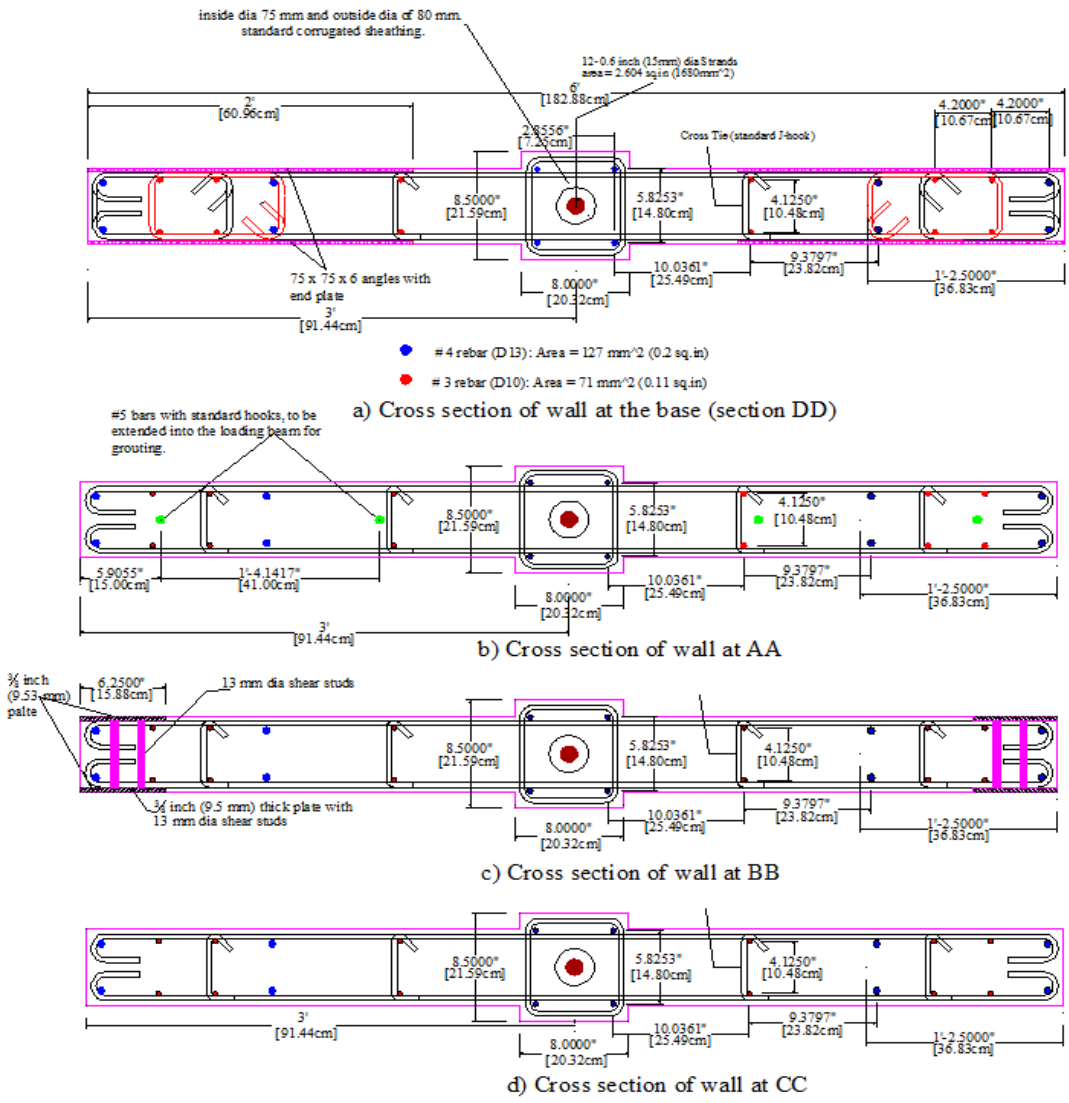

Figure 2.6 Cross-section details of the wall panel at different elevations

2.3 Connector Testing

As previously observed during testing of the PRESSS jointed wall system (Priestley et al. 1999), establishing the contribution of the connectors through component testing was identified as a critical step in quantifying the expected lateral load behavior of the wall system. Consequently, experimental tests were performed on sets of O-connectors at Iowa State University and the National Center for Research for Earthquake Engineering (NCREE), Taiwan. The tests at Iowa State University (ISU) included three uniaxial tensile tests to characterize the material behavior through the coupon tests and quantifying the connector

response via reverse cyclic testing of two sets of O-connectors. In addition, three further sets of O-connectors were subjected to reverse cyclic loading and another set were subjected to a derived seismic displacement history at NCREE. Also, uniaxial tension coupon tests were performed to characterize the material behavior of the connectors tested at NCREE. The measured force-displacement behavior of the O-connector used in the large-scale testing is shown in Figure 2.7. More details about the connector testing and its force-deformation behavior under cyclic loading are presented in reference Aaleti (2009).

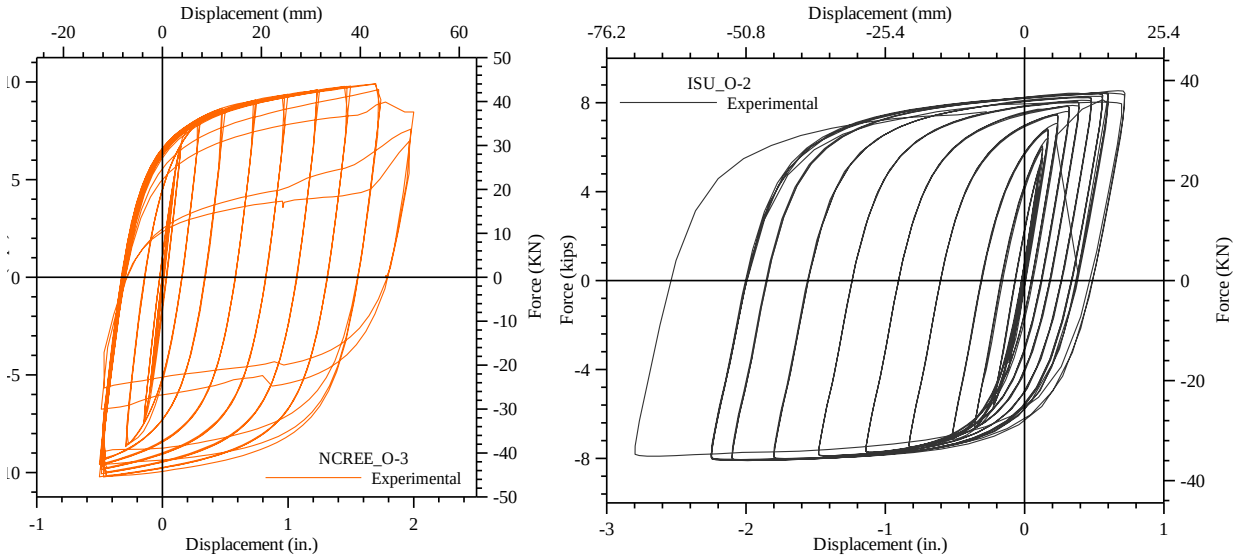

a) Connector tested at NCREE

b) Connector tested at ISU

Figure 2.7 Measured force vs. displacement response of O-connector under reverse cyclic loading

2.4 PreWEC-1 Test Setup

This section discusses the test setup and the loading protocol used for the experimental investigation of PreWEC-1 at NCREE in Taiwan. A schematic of the test setup is shown in Figure 2.8. A 12 ft (3.66 m) long, 4.8 ft (1.44 m) wide precast foundation block with block outs at the bottom and a pocket on the top was cast at a precast plant. The foundation block was brought into the final position on the test floor and was post-tensioned to the strong floor using eight two-inch diameter high strength threaded bars to prevent sliding from occurring during the lateral load testing. The precast wall panel and the CFT columns were erected on a concrete foundation block. A T-shaped beam was placed on the wall to connect the actuator. The erection process of the PreWEC-1 is shown in Figure 2.9.

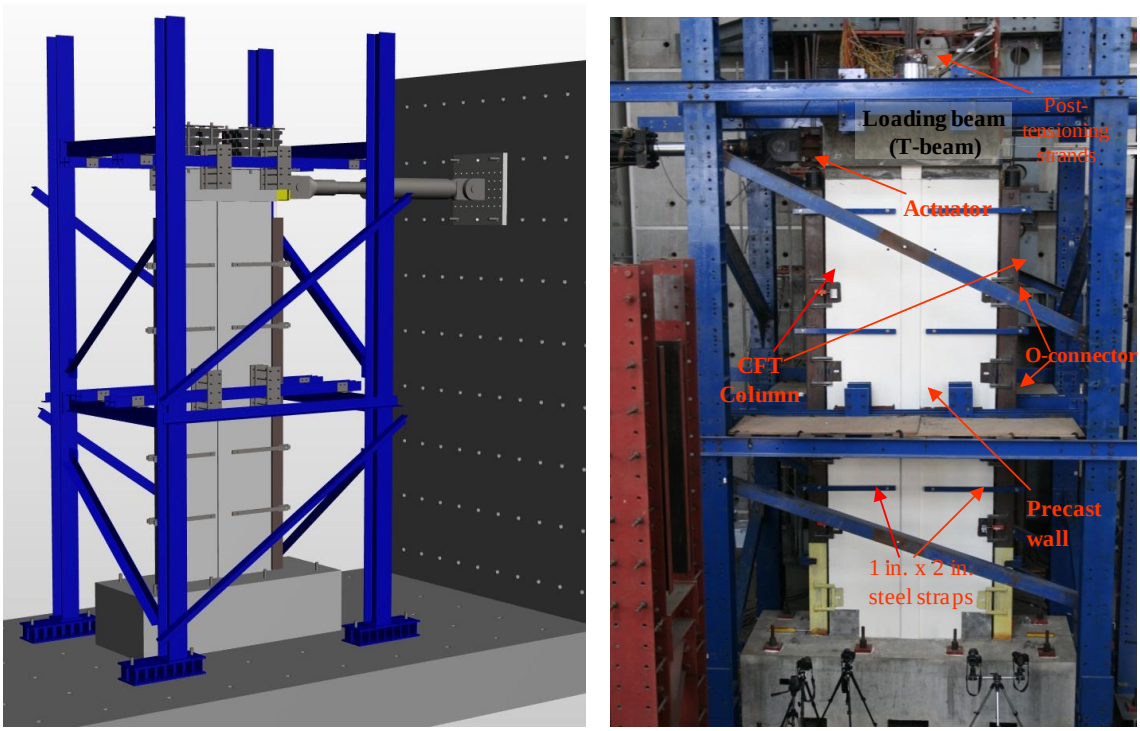

a) Schematic view b) A picture of PreWEC-1

Figure 2.8 The test setup used for the PreWEC system testing

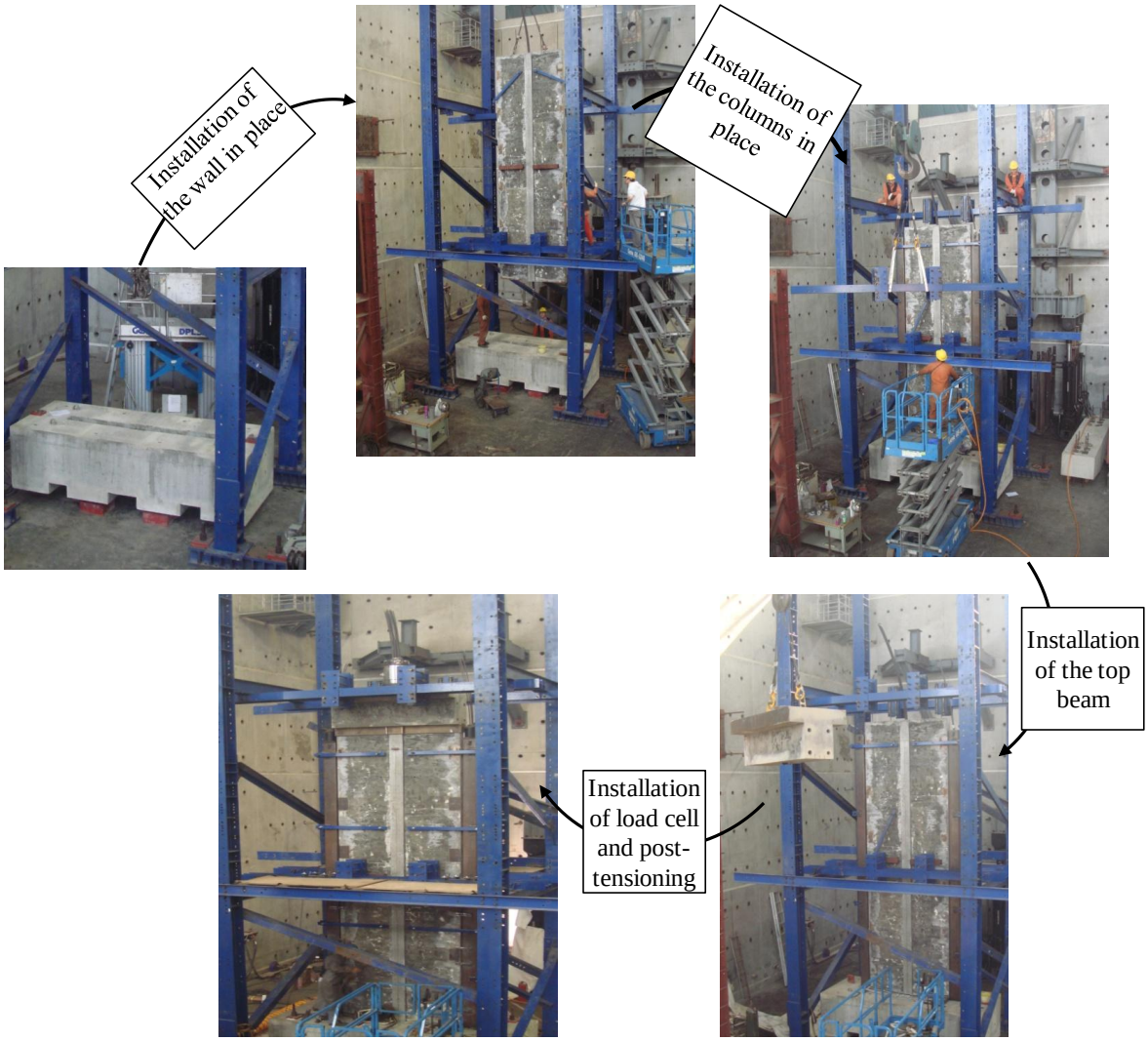

Figure 2.9 PreWEC -1 erecting process

As required by ACI ITG-5.1 (2007) and ACI ITG-5.2 documents (2009), a 1.5 in. (37 mm) thick Pagel® V 1A/40 grout, a high strength steel fiber reinforced grout with a specified compressive strength of 14 ksi (98 MPa) at 14 days, was placed at the interface between the foundation and wall to obtain uniform contact between the PreWEC system elements and the foundation (see Figure 2.10a). The prestressing tendons in the wall and column were anchored at the top of the loading beam (Figure 2.10b) and column, and in the foundation beam at the bottom. All of the post-tensioning strands (12, 0.6 in. dia.) in the precast wall panel were pulled simultaneously using a VSL post-tensioning system to introduce uniform compression in the wall panel and to prevent variation of strand stresses. However, the

strands in the columns were post-tensioned one after the other, until all strands reached similar stresses and the desired total prestressing was reached. The prestressing forces were monitored using load cells placed at top of the columns. Based on the O-connector's measured force-displacement behavior from the experimental investigation at NCREE, five pairs of O-connectors with restrainers (Figure 2.10c) were used at each side of the wall. The dimensions of the O-connectors used in the test are shown in **Error! Reference source not found.**.

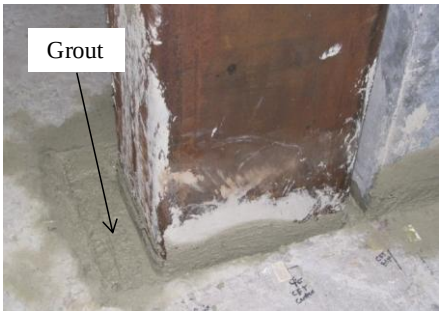

a) Pagel V 1A/40 grout at column-foundation interface

b) Post-tensioning anchor of the wall panel

c) A view of an installed O-connector with restrainer near the base of the wall

d) Steel Struts

Figure 2.10 Close-up of the PreWEC-1 system at different locations

In a typical building, walls are restrained from out-of-plane movement by floor elements. Therefore, to simulate this condition, the test setup included an out-of-plane restraint at the top and at mid-height of the wall, constructed by using rollers supported on steel beams (see Figure 2.11). This arrangement was to prevent twisting and unexpected buckling of the wall during lateral load testing. The out-of-plane supports were used in erecting the wall in the vertical position and a gap of 1/8 to 1/4 in. (3 to 6 mm) was left

between the rollers and the wall during testing to allow small movements as the wall displaced laterally. This arrangement was used to avoid the lateral forces being transmitted to the support frame. The support frame was anchored to the strong floor using high strength threaded bars. Additionally, the wall and the column elements were tied together at four places using 1 in. thick by 2 in. wide (25 mm by 50 mm) steel struts in the horizontal direction. These steel struts were connected to the columns and wall by means of a hinge mechanism to ensure that wall and columns would undergo the same amount of lateral movement without influencing their individual uplift behavior.

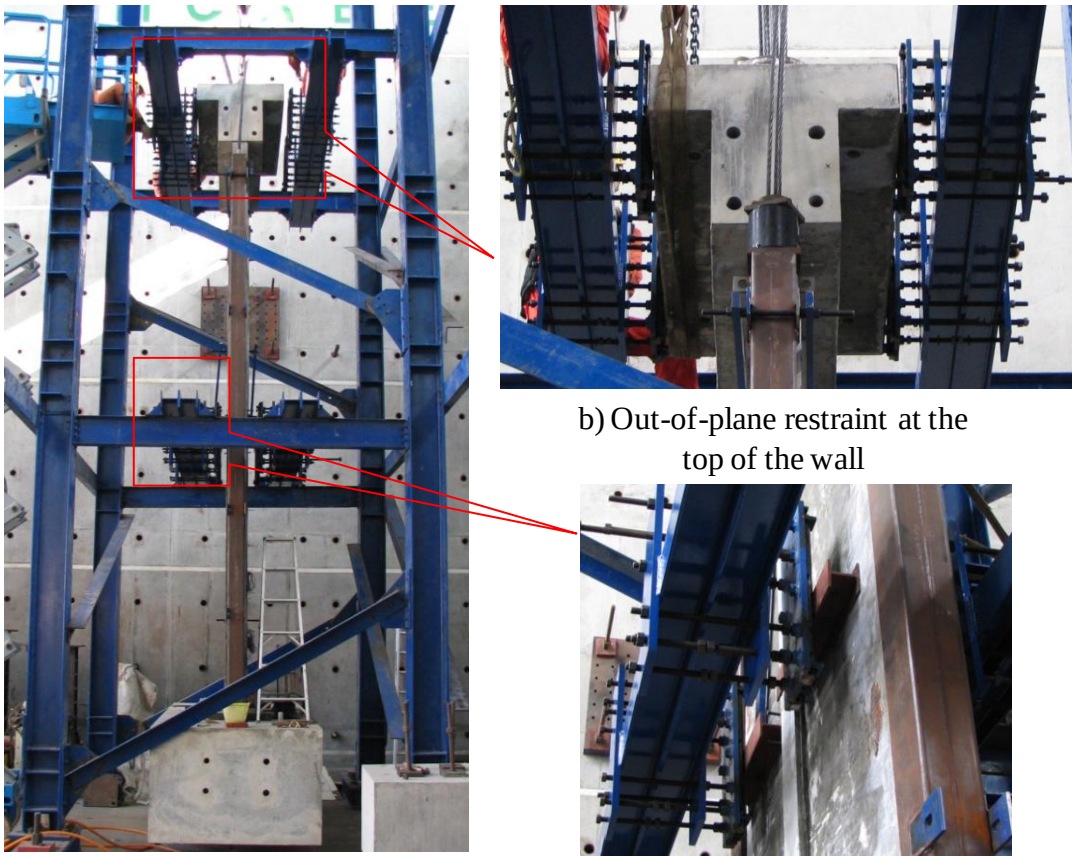

a) Side view of PreWEC-1

b) Out-of-plane restraint at the top of the wall

c) Mid height out-of-plane restraint

Figure 2.11 Out-of-plane restraints added at the top and mid height of PreWEC-1

The wall system was subjected to reverse cyclic lateral loading using a ± 220 kip (± 1000 KN) capacity hydraulic actuator, mounted to a reaction wall at 20 ft (6.1 m) above the wall-to-foundation interface. The actuator was connected to a T-shaped precast loading

beam located at the top of the wall. The interface between the loading beam and the precast wall panel was grouted using a high early strength cement grout (5 ksi) to create a uniform contact between the elements. Similar to the previously tested cast-in-place concrete walls, the wall system was not subjected to any external gravity load.

2.5 Instrumentation

The following section details the various instruments used to measure the performance of the PreWEC system during testing. Several types of instruments were used, including load cells (LC), linear variable differential transducer (LVDTs), string potentiometers (string pots), rotation meters, and strain gauges. Figure 2.12 shows the locations and designations of the displacement gauges and the load cells. A 600 kip load cell (shown as LCwall in Figure 2.12) and two 110 kip load cells (shown as LCcol_S and LCcol_N in Figure 2.12) were placed at the top to measure the forces in the post-tensioning steel of the wall panel, and the south and north columns respectively. LVDTs and string potentiometers (string pots) were used to measure the in-plane global displacements (denoted as SPL25, SPL50 and SPL75 in Figure 2.12) over the height of the test unit, as well as the relative deformations within the wall. The arrangement of the instrumentation at the base of the wall is shown in Figure 2.12.

To measure the uplift of the wall and columns with respect to the foundation block, LVDTs were attached vertically at the wall-foundation interface (see Figure 2.13). LVDTs were also used to monitor any unintentional uplift or horizontal slip of the foundation block (not shown in Figure 2.12), intended to be rigidly connected to the laboratory's strong floor. Two temposonic displacement gauges (denoted as SPLTOP1 and SPLTOP2 in Figure 2.12) were attached to the specimen at the loading level to measure the overall lateral displacement of the system relative to a steel reference frame erected independently of the steel lateral support frame. Rotation devices (RWB, RCS, RCN and RWT in Figure 2.12) were mounted near the bottom of the wall, bottom of the columns, and at the top of the wall to measure the rotations. Any possible slip at the wall-loading beam interface and uplift of the loading beam were monitored, using two LVDTs (LBS and LBUT) mounted to the wall panel at 1 in. (25 mm) from the top T-beam and wall interface.

LVDTs were used to measure the relative displacements between the wall and columns at two different connector levels for each column at the location of connectors as shown in Figure 2.14. The bottom story of the wall was instrumented with string pots in an X-configuration to measure the relative deformation contributions by flexural and shear actions.

A number of embedded concrete and steel strain gauges were used to measure the strain demands in the longitudinal reinforcement, shear reinforcement, confinement hoops, and the confined concrete in the compression regions. Figure 2.15 to Figure 2.17 show the locations of the various strain gauges. Strain gauges were also placed on Concrete Filled Tube (CFT) columns, bottom steel struts, and the O-connectors to measure the strain demand experienced during testing.

During the test, data from all instruments were recorded using a computer based data acquisition system. The data acquisition speed was varied depending on the target displacement. All channels were read and recorded each time the data were saved. However, due to unforeseen reasons, the data from string potentiometers and rotation meters were not recorded upto a lateral drift of ±1%.

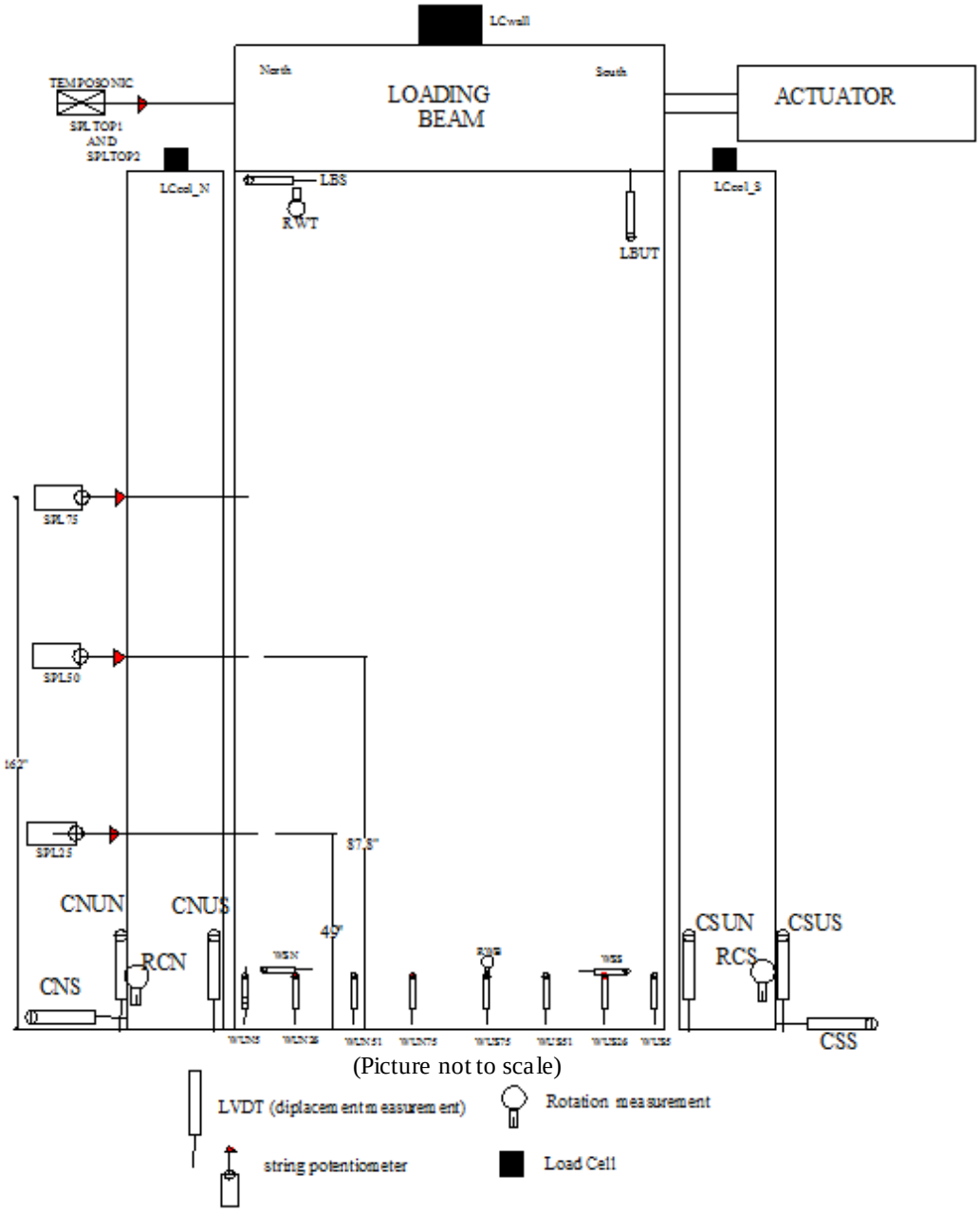

Figure 2.12 A schematic of PreWEC-1 showing load cell and displacement gauge locations

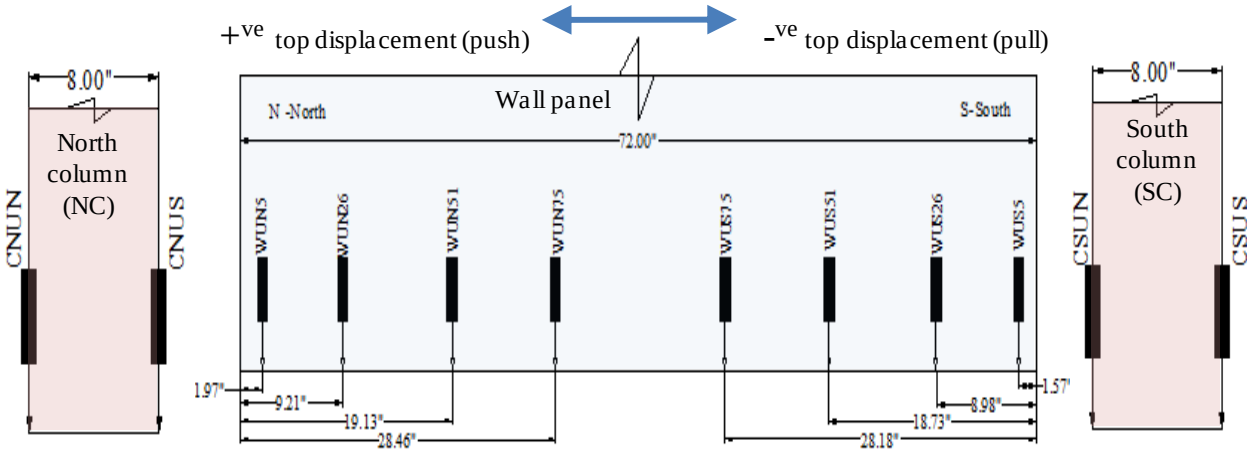

Figure 2.13 Locations of the displacement transducers along the wall and column ends

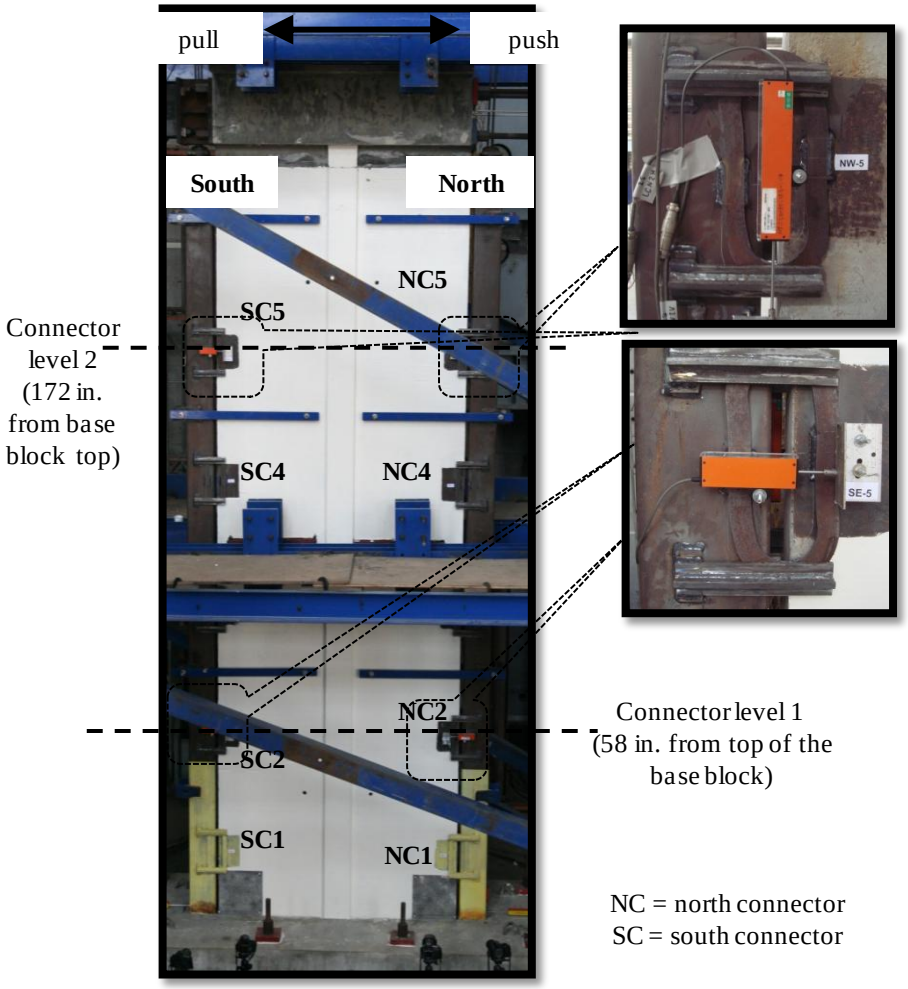

Figure 2.14 Locations of LVDTs used to measure the displacement demands on the O-connector

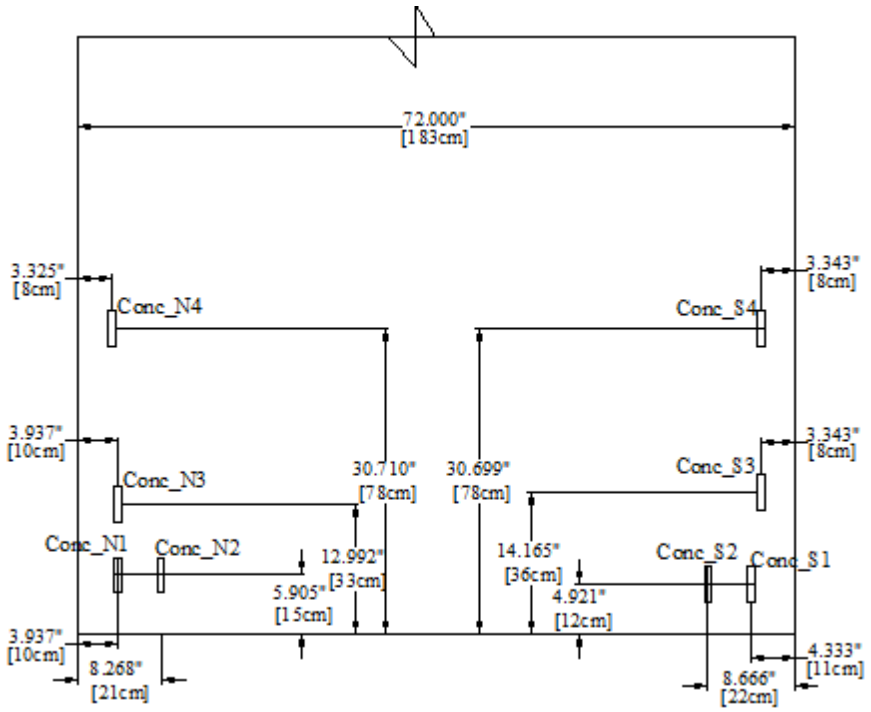

Figure 2.15 Locations of the embedded concrete gauges in the wall panel boundary regions (concrete gauge type: PML-60-2L, gauge factor: 2.09)

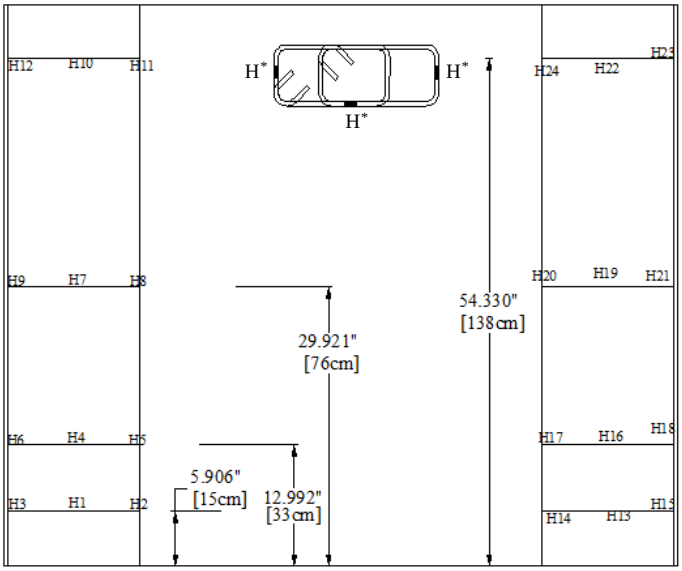

Figure 2.16 Locations of the hoop gauges in the wall panel boundary regions

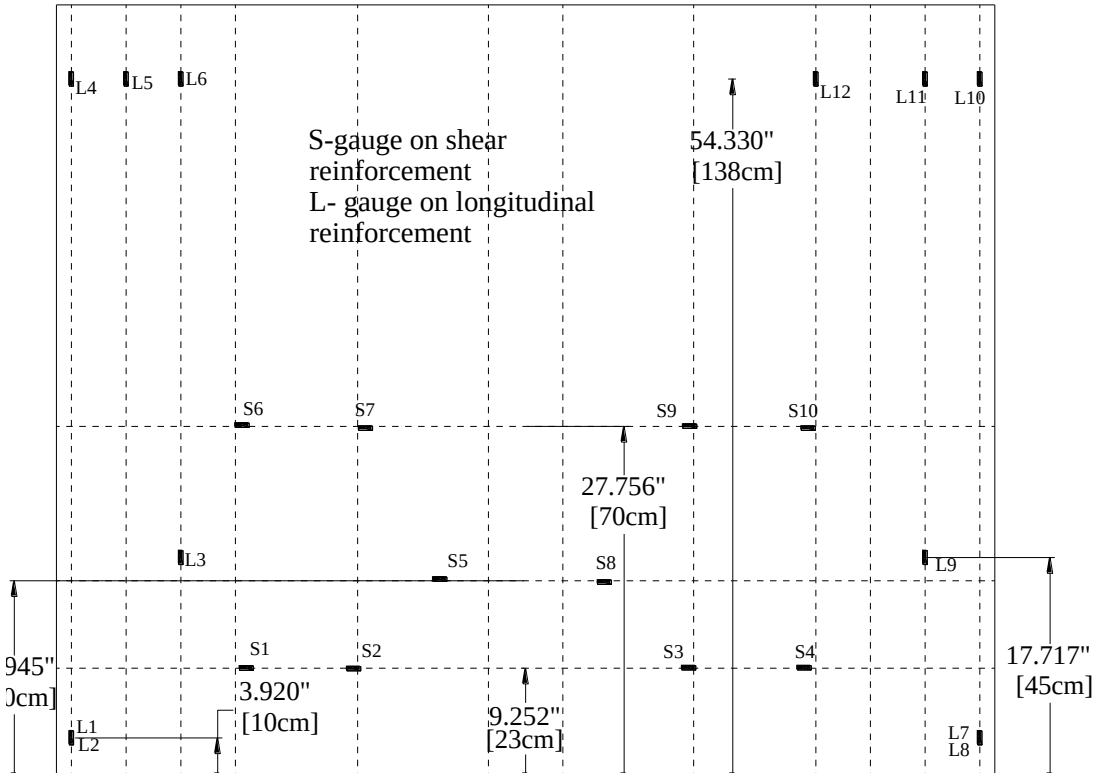

Figure 2.17 Locations of the strain gauges mounted to the longitudinal and shear reinforcement of the wall panel

2.5 Load Protocol

To simulate the seismic effects, the wall was subjected to a pseudo-static reverse cyclic lateral load by the actuator. The cyclic displacement history applied to the wall system is shown in Figure 2.18. For the first four cycles of loading, up to the decompression point of the wall system, the load was applied under a force-controlled mode. Then, the load was applied under the displacement control mode. The displacement targets for the testing were chosen based on the load protocol guidelines recommended by ACI ITG 5.1 document (ACI ITG 5.1 2007) on validating testing of special precast concrete walls for seismic regions. The wall system was subjected to a maximum lateral drift of ±3.5%, with three full reversed

cycles at each target drift up to 3%. Three load cycles were used at each target displacement to ensure the stability of the force-displacement response at that displacement. During testing, the applied lateral displacement to the wall system was controlled using an external temposonic displacement gauges located at the loading height (i.e., 20 ft (6.1 m) from the base of the wall).

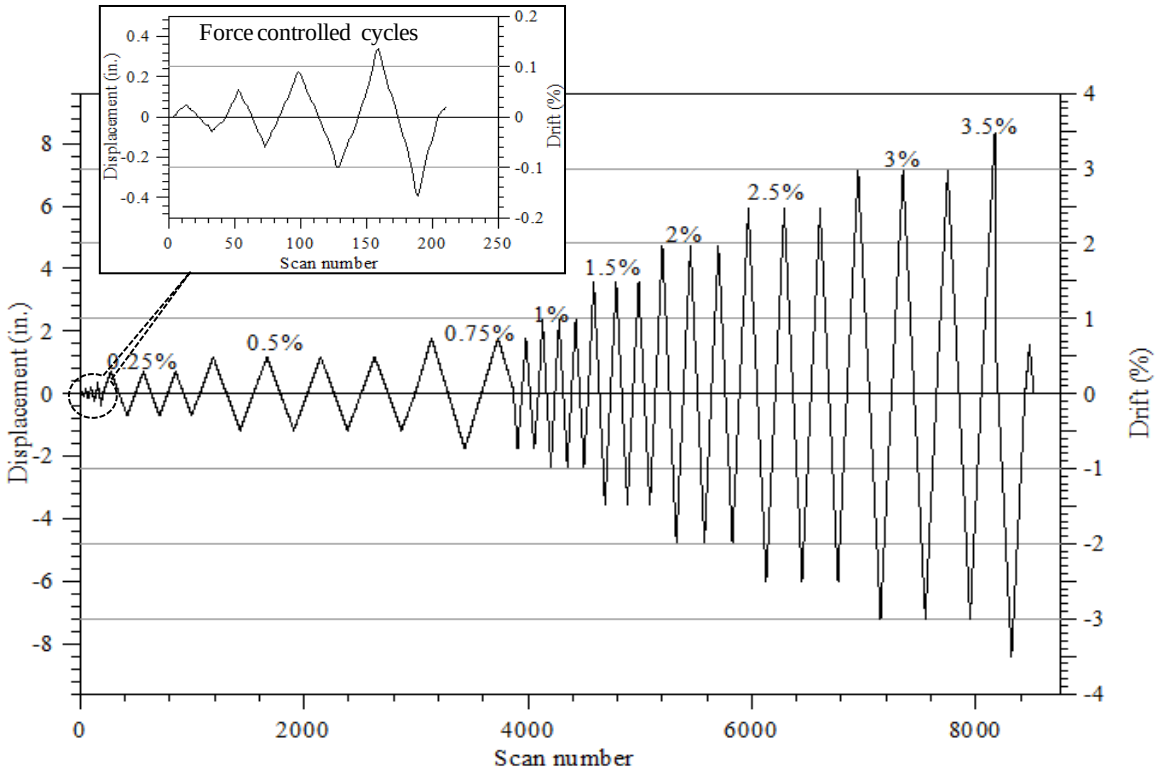

Figure 2.18 The cyclic displacement history used for the PreWEC system testing.

2.6 Experimental Observations and Results

This section presents observations and detailed experimental results from the PreWEC-1 testing. The results include global lateral response of the wall system, connector deformations at different heights, post-tensioning stress variations, wall uplifts, information about the wall panel contact lengths, and strain gauge responses.

2.6.1 Test Observations

PreWEC-1 performed very well with negligible damage to the wall panel and no damage to the end columns. The damage to the wall was limited to spalling of cover concrete

over a 10 in. (25 cm) depth at the bottom corners. The channel placed at the bottom of the wall experienced some bending and its impact on the response of the overall system behavior needed to be further investigated in future tests. The O-connectors behaved as expected, providing sufficient shear transfer and energy dissipation during the reverse cyclic testing. The O-connectors experienced progressive fracture started at the lateral drift ± 3% and eventually failing during 3.5% drift cycles. Even after the connector was fractured, it was able to transmit the forces as the connector ends came into full contact with each other. Consequently, the force-displacement behavior of the PreWEC-1 was not affected by the fracture of the connectors. Figure 2.19 shows the damage state of the PreWEC specimen and RWN at 3% drift.

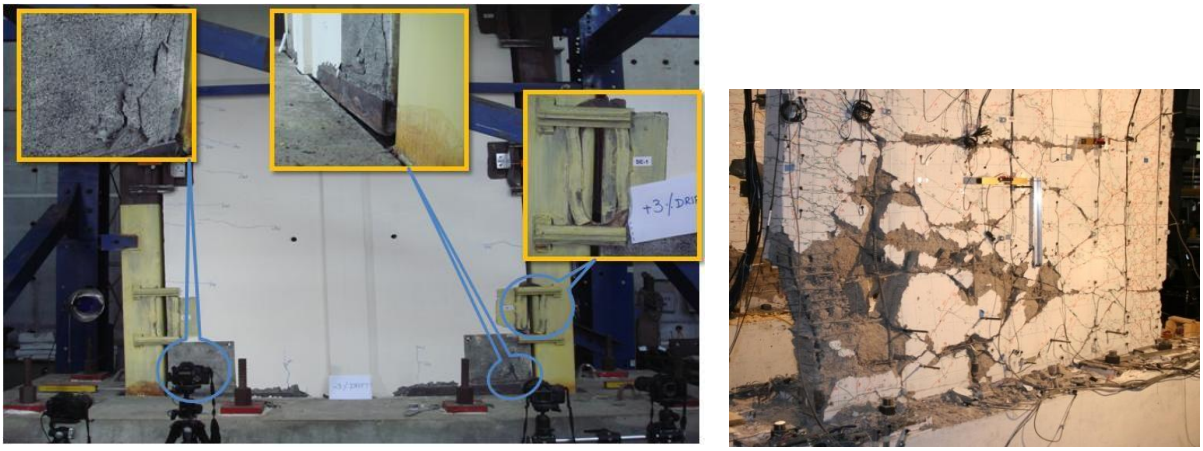

a) PreWEC condition at 3% drift

b) RWN condition at 3% drift

Figure 2.19 Condition of the PreWEC system and RWN at 3% drift

2.6.2 Lateral load response

The lateral load response of the PreWEC-1 system is presented by plotting the base shear as a function of the lateral drift, shown in Figure 2.20a. The cyclic force-displacement hysteretic response of PreWEC-1 was stable. There was no significant strength degradation between the successive cycles imposed at any drift. The PreWEC test unit performed exceptionally well compared to the traditional reinforced concrete walls. The base shear capacity of the PreWEC-1 in the push and pull directions was 115.67 kips (514.2 kN) and 119.3 kips (530.3 kN) respectively. The base shear capacity of the PreWEC system is nearly 12%-15% more than that of the reference cast-in-place concrete wall (RWN) (see Figure

2.20b). Note that the force-displacement response included in Figure 2.20b for RWN assumes the boundary elements at both ends of the wall contained #5 and #6 longitudinal bars, resulting in identical response for the positive and negative displacement directions.

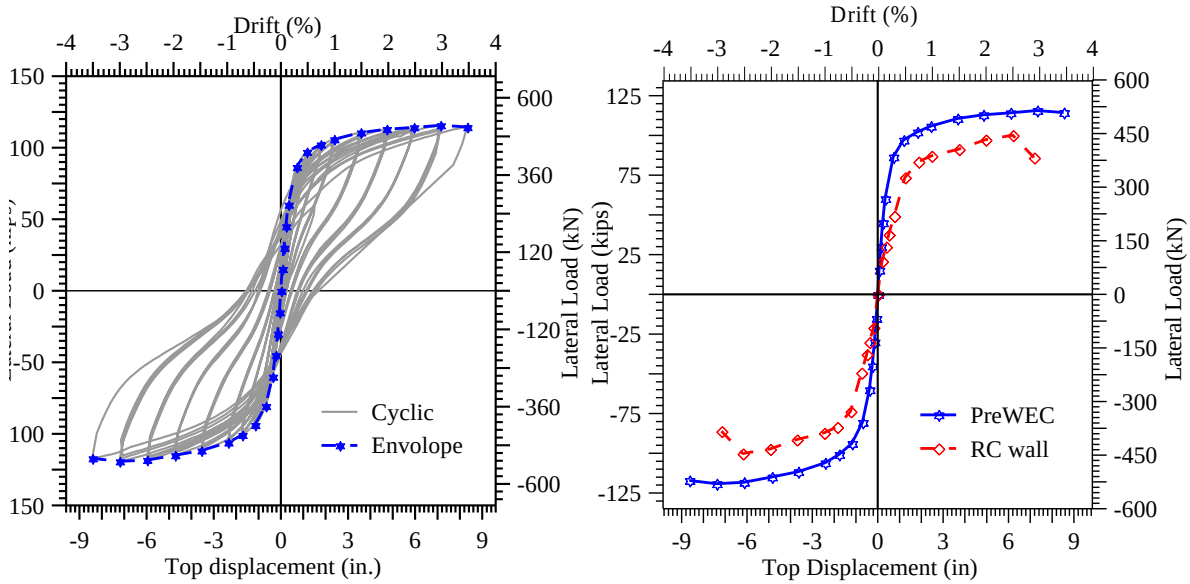

a) PreWEC-1 response

b) Comparison of PreWEC-1 and RWN response envelopes

Figure 2.20 Measured force-displacement response of PreWEC-1

2.6.3 Prestressing steel response

The post-tensioning tendon in the wall panel was at a stress of $0.67f_{pu}$ at the beginning of the test, resulting in a total prestress force of 454.157 kips (2019.18 kN) acting at the center of the wall. The prestressing steel in the north and south column were at a stress level of $0.662f_{pu}$ and $0.677f_{pu}$ after losses, anchoring the columns to the foundations with a force of 112.07 kips (498.3 kN) and 114.68 kips (509.9 kN) respectively.

Figure 2.21 shows the variation of post-tensioning tendon forces in the wall panel and the north and south columns as a function of lateral drift. Figure 2.21a shows the increase in the wall post-tensioning force is linearly proportional to the top displacement until yielding of the tendon occurred. The post-tensioning tendon in the wall panel experienced yielding after a lateral drift of 2% was exceeded, resulting in small loss of initial prestress force and a reduction to the reloading stiffness of the system. The prestress loss in the wall panel was nearly 8.5% after unloading from the ±3% drift. Prestress losses of 4 to 5% were observed in

the column post-tensioning steel at 1% drift, as shown in Figure 2.21b and Figure 2.21c. This observation indicates a possibility of overstressing one of the three strands in the columns, leading to yielding before 2% drift. However, this did not affect the overall behavior of the wall system, as the contribution of the columns to the lateral strength of the system is not significant.

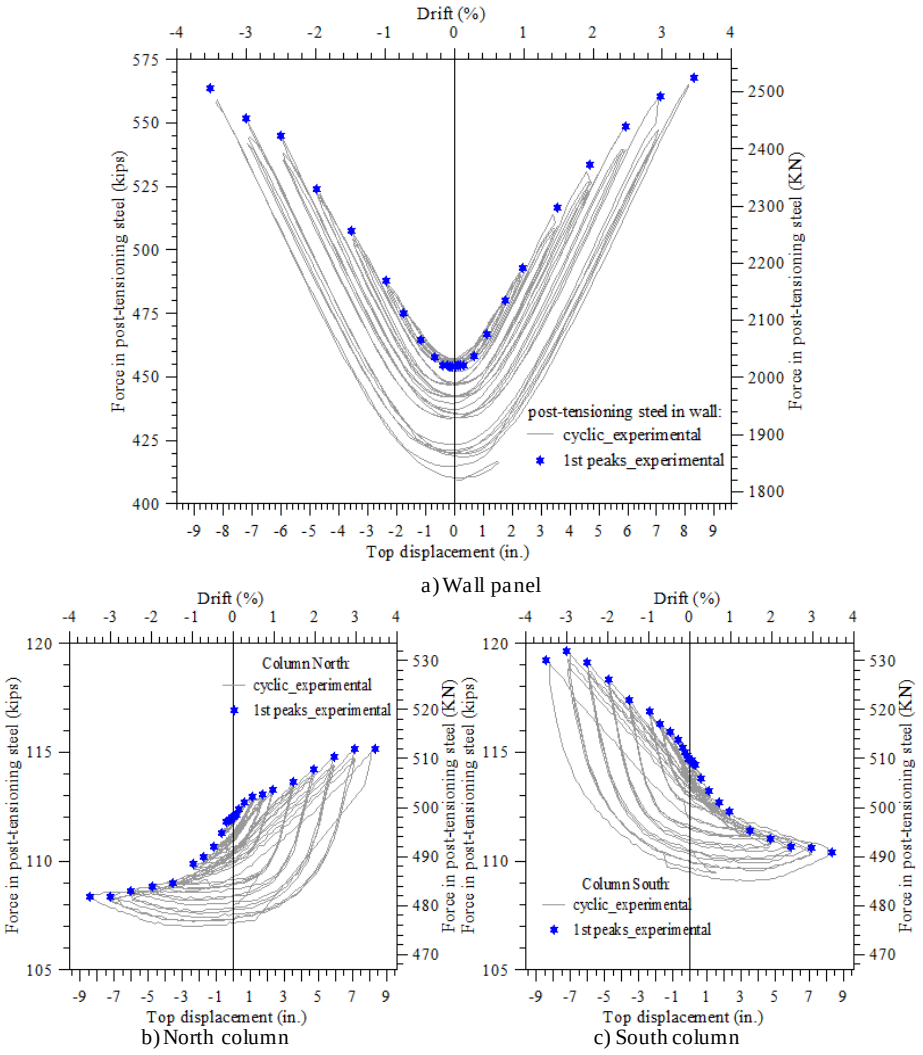

Figure 2.21 Variation of forces in the post-tensioning tendon in the wall panel, and the north and south columns

2.6.4 Wall panel and column uplift

As expected, the flexural deformation of the wall system was concentrated at the wall-to-foundation interface. Displacement transducers (LVDTs) were placed at the wall and column bases as shown in Figure 2.13. The cyclic displacements and displacement at first peaks measured by these LVDT's are shown in Figure 2.22 and Figure 2.23 for the wall and end columns respectively. Figure 2.22 shows that the maximum uplift occurred at the end of the wall (WUN5 and WUS5) was 2 in. (50mm) which is the same as the maximum displacement demand on the O-connector. Additionally, the profiles of the uplift along the wall length for various drift levels in the push and pull direction are presented in Figure 2.24 and Figure 2.25. The contact length for the wall panel was estimated based on the uplift along wall length and Figure 2.26 shows its variation with the top lateral displacement of the wall. It is clear from the Figure 2.26 that the contact length rapidly decreases at the beginning of the loading. The variation of the contact length is not significant after 0.5% drift. This supports the previous observations made by Aaleti and Sritharan (2009) in the case of jointed wall systems.

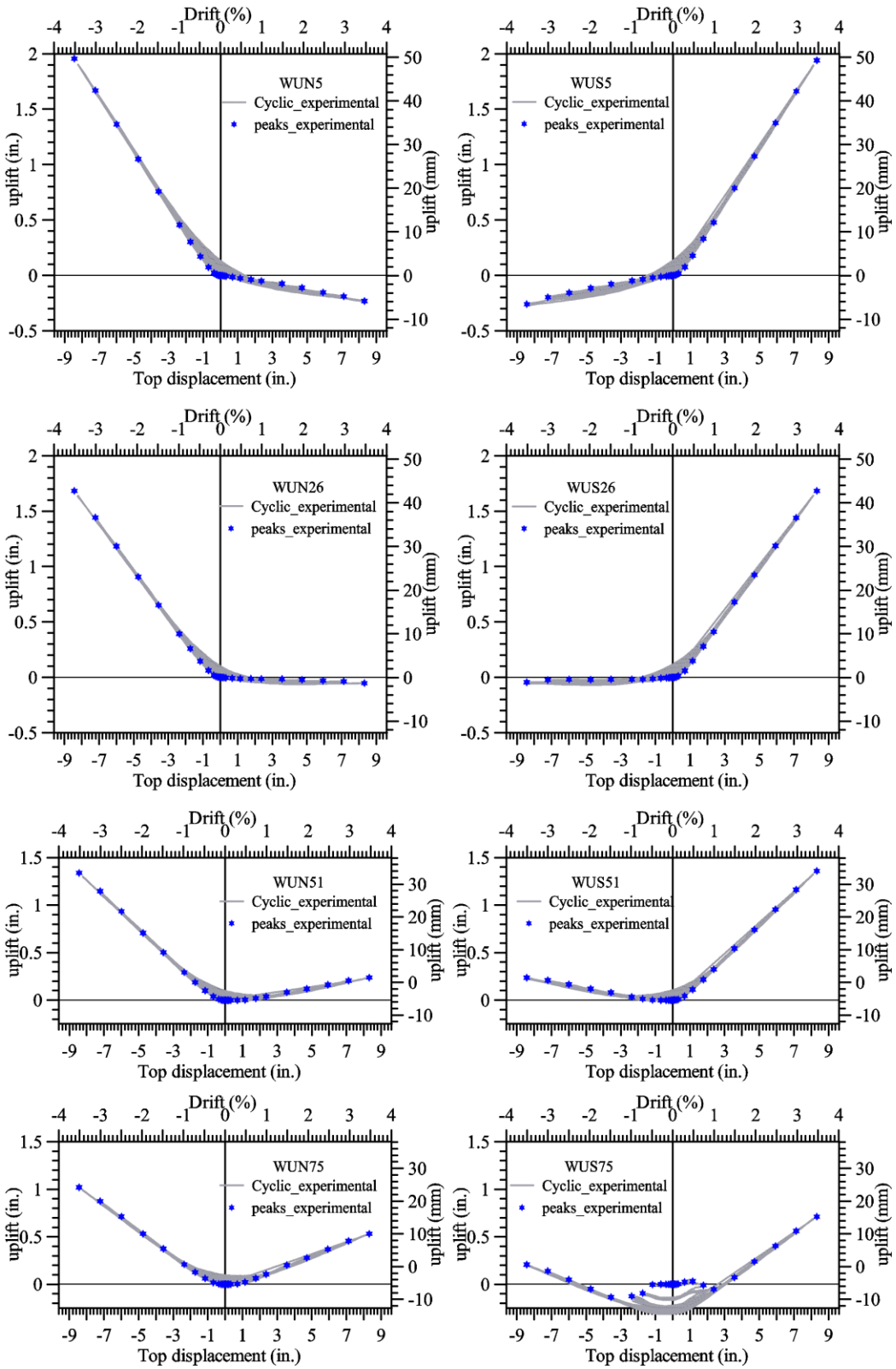

Figure 2.22 Variation of wall panel uplifts along the length with lateral drift

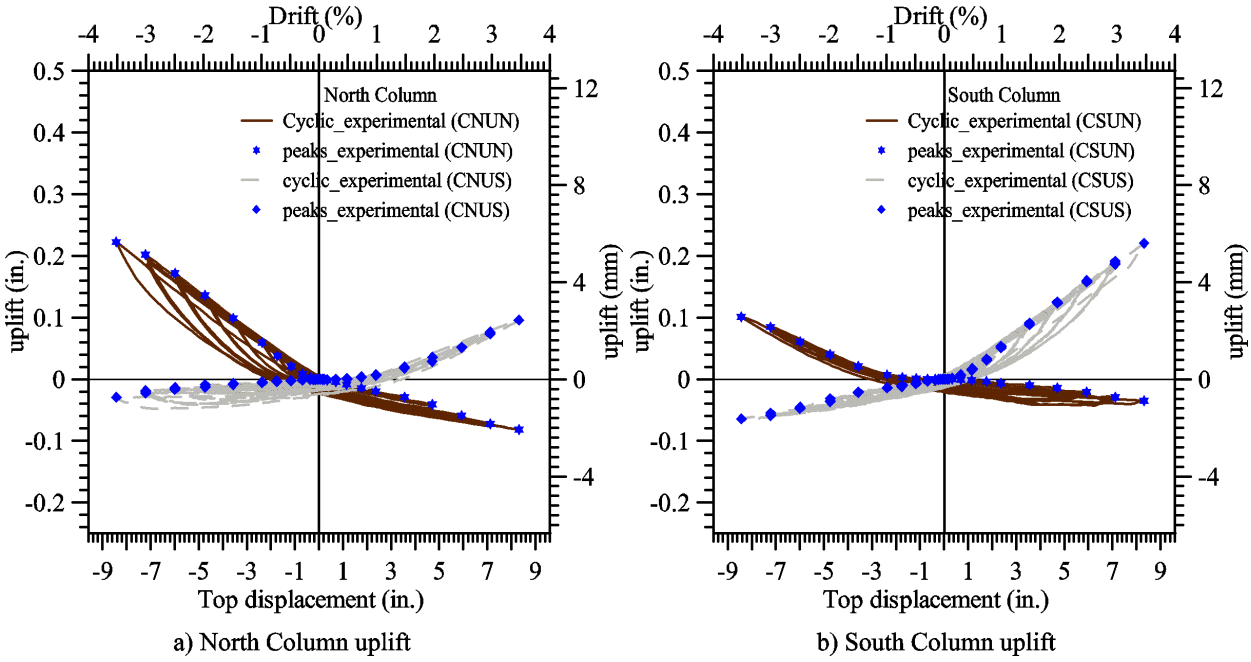

Figure 2.23 End column uplifts on north and south faces as a function of lateral drift

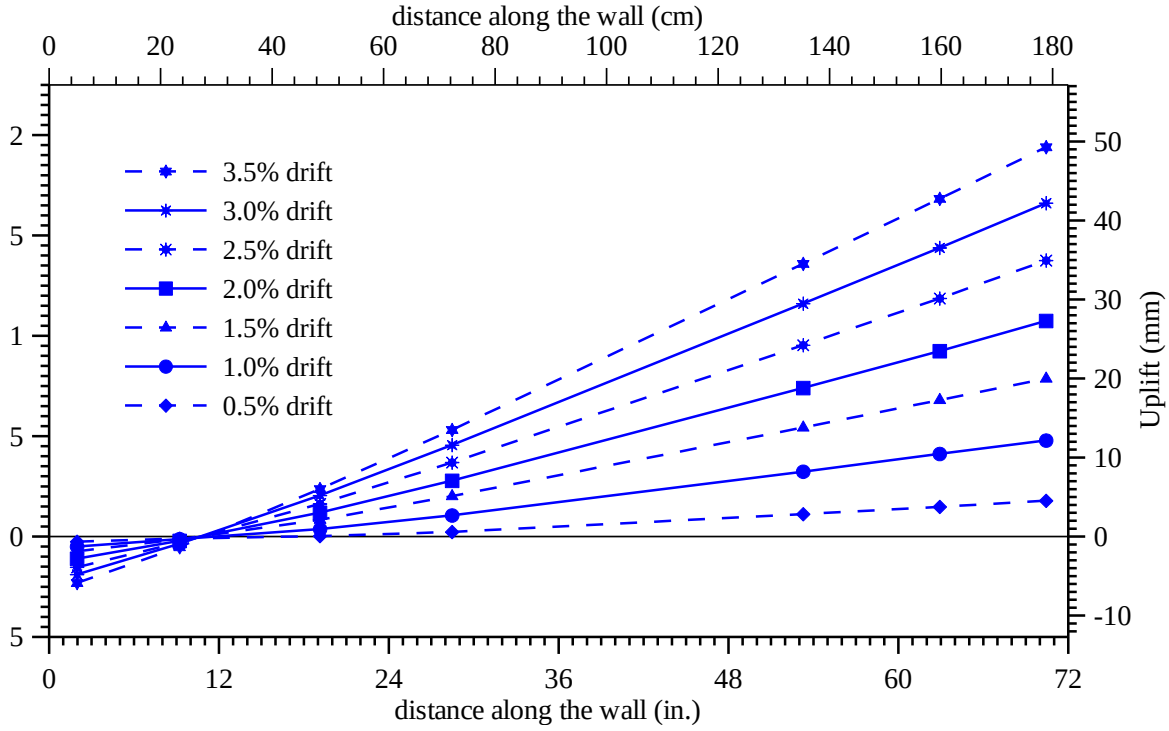

Figure 2.24 The uplift along the wall length at various drift levels in the positive direction of loading

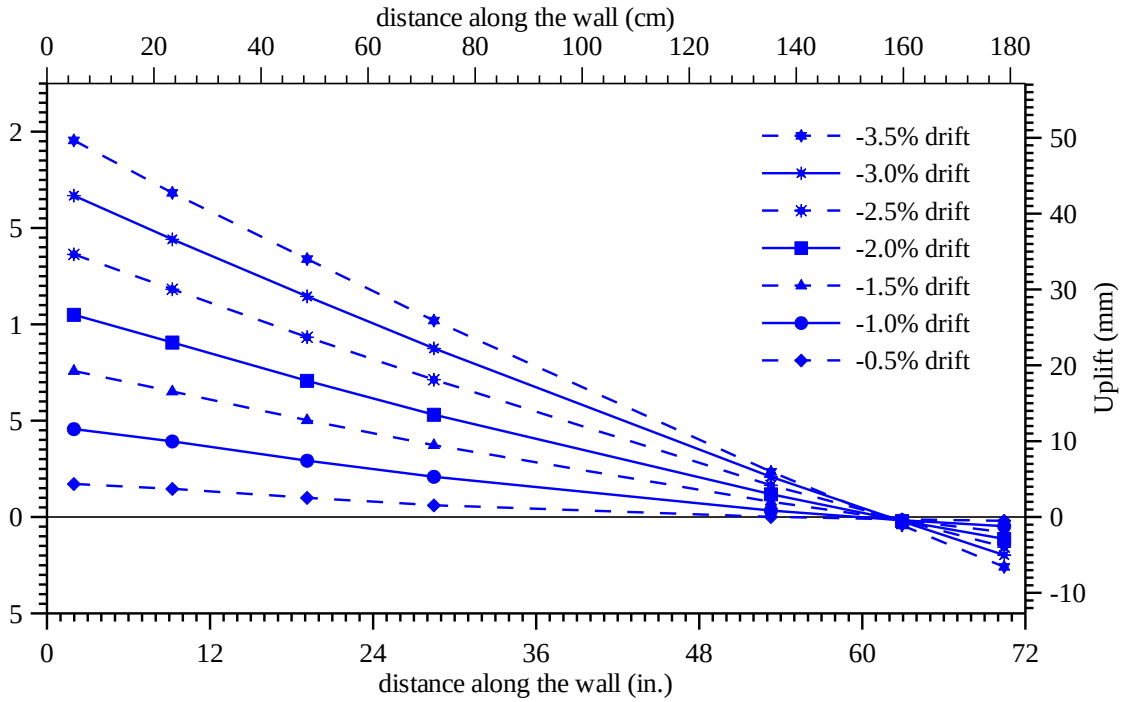

Figure 2.25 The uplift along the wall length at various drift levels in the negative direction of loading

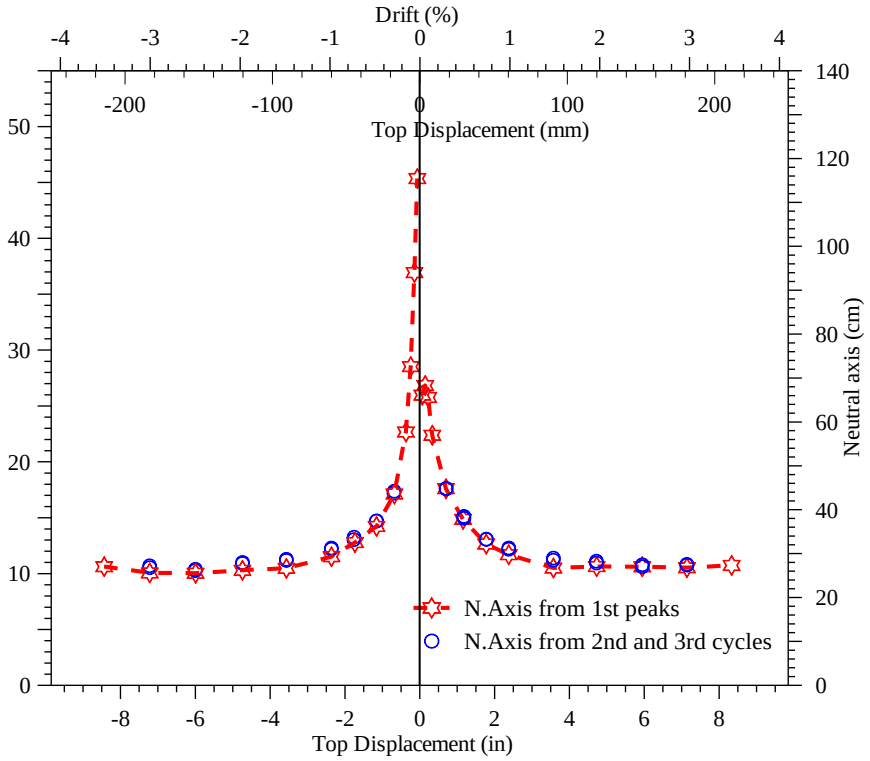

Figure 2.26 Variation of the wall panel contact length with lateral drift

2.6.5 Connector response

The O-connectors performed as expected with a stable response until cracking occurred in the critical regions of the connectors during the third 3% drift cycle. The condition of the bottom most connectors (north and south side) at various drift levels is shown in Figure 2.27. As shown in Figure 2.28, three of the connectors at the top of the wall system underwent a progressive fracture, starting at ± 3.0% drift with eventual failure occurring during 3.5% drift cycles. It is important to note that even after fracture; the connectors were able to transfer forces when the ends of the connectors came into contact with each other. As a result, the wall system showed almost no strength degradation due to the fracture of the connectors, which can be observed in the system force-displacement response in Figure 2.20a.

On both sides of the wall panel the vertical and horizontal deformations that the O-connectors experienced along the vertical joint were measured using two LVDTs near the bottom connector located at 58 in. (1.47 m) from the top of the base block and at the top most connector located at 172 in. (1.83 m) from the top of the base block. Figure 2.14 shows the locations of the LVDTs used for measuring vertical and horizontal displacement demands experienced by the O-connectors. The horizontal LVDTs were used to monitor the horizontal separation between the wall and the column along the vertical joint during testing, while the vertical LVDTS measured the connector displacement demands. Figure 2.30 and Figure 2.31 depict the data obtained from the vertical displacement transducers, which show the vertical displacement demand imposed on the connectors was almost linearly proportional to the top lateral displacement. Additionally, Figure 2.29 shows a time history plot for one of the bottom connectors, which together with Figure 2.30 and Figure 2.31 indicate that the O-connectors underwent a maximum positive displacement of 2.1 inches (53.4 mm) and a maximum negative displacement of 0.55 inches (13.97 mm) in the direction parallel to the side face of the wall panel. The maximum negative displacement does not match with the maximum uplift estimated for the columns (see Figure 2.23), implying the compression at the wall toe should be taken into consideration when estimating the connector displacement. The maximum value of wall compression (obtained from uplift measurements of LVDTs WUS5 and WUN5) was found to be 0.27 in. (6.86 mm), which, when added to the maximum

column uplift of 0.24 in. (6.1 mm) nearly matches with the maximum measured negative displacement of 0.55 in. (13.97 mm). The horizontal LVDTs measured a horizontal movement of 0.09 in. (2.2 mm) and 0.17 in. (4.38 mm) between the wall panel and the end columns at the bottom and top connector levels respectively, which did not seem to have influence connector behavior.

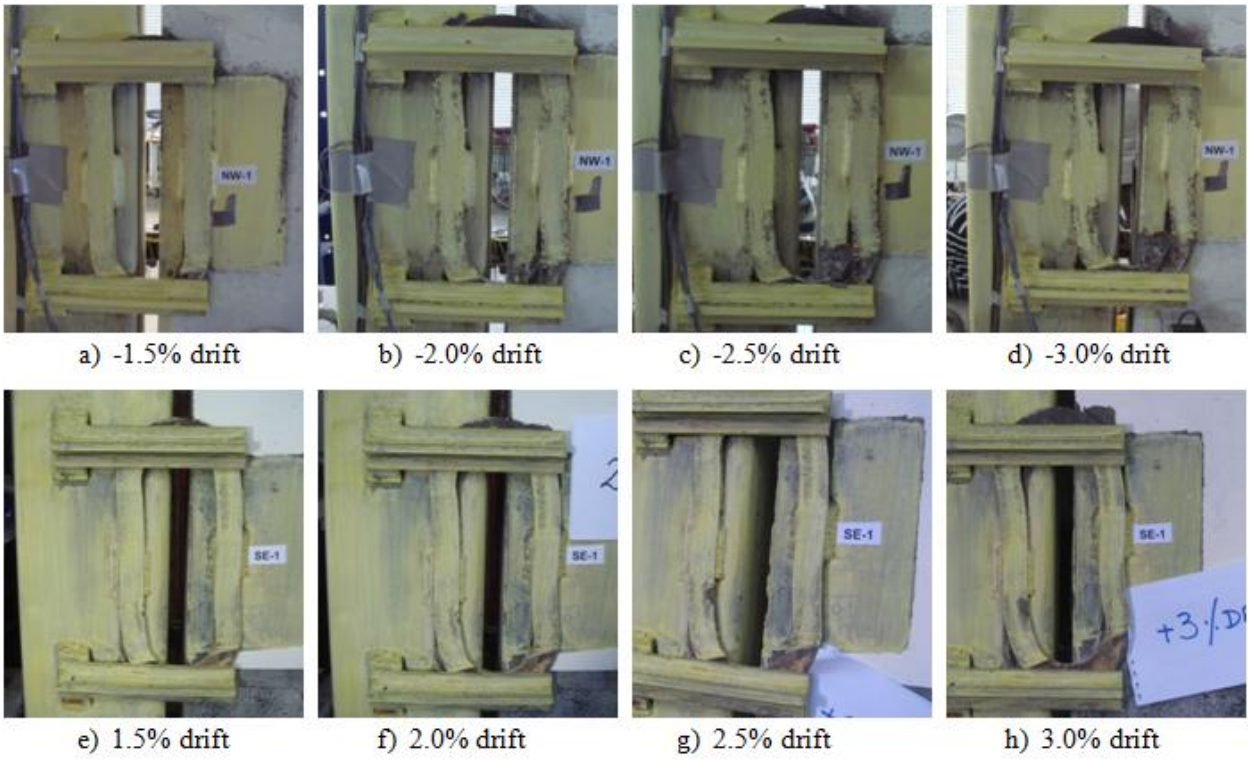

a) -1.5% drift b) -2.0% drift c) -2.5% drift d) -3.0% drift

e) 1.5% drift f) 2.0% drift g) 2.5% drift h) 3.0% drift

Figure 2.27 Condition of the bottom O-connector at various drift levels

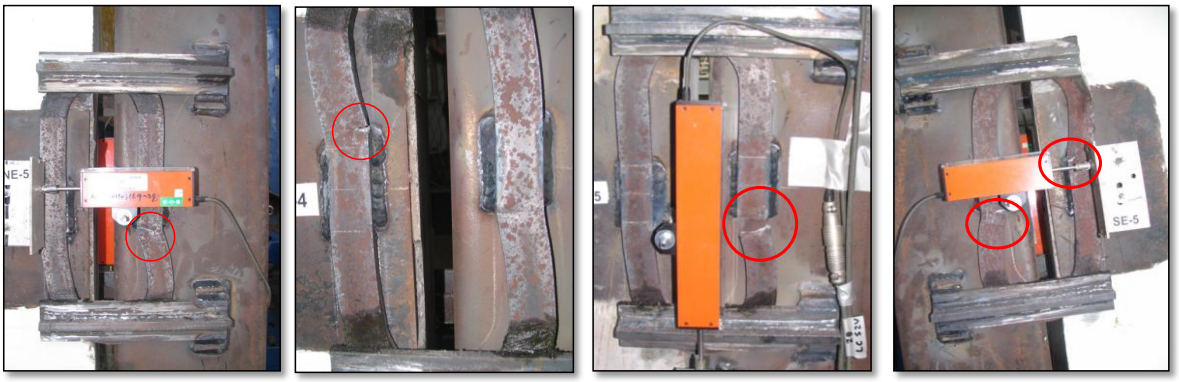

a) Crack initiation at critical regions of connector at 3% drift

b) Fractured connectors at 3.5% drift

Figure 2.28 Progressive fracture of a top O-connector observed during the 3 and 3.5% drift

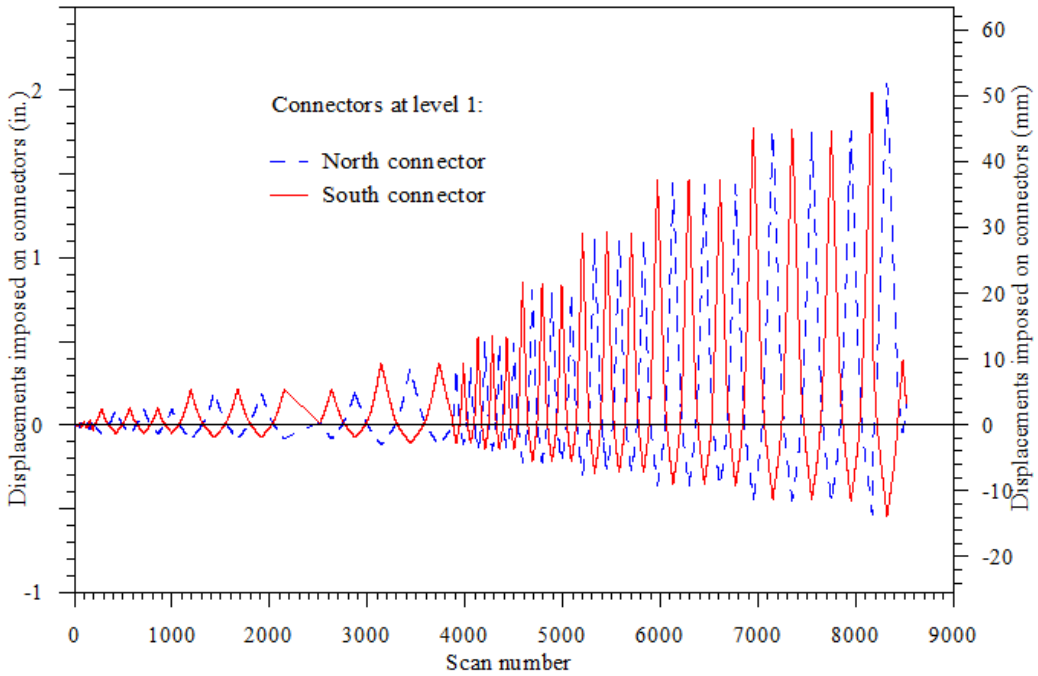

Figure 2.29 Vertical displacement demand recorded for the connector near the base in the direction parallel to the wall side face as a function of the scan number

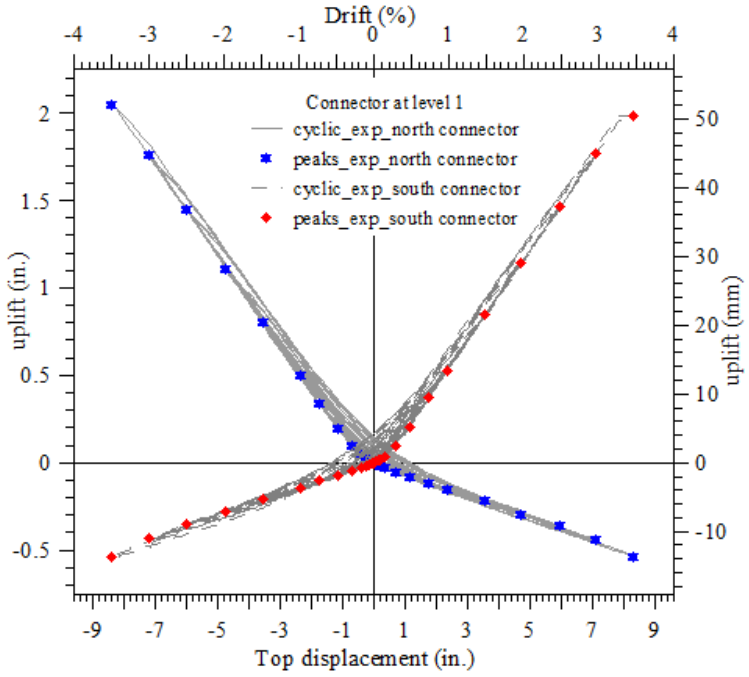

Figure 2.30 Vertical displacement demand recorded for the connector near the base in the direction parallel to the wall side face

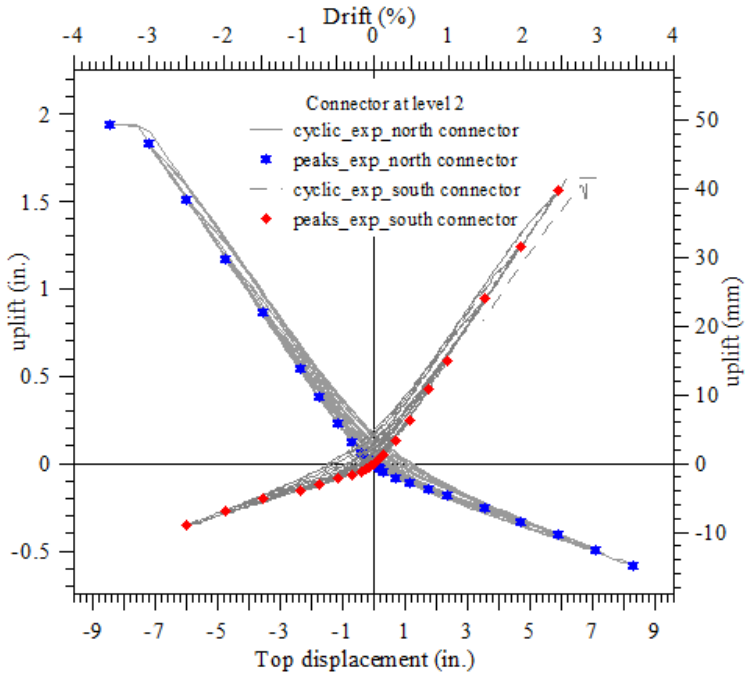

Figure 2.31 Vertical displacement demand recorded for the connector near the top in the direction parallel to the wall side face

2.6.6 Strain in the horizontal straps

The wall panel was secured with three pairs of 1-in. thick, 2-in. wide Grade 60 steel plates, with an objective of providing resistance, if the wall panel was to move away from the columns in the direction parallel to the direction of loading. Gauges mounted on the outside surface of the straps monitored strain demands, which did not exceed 160 με. This corresponds to a maximum force of 4.64 kips (19.6 kN) in each strap.

2.6.7 Strain in the confinement reinforcement

Strain gauges were mounted to the confinement reinforcement placed at the wall ends to estimate the required confinement steel area and the height over which confinement is needed. The details of the hoop strain gauges locations are provided in Section 2.5.

Figure 2.32 and Figure 2.33 show that the hoop strains of gauges located at 5.9 in. and 13 in. above the wall base. Figure 2.32 indicates the strains imposed on the confinement reinforcement did not cause yielding of this reinforcement. This finding is consistent with the test observations, where no damage to the confinement reinforcement or significant spalling of cover concrete in this region was observed during the test. The strain demand on the hoop reinforcement at 13 in. (see Figure 2.33) indicates the hoop reinforcement did not experience yielding. This observation implies the amount of confinement reinforcement required at this level could be reduced

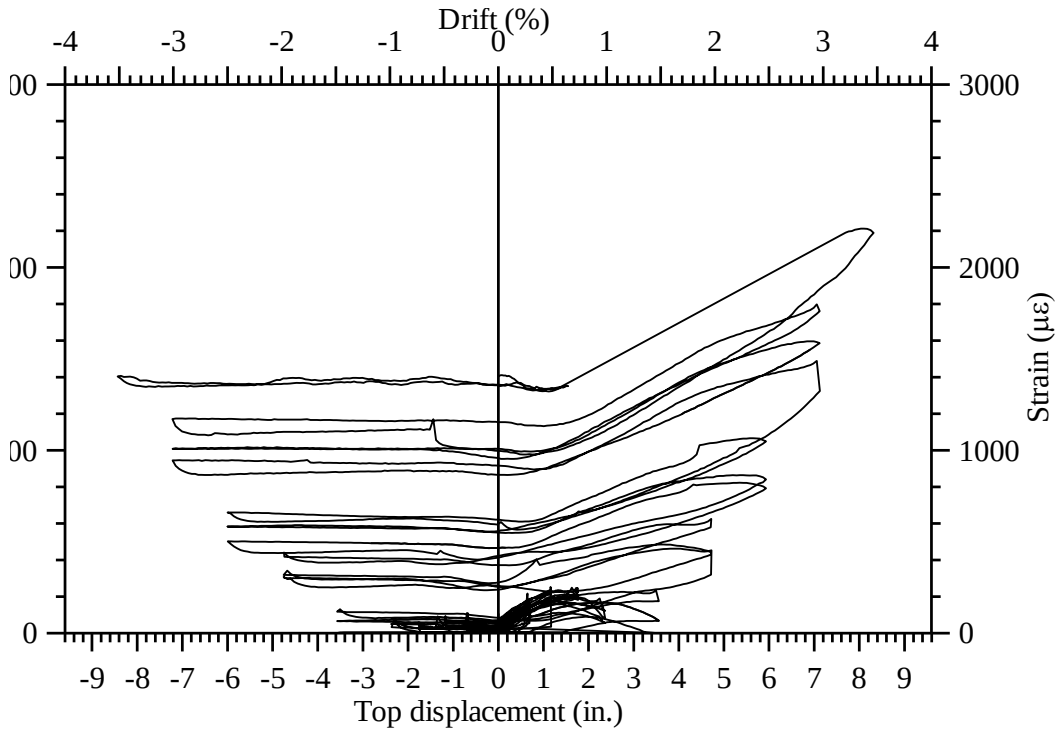

Figure 2.32 Variation of strains recorded by a confinement hoop gauge (H1) located at 5.9 in. from the base of the wall panel.

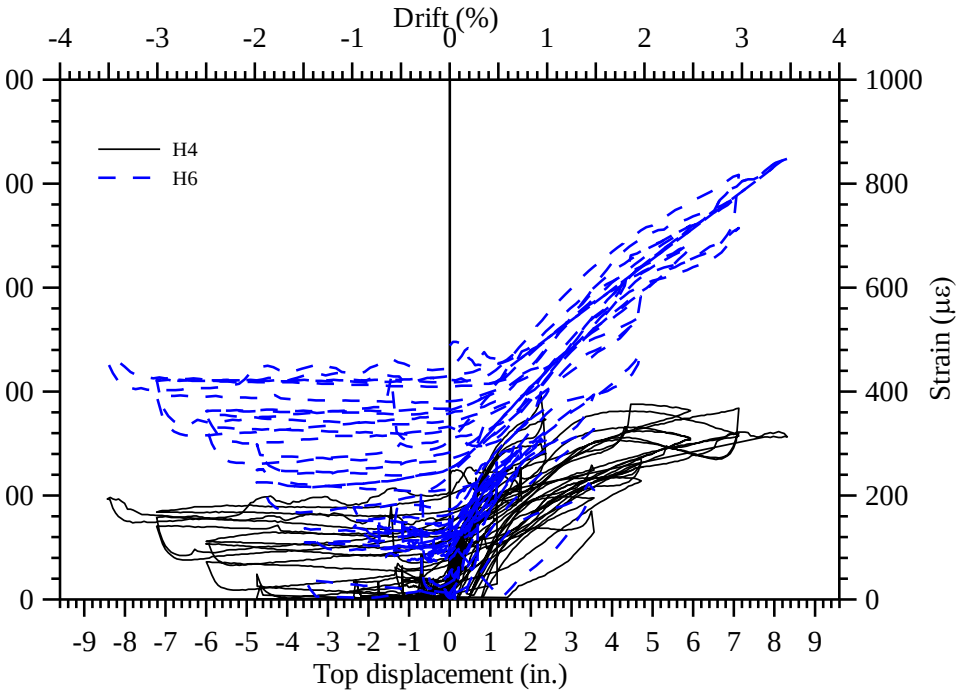

Figure 2.33 Variation of strains recorded by a confinement hoop gauges (H4 and H6) located at 13 in. from the base of the wall panel

2.6.8 Confined concrete strains

Concrete strain gauges were placed in the confined concrete regions of the wall panel at different levels along the wall height to estimate strain demand in the concrete. The distribution of the gauges along the height of the wall provides an estimate for the required height of the confinement region. The location and the distribution of the concrete gauges in the wall panel are shown in Figure 2.15.

Figure 2.34 shows the strain demand in the confined concrete at 5 to 6 in. (12.6 cm to 15.1 cm) from the base of the wall. The strain demand at 15 in. (38 cm) and 33 in. (83.8 cm) along the height of the wall in the north and south confined regions is shown in Figure 2.35. This figure indicates the concrete strain demand at 15 in. (38 cm) above the base of the wall was less than 0.003 in./in. up to 3% lateral drift. The strain demand at 33 inches (83.8 cm) from the wall base is around 0.0012 in./in (see Conc_N4 and Conc_S4 in Figure 2.35) indicating no need for confinement reinforcement in this region.

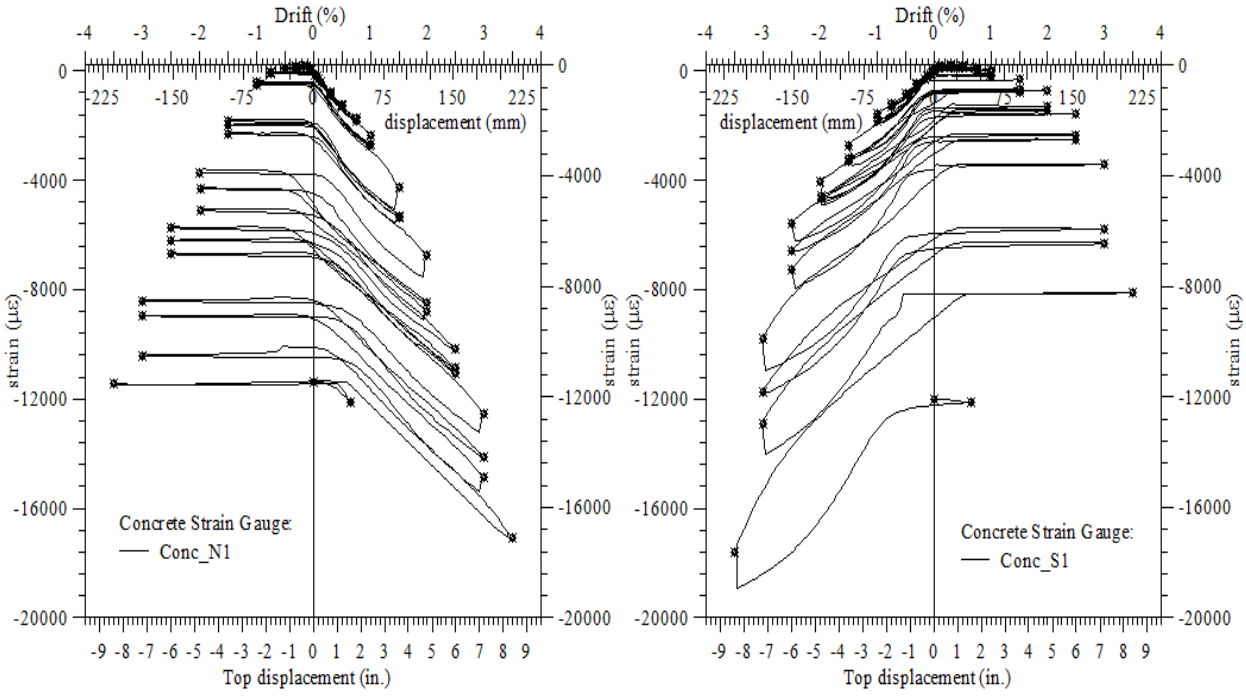

Figure 2.34 Recorded confinement strain demand in wall toe regions at 5 in. to 6 in. from the wall panel base as a function of top displacement

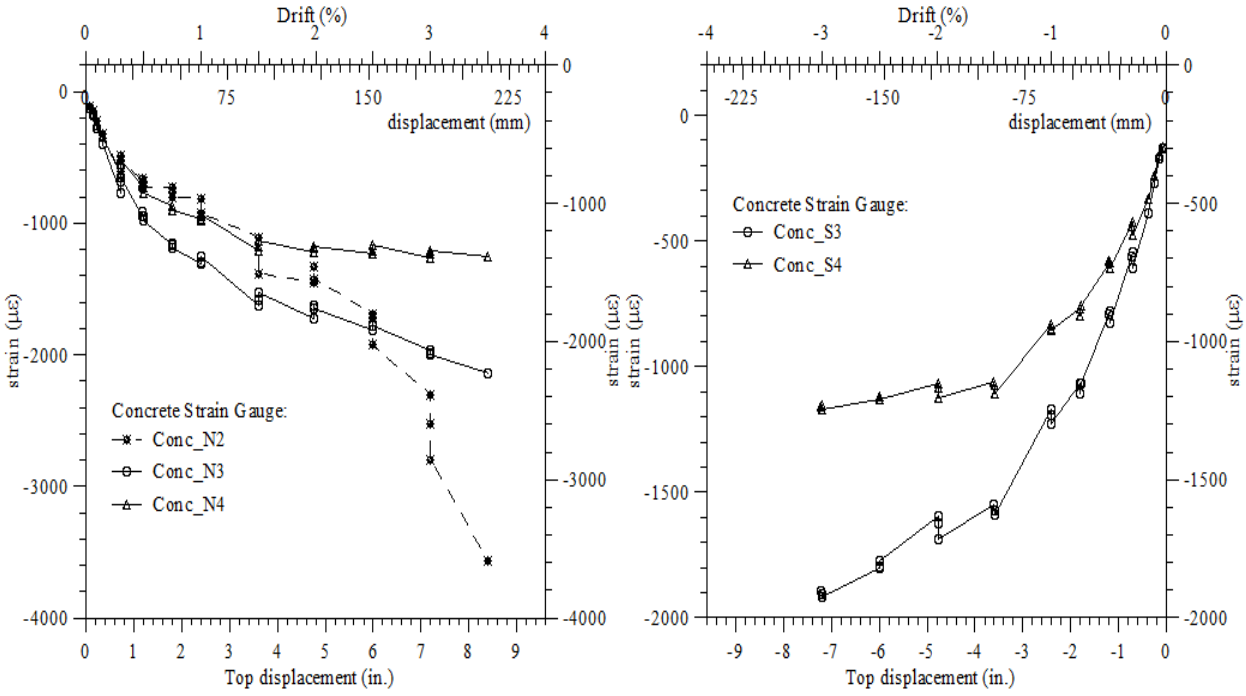

Figure 2.35 Recorded confinement strain demand at 15 and 33 inches from the wall base as a function of top displacement

2.6.9 Energy dissipation capacity

Using the force-displacement response recorded during the test, the amount of energy dissipated by the PreWEC-1 system was quantified in terms of equivalent viscous damping using Eq.(2.1). The majority of the energy dissipation for the wall system was provided by inelastic deformation experienced by the O-connectors. Figure 2.36 shows an example of the experimental hysteresis loop obtained for PreWEC-1 system at +2% drift, which was used in estimating the equivalent viscous damping.

$$\varsigma_{eq} = \frac{2}{\pi}\frac{A_{loop}}{A_{rect}} \tag{2.1}$$

where, A_{loop} is the area enclosed by a hysteresis loop at a given drift, and

A_{rect} is the area of the rectangle circumscribing the hysteresis loop.

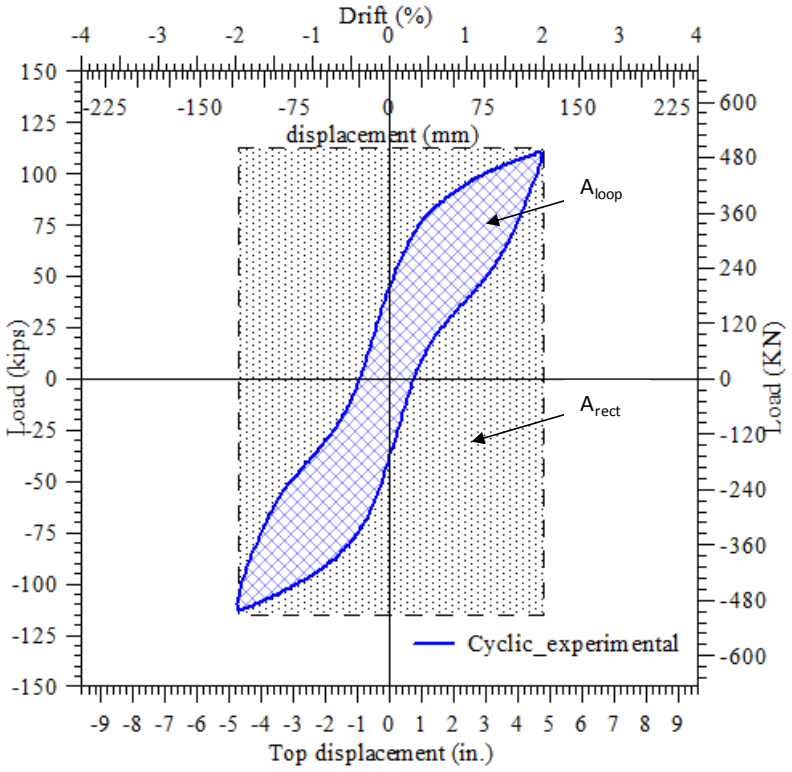

Figure 2.36 Hysteresis loop of the PreWEC system at 2% drift

ACI ITG 5.1 document on validation testing of unbonded precast wall systems uses a relative energy dissipation ratio (β) to characterize the energy dissipation capability of special unbonded precast wall systems. The ratio, β, is defined as the ratio between the energy dissipated by the specimen during the loading cycle at a particular drift level (i.e., A_{loop}), and the energy that would be dissipated by an equivalent elasto-plastic system. Accordingly β is defined by Eq. (2.2).

$$\beta = \frac{A_{loop}}{A_{rect}} \tag{2.2}$$

Figure 2.37 shows the calculated values for the equivalent viscous damping and the relative energy dissipation ratio of PreWEC-1 for drifts ranging between 0.25 and 3.5%. As can be seen, PreWEC specimen exhibited excellent relative energy dissipation ratios throughout the test, with β values ranging from 5% at low drift levels to nearly 27% at 3.0% drift. It is worth mentioning that a β value of 12.5% is specified in the ACI-ITG 5.1 document (ACI ITG 5.1

2007) as the minimum acceptable value behavior of unbonded post-tensioned precast wall systems for seismic loading. In terms of equivalent viscous damping, PreWEC-1 exhibited 3 to 17% of damping.

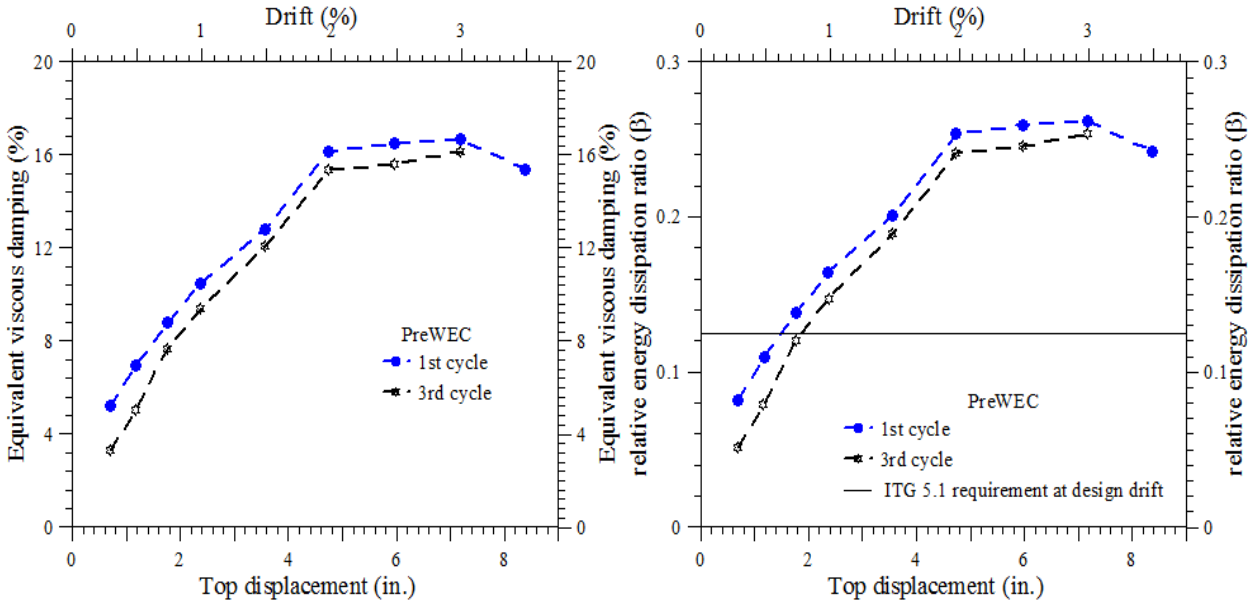

a) Equivalent viscous damping b) Relative energy dissipation ratio

Figure 2.37 Measured equivalent viscous damping and relative energy dissipation ratio for PreWEC-1

2.6.10 Code Validation of PreWEC-1 Behavior

This section examines the PreWEC-1 performance against the acceptance criteria established for special unbonded post-tensioned precast walls, ACI-ITG 5.1 (2007). The PreWEC system can be deemed to have performed satisfactorily when all of the following criteria of ITG-5.1document are met for both directions of in-plane response, making the application of this system viable in construction practice.

Criteria-1*:* "*In cycling up to the drift level given by Sec.7.4 through 7.6, fracture of reinforcement or coupling elements, or other significant strength degradation, shall not occur. For a given direction, peak lateral strength during any cycle of testing to increasing displacement shall not be less than 0.8 times* E_{max} *for that direction."*

From the experimental response and observations presented in Section 2.6.2 Lateral load response, it is clear that the lateral force did not decrease as the lateral drift increased. The maximum drift level required by ITG for the PreWEC specimen is calculated using section 7.4 of ITG 5.1 document and is equal to 3%. As presented in Section 2.6.5 Connector response, coupling elements (O-connectors) began to fracture only at 3% drift, which is the same as the maximum drift level required by ITG 5.1.

Criteria-2: *"For cycling at the given drift level for which acceptance is sought in accordance with Sec.7.4, 7.5 or 7.6, as applicable, the parameters describing the third complete cycle shall have satisfied the following:*

1. The relative energy dissipation ratio shall be not less than 1/8; and

2. The secant stiffness between drift ratios of -1/10 and +1/10 of the maximum applied drift shall be not less than 0.10 times the stiffness for the initial drift ratio specified in Sec. 7.3.

3. The force in any vertical unbonded tendon in any wall shall not exceed 0.95 times the measured yield strength of the prestressing steel of that tendon at 1% elongation.

4. The maximum relative displacement between the base of a wall and the adjacent foundation (shear-slip) shall not exceed 0.06 in (1.5 mm)."

From Figure 2.37, it can be clearly seen that the relative energy dissipation ratio of the PreWEC system for the 3rd complete cycle is greater than 0.125 for drifts greater than 0.75%. Thus, the PreWEC-1 system satisfied this requirement. Figure 2.38 shows the secant stiffness between drift ratios of -1/10 and +1/10 of the maximum applied drifts of 2 and 3%, which are 0.21 and 0.11 times the initial stiffness of the PreWEC system. The measured force of the post-tensioning tendons in the wall panel at 2% design drift is less than 95% of the measured yield force of the prestressing steel (see Figure 2.21). The measured maximum relative displacement between the base of a wall and the adjacent foundation (shear-slip) was 0.044 in. (1.13 mm), less than the acceptable value of 0.06 in. (1.5 mm).

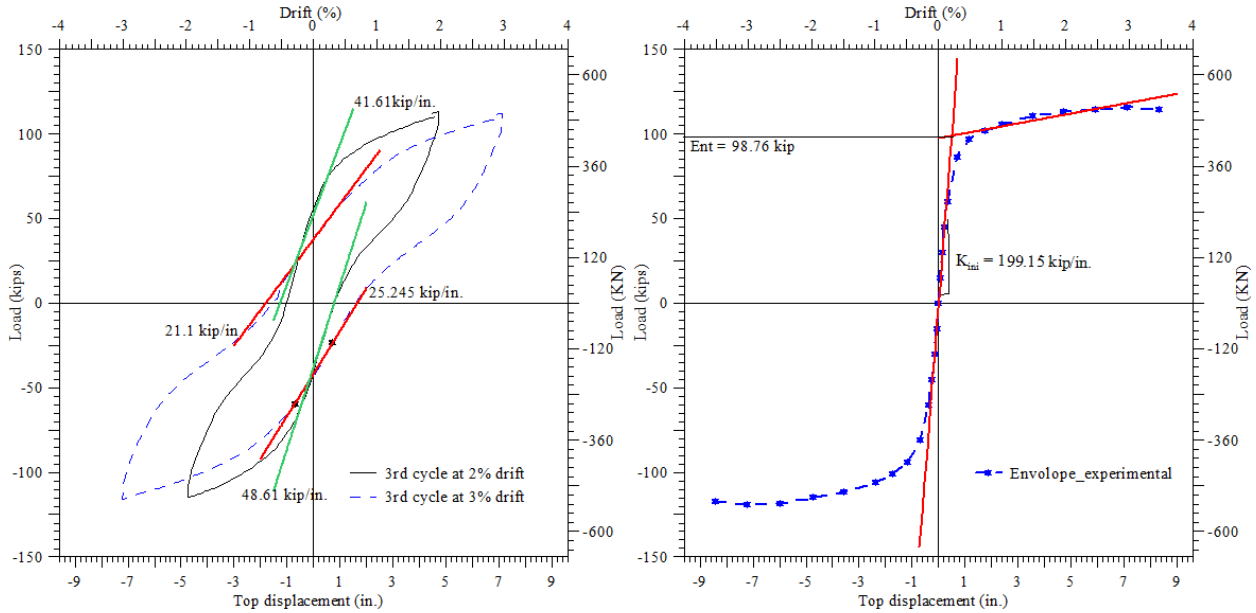

a) Secant stiffness b) Initial stiffness

Figure 2.38 Secant stiffness and initial stiffness at 2% and 3% drifts for the PreWEC-1

In summary, the PreWEC-1 satisfied the requirements of the ITG 5.1 document for good performance. However, ITG 5.1 requires at least two specimens are to be tested to validate the performance requirements. So, to implement the PreWEC system in practice, another test should be conducted.

Chapter 3
Analytical Investigation of the PreWEC System and Its Components

3.1 Introduction

Analysis methods suitable for examining monotonic behavior of the PreWEC system and the O-connector are presented, and their accuracy is verified using the test data. An analytical procedure was developed and validated previously by Aaleti and Sritharan (2009) to establish the monotonic behavior of the unbonded post-tensioned precast wall systems. By incorporating the experimental observations (about the connector deformation) from the large-scale testing of PreWEC (presented in Chapter 2) into this analytical procedure, a modified analytical procedure is established for the PreWEC system.

Following a step-by-step presentation of the analysis procedures in the next section, validation of the simplified analysis procedures are presented, using test data obtained from the large-scale testing of the PreWEC system.

3.2 Simplified Analytical Procedures

This section presents simplified methods to estimate the lateral load behavior of the PreWEC system along with the force-deformation behavior of the O-connector used as an external energy dissipater.

3.2.1 O-connector

This section presents an analytical method to theoretically characterize the force-displacement response envelope of the O-connector. The connector was modeled using a series of frame elements to establish the force-displacement behavior. For this purpose, the fiber based beam-column element available in OpenSees (OpenSees 2007) was used. Taking advantage of the symmetry, only the top half portion of the O-connector was modeled as shown in Figure 3.1. The O-connector was modeled using 2-D nonlinear forced-based beam-column elements located along the center line. The circular portion of the connector was

discretized into twelve segments as shown in Figure 3.1b. The weld at the center of the connector was assumed to act as a rigid connection and thus modeled with a node restrained in all degrees of freedom direction. A single force-based beam-column element with four integration points was used to model the vertical legs of the connector, whereas, the circular portion of the connector was modeled using twelve force-based beam-column elements with three integration points for each element. The location of integration points followed the Gauss-Lobotto scheme. For example, in an element with four integration points, the integration points are located at both ends of the element (-1.0 and 1.0 in an isoparametric formulation), and at points located at a distance of 0.2764 times the length of the element from both ends (-0.4472, 0.4472) of the element.

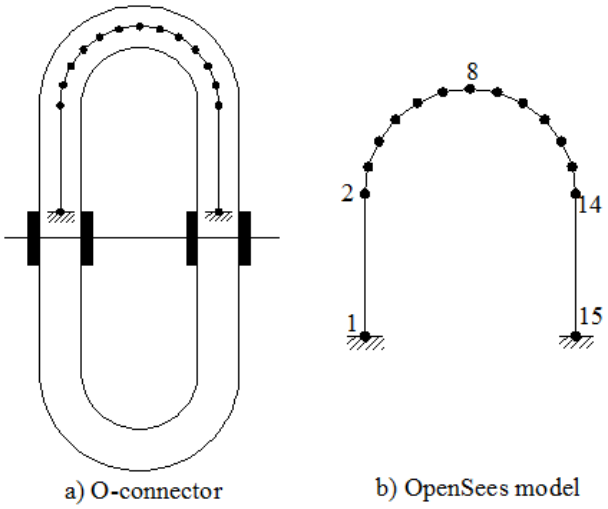

Figure 3.1 A fiber based beam-column model of the O-connector

A fiber section was used to represent the cross section of the connector. The connector cross-section was discretized using fibers with approximate cross section of 0.025 in. x 0.05 in. The stress-strain behavior of the connector material was modeled using a bilinear curve (i.e., *Steel02* in OpenSees). The O-connector was monotonically loaded by applying the measured maximum peak displacement from the O-connector test to node 15 in the vertical direction.

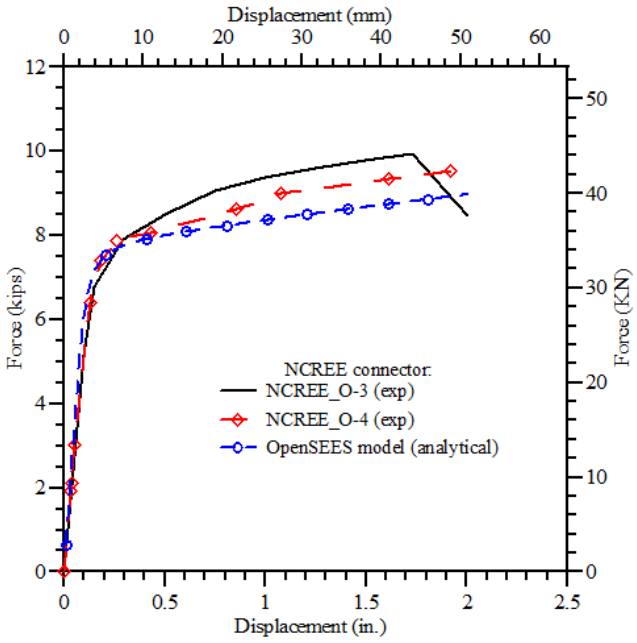

Figure 3.2 Comparison of the experimental and calculated force-displacement response of the O-connector tested at NCREE

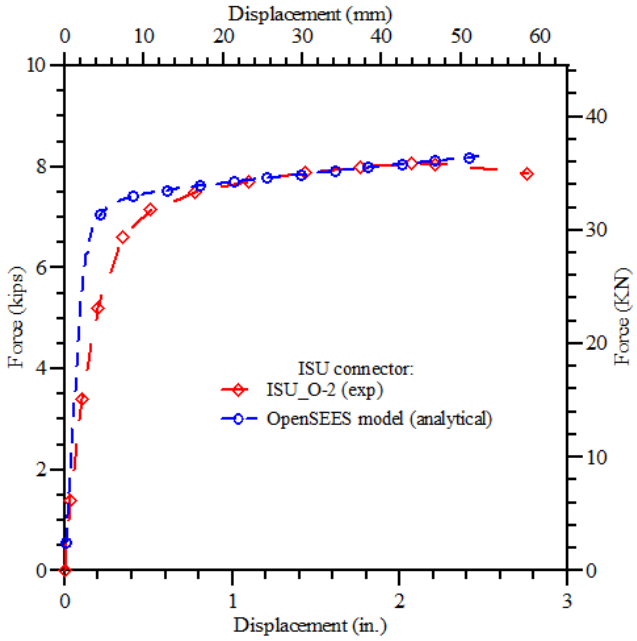

Figure 3.3 Comparison of the experimental and calculated force-displacement response of the O-connector tested at ISU

The measured envelope responses of the NCREE and ISU O-connectors and that calculated for the OpenSEES model are shown in Figure 3.2 and Figure 3.3 respectively. From these

figures, it is clear that the OpenSEES model underpredicted the strength of the O-connector tested at NCREE by an average of 15%. The initial stiffness of the ISU O-connector was overestimated by the analytical model. In conclusion, a simple beam-column element can be used to estimate the force-displacement characteristics of the O-connector.

3.2.2 PreWEC System Analysis Procedure

Similar to other unbonded post-tensioned wall systems analysis, the conventional section analysis cannot be applied to the PreWEC system because of the nonexistence of strain compatibility condition between the unbonded post-tensioning steel and concrete at the section level. Therefore, to analyze a PreWEC wall system, a non-iterative procedure is presented in this section by establishing a relationship between the neutral axis depth and the base rotation for the wall panel and the columns. This relationship is based on the neutral axis depth estimated at a base rotation of 2% and is found from an iterative procedure involving the force equilibrium and geometric compatibility conditions. Similar to other unbonded precast wall systems (Aaleti and Sritharan 2009), the following assumptions are made in the analysis procedure:

1. The wall panel and the columns are provided with adequate out-of-plane bracing, preventing them from experiencing torsional and out-of-plane deformations.
2. The dimensions and material properties of the wall panel, columns and connectors are known.
3. The fiber grout pad located at the interface between the wall panel and the foundation does not experience any strength degradation.
4. The wall panel and the columns will undergo the same lateral deformation at every floor level due to the rigid floor assumption.
5. The wall panel base has adequate friction resistance, such that it will not undergo any relative lateral movement at the base with respect to the foundation.
6. The connectors and the post-tension steel anchors remain fully effective for the entire analysis.
7. All vertical joints in a PreWEC wall system have the same number of connectors.

Presented below are descriptions of the different steps of the proposed analysis procedure. It is expected that the analysis of the wall system be performed in the following order: 1) wall panel 2) leading column, and 3) the trailing column.

Step 1: Define dimensions, reinforcement details, and material properties

The following variables are defined in this step.

System Dimensions

h_w = height of the wall system,

t_w = thickness of wall,

L_s= total length of the wall system,

l_w = length of wall

l_{col} = width of column, and

t_{col} = depth of column

Post-tensioning Steel

Wall panel:

A_{pt} = area of a post-tensioning tendon,

$n_{pt,w}$ = number of post-tensioning tendons in wall,

$h_{u,w}$ = unbonded length of the post-tensioning tendon in wall,

$x_{pt,i}$ = location of the i^{th} post-tension tendon from the rocking edge of the wall,

E_p = modulus of elasticity of the post-tensioning tendon,

$f_{pi,w}$ = initial stress in the post-tensioning tendon in the wall,

f_{py} = yield strength of the post-tensioning tendon, and

$A_{p,w}$ (= $n_{pt,w}\, A_{pt}$) = total area of post-tensioning steel in wall.

Columns:

$n_{pt,\,col}$ = number of post-tensioning tendons in column,

$x_{pt,col}$ = location of the post-tensioning steel from the rocking edge of the column. Note that in a PreWEC system, the post-tensioning steel in columns is located at the center of the columns. Thus, $x_{pt,col} = 0.5l_{col}$.

$A_{p,col}$ (= $n_{pt,col}$ A_{pt}) = total area of post-tensioning steel in each column, and

$f_{pi,col}$ = initial stress in the post-tensioning steel in each column.

Confinement Details

A_s = area of confinement steel (which may be taken as $0.5(A_{sx}+A_{sy})$,

A_{sx} = area of confinement steel in the x-direction,

A_{sy} = area of confinement steel in the y-direction,

s = spacing of the confinement reinforcement,

l_{cr} = length of confinement area, and

f_y = yield strength of the mild steel reinforcement.

Concrete Properties

$f_c^{'}$ = compressive strength of unconfined concrete,

$f_g^{'}$ = compressive strength of grout,

$f_{cc,w}^{'}$ = confined concrete strength in wall panel (from Mander's confinement model),

$f_{cc,col}^{'}$ = confined concrete strength in end columns (from Mander's confinement model),

ε_{cc}= concrete strain at $f_{cc,w}^{'}$,

ε_{cu} = strain capacity of confined concrete in wall panel, and

γ_c = concrete density.

Connector Details:

n_{con} = number of connectors per joint,

f_{con} = downward connector force acting on the wall at a given displacement,

f'_{con} = upward connector force acting on the wall at a given displacement, and

Δ_{con} = deformation of the connector parallel to the vertical face of the wall.

(Use a reliable force-displacement response of the O-connector to determine the values of f_{con} *and* f'_{con} for a given Δ_{con}, see Figure 3.3)

Step 2: Decompression point

In this step, the decompression point is established, which defines the beginning of a gap opening at the wall panel base and corresponds to the condition that makes the stress in the extreme concrete fiber furthest from the rocking edge of the wall reaching a value of zero. Assuming a linear strain distribution at the critical section due to the moment induced by the decompression force (F_{dec}), the following equations are used to determine the corresponding moment resistance. The decompression moment capacities of the wall ($M_{dec,w}$) and columns ($M_{dec,col}$) are calculated from the elastic flexural formula $\sigma = \frac{Mc}{I}$ and substituting the values for the neutral axis depth (c) and the moment of inertia (I):

$$M_{dec} = \frac{\sigma I}{c}$$

where σ = stress in the wall panel or columns due to the initial prestress force (F_{pi}) and the total gravity load (P_D) and I = moment of inertia of wall panel or columns based on the gross section properties. Hence,

$$\sigma_w = \frac{P_{D,w} + \sum_{1}^{n_{pt,w}} f_{pi,w} A_{pt}}{l_w t_w} \text{ and } \sigma_{col} = \frac{P_{D,col} + \sum_{1}^{n_{pt,col}} f_{pi,col} A_{pt}}{l_{col} t_{col}} \quad (3.1)$$

$$I_w = \frac{1}{12} t_w l_w^3 \text{ and } I_{col} = \frac{1}{12} t_{col} l_{col}^3 \quad (3.2)$$

$$c_w = \frac{l_w}{2} \text{ and } c_{col} = \frac{l_{col}}{2} \quad (3.3)$$

Hence, the decompression moment capacity of the wall system (M_{dec}) is given by

$$M_{dec} = M_{dec,w} + \sum M_{dec,col} = \frac{1}{6} l_w \left[P_{D,w} + \sum_{1}^{n_{pt,w}} f_{pi,w} A_{pt} \right] + \frac{1}{3} l_{col} \left[P_{D,col} + \sum_{1}^{n_{pt,col}} f_{pi,col} A_{pt} \right] \quad (3.4)$$

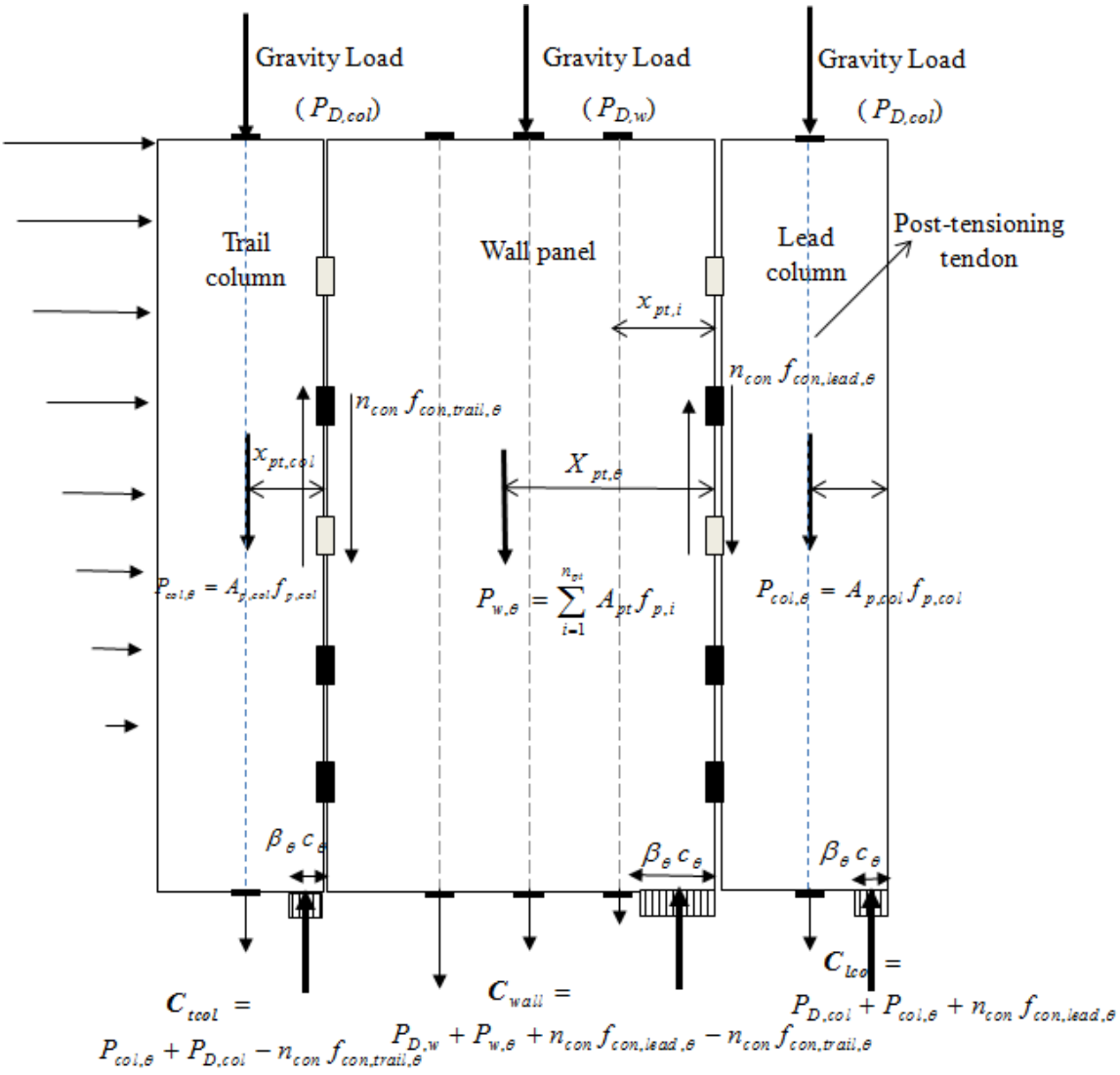

Figure 3.4 Various forces acting on a PreWEC system at base rotation θ

Step 3: Neutral axis depth at 2% base rotation

The neutral axis depth that satisfies the vertical direction force equilibrium at the wall system base is found for the wall panel and each column through an iteration process with an assumed neutral axis depth as the initial value. The following sub-steps are used in this process.

Estimating the n.axis depth for wall panel:

1. *Assume a neutral axis depth (c) for the wall panel*
2. *Determine the total gravity load on wall ($P_{D,w}$)*

$$P_{D,w} = \gamma\, l_w t_w h_w + w_{floor} l_w \tag{3.5}$$

where w_{floor} is the uniform dead load acting on the wall panel.

3. *Determine the stresses and strains in the post-tensioning tendons*
   - The elongation of the i^{th} post-tensioning tendon at 2% base rotation is:

$$\Delta_{p,i} = 0.02*(x_{pt,i} - c) \tag{3.6}$$

   - The strain in this post-tensioning tendon is:

$$\varepsilon_{p,i} = \frac{\Delta_{p,i}}{h_{u,w}} + \frac{f_{pi,w}}{E_p} \tag{3.7}$$

   - Determine the corresponding stress in the i^{th} post-tensioning tendon ($f_{p,i}$) from the stress-strain curve of the post-tensioning steel. The above steps should be repeated until stresses in all post-tensioning tendons in the wall panel are obtained.
   - The total post-tension force in the wall is, therefore,

$$P_w = \sum_{1}^{n_{pt,w}} f_{p,i} A_{pt} \tag{3.8}$$

4. *Determine the forces in the vertical connectors*
   - Estimate the deformation of the connector attached to the trailing column by equating it to the uplift at the wall panel end. Hence,

$$\Delta_{con,trail} = 0.02*(l_w - c) \tag{3.9}$$

   - Calculate the corresponding force in the vertical connector ($f_{con,trail}$) from the force-displacement response of the connector (O-connector, Figure 3.2).
   - Estimate the deformation of the connector attached to the leading column by equating it to the sum of penetration of the wall panel at rocking end and the uplift of the leading column. Hence,

$$\Delta_{con,lead} = 0.02*\left[c + l_{col} - \frac{f_{pi,col} A_{p,col} + n_{con} f_{con.lead}}{0.85\, f'_{cc,col}\, t_{col}} \right] \tag{3.10}$$

As shown in Eq(3.10), the deformation of the connector depends on the connector force ($f_{con,lead}$) which in turn depends on the connector deformation. Therefore, an iteration involving the connector force is performed to arrive at the connector deformation.

- Calculate the corresponding force in the vertical connector ($f_{con,lead}$) from the force-displacement response of the connector (see an example in Figure 3.2).

5. *Determine the new neutral axis depth*

   Assuming a uniform compressive stress acting at the wall panel base over a length of βc, where c is the neutral axis depth, the resultant compressive force is obtained as follows:

$$C = (\beta c)\left(\alpha f'_{cc,w}\right) t_w \tag{3.11}$$

where α and β are the equivalent rectangular block constants and are given by

$$\alpha = \frac{2*\left(0.98 - 0.0022 f'_c\right) r}{r - 1 + 2^r} \text{ and } r = 1.24 + 0.01*\left(\frac{f'_c - 4.0}{0.25}\right); \beta = 0.96 \tag{3.12}$$

- Calculate the resultant compressive force from equilibrium of forces (see Figure 3.4)

$$C = P_w + P_{D,w} + n_{con} f_{con,trail} - n_{con} f_{con,lead} \tag{3.13}$$

- Calculate the neutral axis depth at the wall base

$$c = \frac{C}{\alpha\beta f'_{cc,w} t_w} \tag{3.14}$$

Iterate the above sub-steps until c calculated in Eq. (3.14) converges to the assumed c value at the beginning.

Estimating the neutral axis depth for end columns:

1. *Assume a neutral axis depth (c) for the column*
2. *Determine the total gravity load on each column ($P_{D,col}$)*

$$P_{D,col} = \gamma\, l_{col} t_{col} h_w + w_{floor} l_{col} \tag{3.15}$$

where w_{floor} is the uniform dead load acting on the wall panel.

3. *Determine the stresses and strains in the post-tensioning tendons*

   - The elongation of the post-tensioning tendon at 2% base rotation is:

$$\Delta_p = 0.02*(x_{pt,col} - c) \tag{3.16}$$

   - The strain in this post-tensioning tendon is:

$$\varepsilon_p = \frac{\Delta_p}{h_{u,col}} + \frac{f_{pi,col}}{E_p} \tag{3.17}$$

   - Determine the corresponding stress in the post-tensioning tendon ($f_{p,col}$) from the stress-strain curve of the post-tensioning steel. The total post-tension force in the column is, therefore,

$$P_{col} = f_{p,col} A_{p,col} \tag{3.18}$$

4. *Determine the forces in the O- connectors*

   The connector forces acting along the vertical joints are calculated in the sub step 4 of the wall panel neutral axis determination.

5. *Determine the new neutral axis depth*

   Assuming a uniform compressive stress acting at the wall panel base over a length of βc, where c is the neutral axis depth, the resultant compressive force is obtained as follows:

$$C = (\beta c)\left(\alpha f'_{cc,col}\right) t_{col} \tag{3.19}$$

   Where α and β are the equivalent rectangular block constants and are given by

$$\alpha = \frac{2*\left(0.98 - 0.0022 f'_c\right) r}{r - 1 + 2^r} \text{ and } r = 1.24 + 0.01*\left(\frac{f'_c - 4.0}{0.25}\right);\ \beta = 0.96 \tag{3.20}$$

   - Calculate the resultant compressive force from equilibrium of forces (see Figure 3.4)

$$C = \begin{cases} P_{col} + P_{D,col} + n_{con} f_{con,lead} & \textit{for leading column} \\ P_{col} + P_{D,col} - n_{con} f_{con,trail} & \textit{for trailing column} \end{cases} \tag{3.21}$$

   - Calculate the neutral axis depth at the wall base

$$c = \frac{C}{\alpha\beta f'_{cc,col} t_{col}} \tag{3.21}$$

Iterate the above sub-steps until c calculated in Eq.(3.21) converges to the assumed c value at the beginning.

Step 4: Select a base rotation (θ)

Choose a value for θ in the range between zero and $\theta_{ultimate}$, where $\theta_{ultimate}$ may be taken as 3% or $1.5\theta_{design}$.

Step 5: Determine forces acting on the wall and columns at selected base rotation θ

1. *Determine the neutral axis depth of wall panel and end columns* ($c_{\theta,w}$ $c_{\theta,lcol}$ $c_{\theta,tcol}$) *corresponding to base rotation* θ

   From experimental data and analysis based on the monolithic beam analogy (MBA) approach on precast walls with unbonded post-tensioning, it was found that the neutral axis depth does not significantly vary beyond an interface rotation of about 0.5% as illustrated in Figure 3.5 (see Figure 2.26 in Section 2.6.4 for experimental confirmation). Consistent with this observation, the neutral axis depth determined at 2% base rotation in *Step 3* is used in the simplified analysis procedure to establish a trilinear relation between the neutral axis depth and the interface rotation at the wall base. This is demonstrated in Figure 3.5, where Point 1 corresponds to the wall length at zero percent base rotation and Points 2 and 3 are defined at base rotations of 0.1 and 0.5%, respectively. The neutral axis depth (*c*) at Point 3 is taken as that found at 2 percent rotation in *Step 3*, whereas the neutral axis depth is approximated as 2c at Point 2.

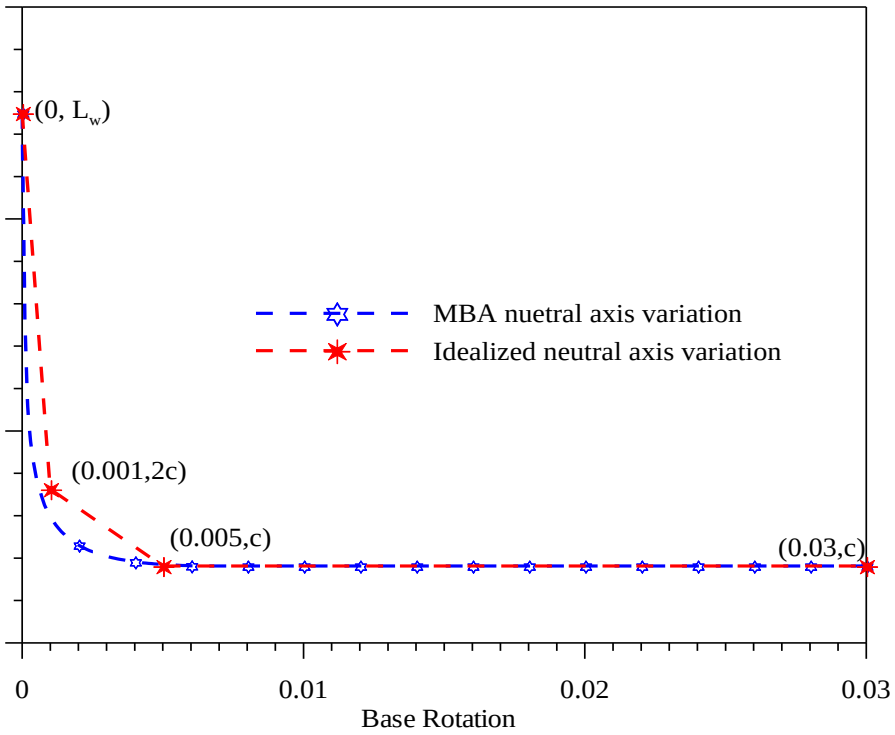

Figure 3.5 An illustration of trilinear idealization used for the neutral axis depth at the base of a wall with unbonded post-tensioning as a function of base rotation

2. *Determine stresses and strains in the wall panel post-tensioning steel*

- The elongation of the post-tensioning tendon:

$$\Delta_{p,i} = \theta\left(x_{pt,i} - c_{\theta,w}\right) \tag{3.23}$$

- The strain in the post-tensioning tendon:

$$\varepsilon_{p,i} = \frac{\Delta_{p,i}}{h_{u,w}} + \frac{f_{pi,w}}{E_p} \tag{3.24}$$

- Determine the stress in the i^{th} post-tensioning tendon ($f_{p,i}$) from the stress-strain curve of the post-tensioning steel. The above steps should be repeated to determine the stresses in all post-tensioning tendons.
- The total post-tensioning force in the wall at the selected base rotation θ

$$P_{w,\theta} = \sum_{1}^{n_{pt}} f_{p,i} A_{pt} \tag{3.25}$$

- Calculate the location of the resultant post-tensioning force from the rocking edge using Eq. (3.26) (see Figure 3.4).

$$X_{pt,\theta} = \frac{\sum_{1}^{n_{pt}} f_{p,i} A_{pt} x_{pt,i}}{P_{\theta}} \tag{3.26}$$

3.*Determine the stresses and strains in the end column post-tensioning tendons*

- The elongation of the post-tensioning tendon at base rotation θ is:

$$\Delta_p = \theta^* (x_{pt,col} - c_{\theta,col}) \tag{3.27}$$

Where, $c_{\theta,col} = \begin{Bmatrix} c_{\theta,lcol} & for\ lead\ column \\ c_{\theta,tcol} & for\ trail\ column \end{Bmatrix}$

- The strain in this post-tensioning tendon is:

$$\varepsilon_p = \frac{\Delta_p}{h_{u,col}} + \frac{f_{pi,col}}{E_p} \tag{3.28}$$

- Determine the corresponding stress in the post-tensioning tendon ($f_{p,col}$) from the stress-strain curve of the post-tensioning steel. The total post-tension force in the column is, therefore,

$$P_{col,\theta} = f_{p,col} A_{p,col} \tag{3.29}$$

4. *Determine the forces in the vertical connector*

- Calculate the connector deformations by using following equations

$$\Delta_{con,trail} = \theta^* (l_w - c_{\theta,w}) \tag{3.30}$$

$$\Delta_{con,lead} = \theta^* \lfloor c_{\theta,w} + l_{col} - c_{\theta,lcol} \rfloor \tag{3.31}$$

- Calculate the corresponding downward connector forces ($f_{con,lead,\theta}$ and $f_{con,trail,\theta}$) using an appropriate force-displacement response envelope (see an example in Figure 3.2).

5. *Calculate the resultant concrete compressive force at the wall system base*

From the equilibrium of forces in the vertical direction (see Figure 3.4)

$$\begin{aligned} C_{wall} &= P_{w,\theta} + P_{D,w} + n_{con} f_{con,trail,\theta} - n_{con} f_{con,\,lead,\theta} && \text{for wall panel} \\ C_{lcol} &= P_{col,\theta} + P_{D,col} + n_{con} f_{con,lead,\theta} && \text{for leading column} \\ C_{tcol} &= P_{col,\theta} + P_{D,col} - n_{con} f_{con,trail,\theta} && \text{for trailing column} \end{aligned} \tag{3.32}$$

Step 6: Compute the resisting moment of the wall system

For the leading column,

$$M_{lcol} = 0.5 l_{col} n_{con} f_{con,lead,\theta} + P_{col,\theta}(x_{pt,col} - 0.5 l_{col}) + C_{lcol}(0.5 l_{col} - 0.5 \beta_\theta c_{\theta,lcol})$$

For the wall panel,

$$M_{wall} = 0.5 l_w (f_{con,lead,\theta} + f_{con,trail,\theta}) + P_{w,\theta}(X_{pt,\theta} - 0.5 l_w) + C_{wall}(0.5 l_w - 0.5 \beta_\theta c_{\theta,w}) \quad (3.33)$$

For the trailing column,

$$M_{tcol} = 0.5 l_{col} n_{con} f_{con,trail,\theta} + P_{col,\theta}(x_{pt,col} - 0.5 l_{col}) + C_{tcol}(0.5 l_{col} - 0.5 \beta_\theta c_{\theta,tcol})$$

In the above equations, $0.5\beta_\theta c_{\theta,w}$ represents the distance to the resultant compression force from the rocking edge of the wall. At the decompression point, the compressive stress variation at the wall bases is expected to be triangular and hence the β_θ value is taken as 0.67 in order to locate the resultant compressive force at the appropriate location. Using Eq. (3.35), and assuming a linear variation for β_θ between the decompression point and θ up to 0.1%, the value of β_θ is approximated for small θ values using Eq. (3.36)

$$\beta_\theta = 0.66 + 146.9\theta \text{ for } \theta \le 0.001 \quad (3.34)$$

For base rotations in the range of 0.1% and $\theta_{ultimate}$ (e.g., 3%), β_θ is obtained from Eq.(3.35), which was based on Eq. A.11 (Sritharan et al. 2007)

$$\beta_\theta = 1.0 + 0.12 \ln\left(\frac{c_{\theta,w}\theta}{0.06 h_w \varepsilon_{cu}}\right) \text{ for } 0.001 < \theta \le 0.03 \quad (3.35)$$

Repeat *Steps 4* through *6* and obtain moment resistance of the wall for all θ values.

Step 7: Compute the resisting moment of the entire wall system

The moment resistance of the wall system as a function of base rotation may be obtained by summing the resistance of the wall panel and the end columns at each selected value of θ using Eq. (3.36).

$$M_{wall\ system} = M_{lcol} + M_{wall} + M_{tcol} \tag{3.36}$$

3.3 Experimental Validation

This section presents validation for the simplified analysis procedure presented in Section 3.2.2, by comparing selected analysis results with available experimental data from PreWEC-1. The selected responses include the envelopes of the base shear capacity as a function of the top floor lateral displacement, connector deformation, and neutral axis depths at the wall base, the confined concrete strains at the bottom corner near the wall base.

3.3.1 Base Shear Capacity

Figure 3.6 compares the base shear vs. the top lateral displacement established for PreWEC-1 with those calculated from the simplified analysis procedure. It is seen that the simplified analysis procedure provides a good estimate for the base shear vs. lateral displacement response envelope. At the top floor displacement of 7.2 inches, the calculated base shear resistance from the simplified analysis method is only 1.3% below the experimental value. At the design drift of 2%, the simplified analysis procedure underestimated the base shear resistance of the PreWEC system by 4.9%.

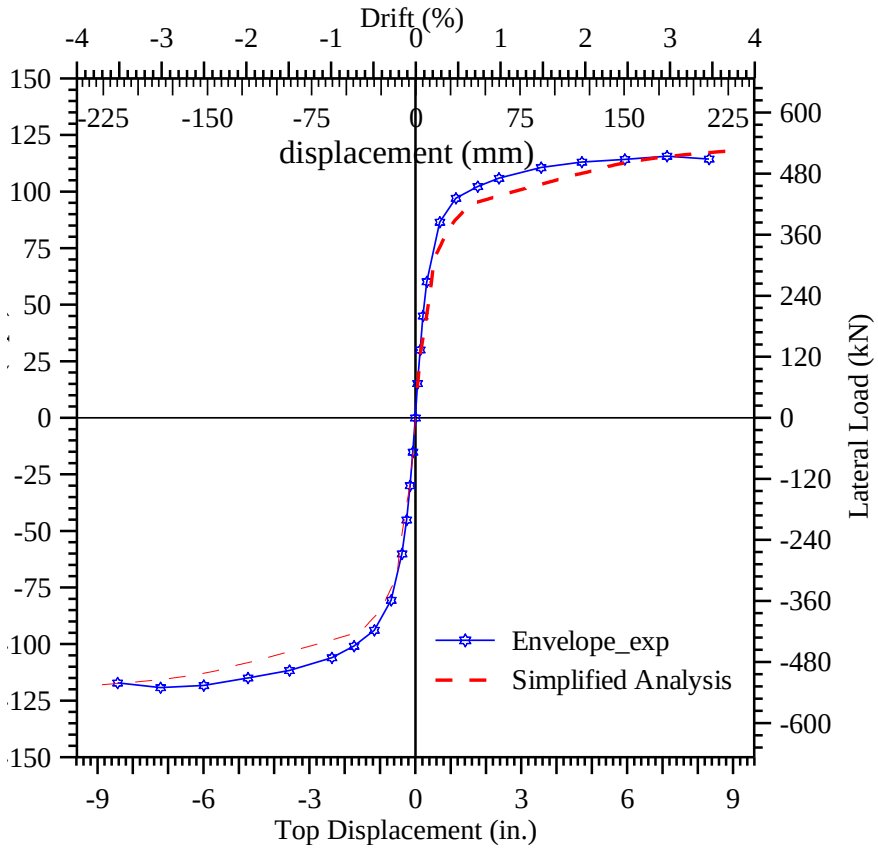

Figure 3.6 The base shear vs. top floor displacement for the PreWEC system

3.3.2 Neutral axis depth

The neutral axis depth calculated using the simple analysis procedure for the PreWEC system is compared with those obtained from experimental data in Figure 3.7. It is seen from the figure that the simplified method provides a good estimate for the neutral axis depth for the wall panel. There are some differences that exist between the analytical and extracted neutral axis depths, which are largely responsible for the small underestimation of the base shear in Figure 3.6. Furthermore, Figure 3.7 confirms the assumption of using a constant neutral axis for base rotations above a small threshold value is acceptable.

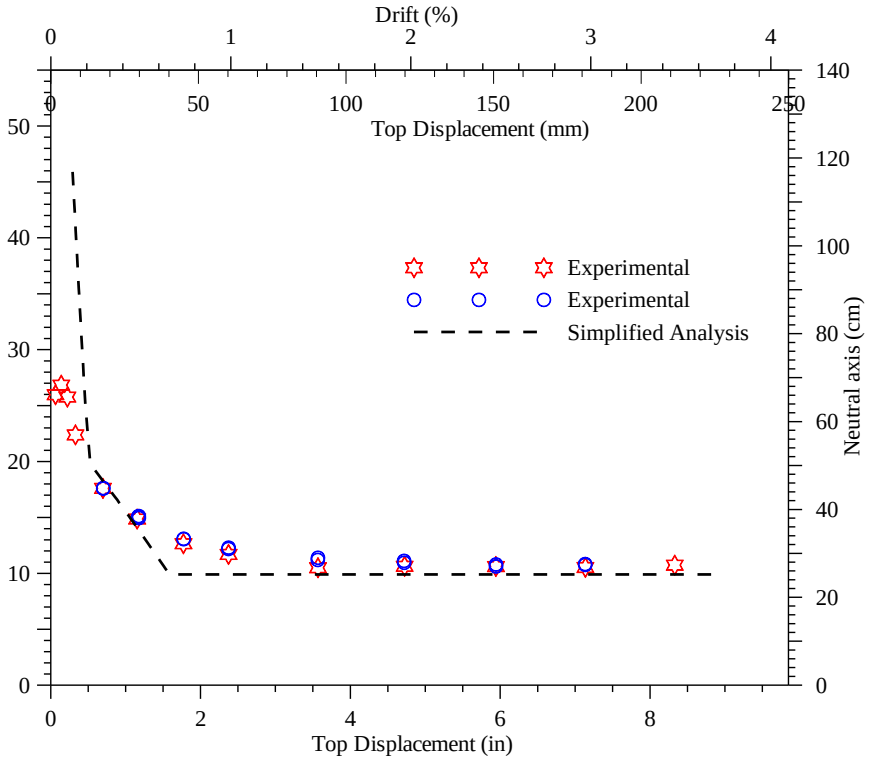

Figure 3.7 The variation of the neutral axis depth of the wall panel with top displacement

3.3.3 Connector displacements

Figure 3.8 compares the calculated displacement with the experimental data for both the trailing and leading connectors as a function of lateral displacement. The analysis procedure captured the connector displacement accurately.

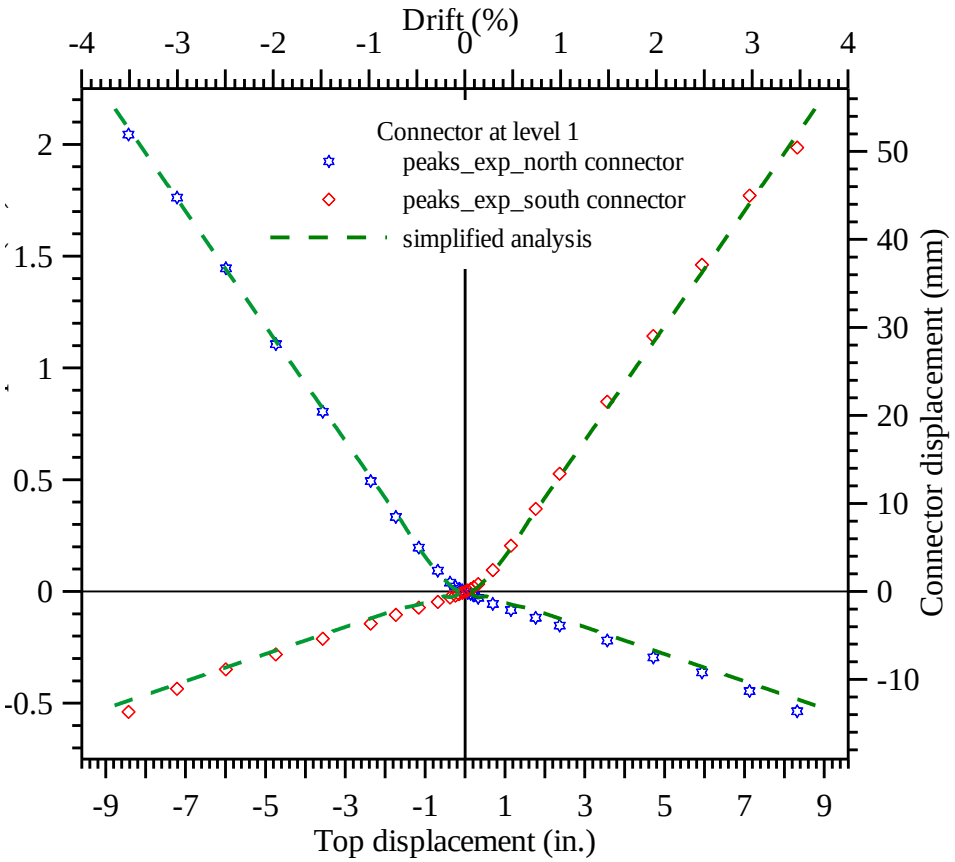

Figure 3.8 Comparison of experimental and analytical connector displacement as a function of top displacement

3.3.4 Concrete confinement strain

The strain data obtained from a concrete gauge (conc_N1) is compared with the analysis results in Figure 3.9, in which the analytical values were obtained using the equation proposed by Aaleti and Sritharan (2009). This concrete gauge was located in the confined concrete region at a distance of 3.94 in. from the compression wall end and at a height of 5.9 in. from the wall base. Given the simplicity used in the analysis approach, the comparison between the measured and calculated strains is remarkably good. The confined concrete strains are overestimated by the analysis. However, this is not of a serious concern for two reasons: 1) the behavior of compression toe region in the PreWEC wall system was expected to be complex and 2) the confined concrete models are inherently conservative. Therefore, basing the confinement reinforcement on the estimated strains will provide reserve strain capacity as much as 50% above the maximum strains expected based on the theoretical

confinement models. The analysis and design methods are targeted to obtain more accurate results at a design base rotation of 2% (corresponding to a drift of slightly above 2%). It is observed in Figure 3.9 that the measured and estimated strains show good agreement at lateral displacements near the design drift.

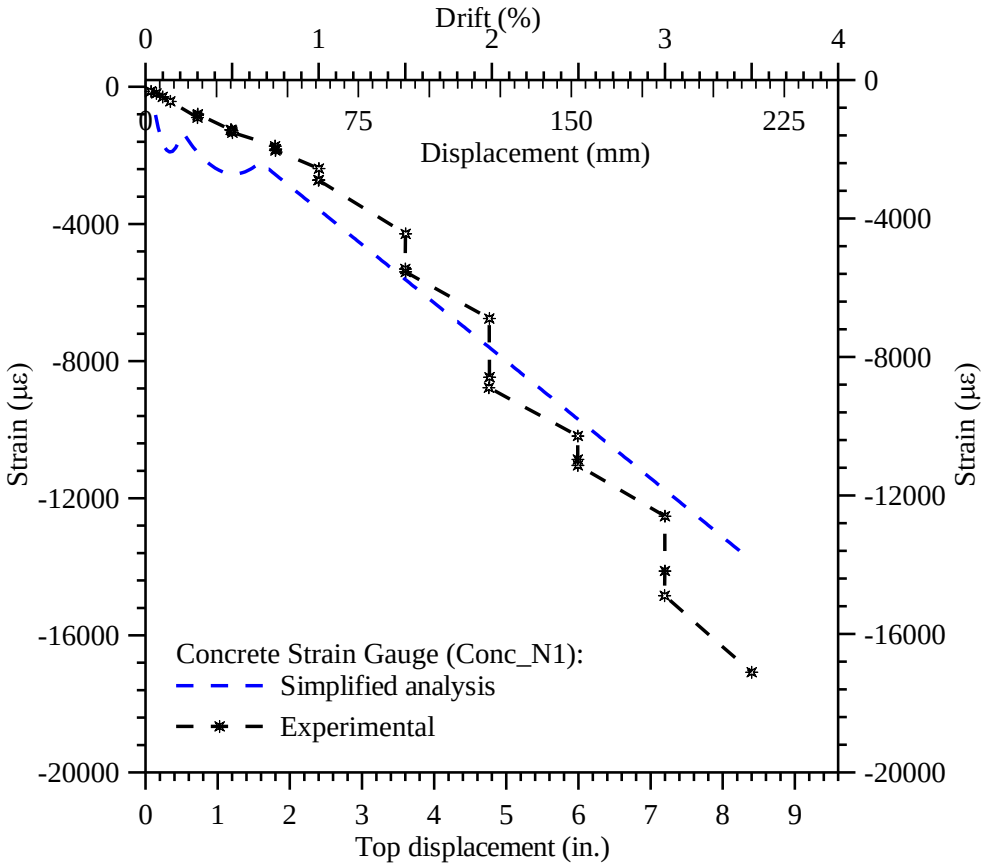

Figure 3.9 Variation of confined concrete strain with the top displacement of the PreWEC system

Chapter 4
Design Methodology

This chapter presents a seismic design procedure for the PreWEC system. A design methodology was proposed by Sritharan et al. (2007) for the unbonded jointed wall systems incorporated into an ACI ITG 5.2 document (ACI ITG5.2 2009) on design of unbonded post-tensioned precast walls for seismic regions. A similar approach is used while arriving at the design methodology for the PreWEC system.

4.1 Methodology

Similar to the jointed wall system, the lateral load resistance of a PreWEC system at a given drift depends on the geometry of the system, the amount of post-tensioning steel, the number of vertical connectors, initial prestressing force, and the force-displacement response of the vertical connector. Also, based on the experimental observations along with the analytical investigation on characterizing the lateral load behavior of PreWEC systems with O-connectors as energy dissipating devices, the following observations are made.

1. The post-tensioning force in the columns does not vary significantly from the initial value during lateral loading. This is expected as the length of the column is small and does not cause significant elongation of the tendon. Therefore, for design purposes, it is reasonable to assume that the post-tensioning force in the columns at the design drift is the same as the initial value.
2. The contribution of end columns towards the total moment capacity of the wall system is not significant. The post-tensioning provided in the columns is typically designed to keep the columns from fully uplifting from the foundation.
3. The hysteretic behavior of the PreWEC system does not match with the idealized flag-shaped hysteresis. The displacement/force corresponding to the change in unloading slope of the wall system is dependent on the cyclic behavior of the O-connector and can be seen in Figure 4.1. The change in the unloading slope takes place at a displacement where the connector force is reversed and reaches yield force in other direction.

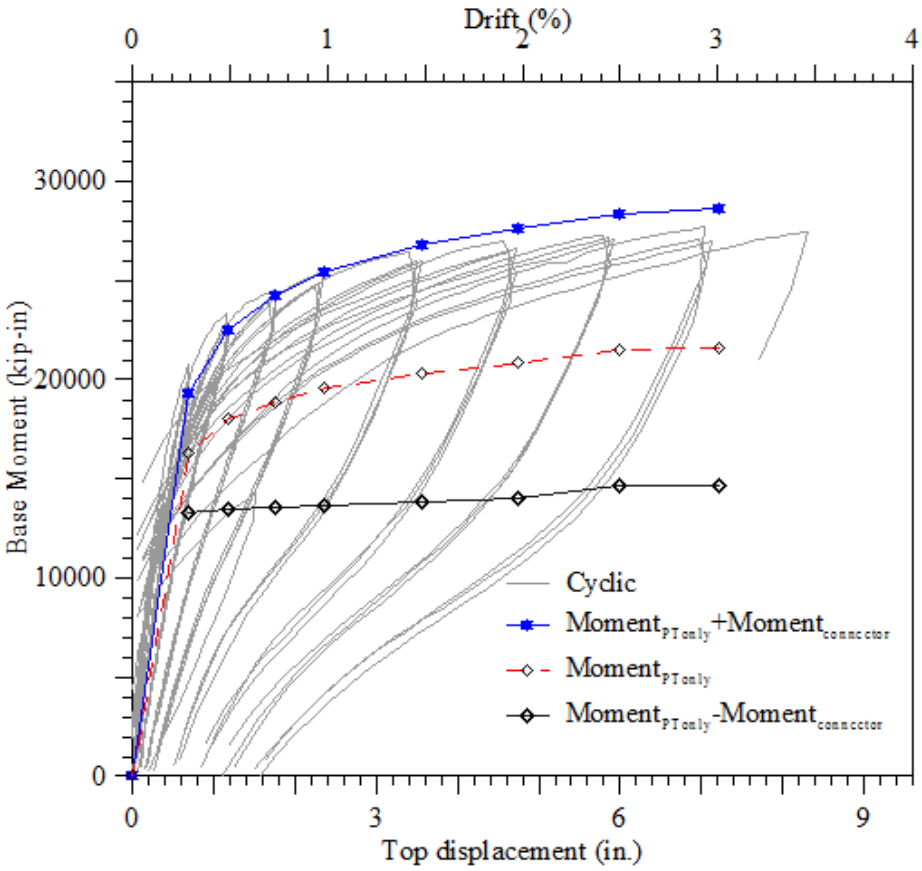

Figure 4.1 Change of unloading stiffness location for PreWEC-1

Consistent with the design methodology proposed for the jointed wall systems, the following assumptions are made for the design of PreWEC systems: 1) the wall system will undergo in-plane deformations only. Torsion and out-of-plane deformations are prevented by providing adequate out-of-plane bracing. 2) Both vertical joints contain an equal number of identical connectors and a dependable force vs. displacement response envelope is available for the connector (e.g., see Figure 3.2). 3) The wall panel and columns undergo the same lateral displacement at the floor and roof levels due to the rigid floor assumption. 4) The strength of fiber grout placed between the wall base and foundation is greater than the strength of the concrete in the wall panel. 5) The post-tensioning steel in the wall panel reaches the yield strain at the design drift. The corresponding rotation at the wall base is assumed to be θ_{design}, which may be taken as 2%. Alternatively, use an acceptable wall design drift to estimate a suitable value for $\theta_{design.}$

The proposed design procedure consists of eight design steps: 1) defining the material properties and wall system dimensions; 2) defining the required design base moment resistance for the wall system, M_{design}; 3) estimating the required number of connectors, N_{con}, and the force resisted by a connector at design drift, θ_{design}; 4) estimating the area of the post-tensioning steel, A_p; 5) estimating of an initial stress for the post-tensioning steel, f_{pi}; 6) estimating the nominal moment capacity of the wall system, M_n ; 7) designing of confinement reinforcement for the boundary elements and 8) shear design.

4.2 Design Steps

The following seven steps are recommended for the design of the jointed wall systems.

Step 1: Material properties and wall dimensions

- Select the following material properties.

  Prestressing tendon: Modulus of elasticity (E_p) and yield strength (f_{py}).

  Concrete: Unconfined concrete strength ($f_c^{'}$), elastic modulus of concrete (E_c) which may be approximated to $57,000\sqrt{f_c^{'}(psi)}$ or $4800\sqrt{f_c^{'}(MPa)}$, and appropriate coefficient of friction between the precast wall base and foundation (μ).

  Connector: Force vs. displacement response envelope.

- Establish the wall dimensions.

  Select the total length of the wall system (L_s) or length of a single wall (L_w), wall height (H_w), wall thickness (t_w), column length (l_{col}) and column thickness (t_{col}). The height and length of the wall system can be determined from the architectural drawings or from preliminary design calculations.

  Stanton and Nakaki (2002) suggest that H_w/L_w should be more than 2.0 to ensure flexural dominant behavior by each wall.

  The following guidance may be used to determine an initial value for the wall thickness:

1. Select a value in the range of $h_{story}/16$ to $h_{story}/25$, where h_{story} is the story height (Englekirk 2003);
2. Ensure the selected wall thickness is sufficient to limit the shear stress in the wall to the permissible limit specified in the current building standard (e.g., ACI 318-08, 2008); and
3. The selected wall thickness should be sufficient to accommodate the required confinement reinforcement at the wall ends without causing any construction difficulties.

Step 2: Required design moment resistance

Using a force-based design (FBD) or direct displacement-based design (DDBD) procedure, arrive at the required base moment resistance for the wall system (M_{design}). Hence, the precast wall system should be designed such that

$$\phi M_n \geq M_{design} \tag{4.1}$$

where ϕ is the flexural strength reduction factor and M_n is the nominal moment capacity of the wall system at the design drift.

Step 3: Force resisted by the connector

- Assuming vertical relative displacements between the wall panel and columns at both vertical joints to be $0.9L_w\theta_{design}$ and $(0.1L_w+l_{col})*\theta_{design}$, estimate the corresponding forces in the connectors (F_{con1} *and* F_{con2}) at the design drift from the force-displacement envelope curve available for the O- connector (see example in Figure 3.2).
- For the wall systems described above, a symmetric lateral response is expected when they are subjected to symmetric cyclic loading. For such systems, the hysteretic energy dissipation can be correlated to equivalent viscous damping using Eq. 4.2.

$$\zeta_{eq} = \frac{2}{\pi}\frac{A_{loop}}{A_{rect}} \tag{4.2}$$

where A_{loop} is the area enclosed by a symmetric hysteresis loop at the design drift and A_{rect} is the area of the rectangle circumscribing the hysteresis loop.

- The number of connectors should be determined such that a desired level of equivalent damping is incorporated in the wall system. If O- connectors, as successfully used in the PreWEC system test, are chosen, then the required number of connectors may be established from Eq.(4.3) to ensure the wall system would have a desired level of equivalent damping. The cyclic force-displacement response of a PreWEC system is approximated to a polygon (ABCDEF) as shown in Figure 4.4a. The equation for the equivalent viscous damping of the PreWEC system is derived by using the Eq.4.2 and is presented below in Eq.(4.4). Figure 4.4b presents the accuracy of the proposed equivalent viscous damping equation.

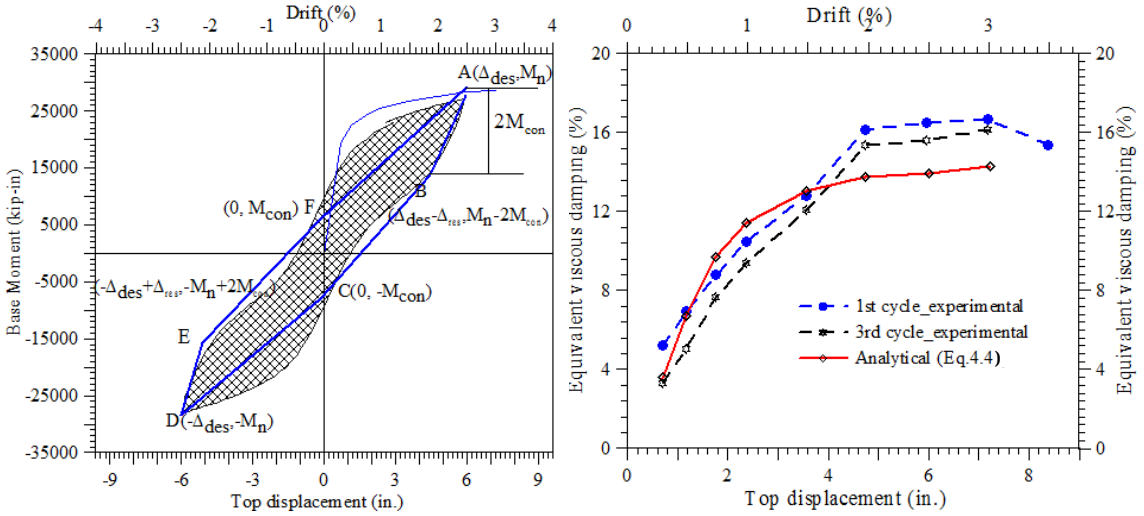

a) Approximation of cyclic response

b) Equivalent viscous damping comparison

Figure 4.4 Multi-linear approximation of the force vs. displacement hysteretic loop of PreWEC-1

$$N_{con} = \frac{\pi\left(2\Delta_{des}\zeta_{eq} + 0.5\Delta_{res}\right)M_n}{\left(4\Delta_{des} - \Delta_{res}\right)F_{con,avg}\left(L_w + l_{col}\right)} \tag{4.3}$$

$$\zeta_{eq} = \frac{2}{\pi}\frac{\left(4\Delta_{des} - \Delta_{res}\right)M_{con} - M_n\Delta_{res}}{4M_n\Delta_{des}} \tag{4.4}$$

where, N_{con} is the number of connectors in each vertical joint between the precast wall and columns.

ζ_{eq} is the required level of equivalent viscous damping, which should be in the 15 to 20% range to ensure that the wall system will have adequate damping.

Δ_{des} is the design displacement of the wall system.

Δ_{res} is the displacement from the design level displacement, at which the wall system's force-displacement response has a change in slope and is given by $\Delta_{res}= 2F_{con,avg}/k_1$

k_1 is initial stiffness of the O-connector.

$F_{con,avg}$ is the average of connector forces at the vertical joints. It is equal to $0.5*(F_{con1}+F_{con2})$.

Step 4: Required area of the post-tensioning steel and initial stress in end columns

The area of post-tensioning steel ($A_{p,col}$) and the initial stress ($f_{pi,col}$) in the end columns is designed such that the total initial prestress force is greater than the connector force along the vertical joint. Therefore,

$$P_{D,col} + A_{p,col} f_{pi,col} = \Gamma F_{con1} n_{con} \tag{4.5}$$

where, Γ is a safety factor against the column uplift, whose value can be assumed to be between 1.25 to 1.5. $f_{pi,col}$ can be assumed to be around $0.8f_{py}$

Step5: Required area of the post-tensioning steel in wall panel

The area of the required post-tensioning steel is determined based on the design moment capacity of the wall panel, $M_{design,\ wall}$. The design moment for the wall panel can be determined by Eq.(4.6).

$$M_{design,wall} = \frac{M_{design}}{\phi} - l_{col}\, n_{con}\, F_{con,avg} - 2M_{dec,col} \tag{4.6}$$

where, $M_{dec,col}$ is the decompression moment capacity of the end column. The decompression moment is equal to $\frac{1}{3} l_{col} \left[P_{D,col} + f_{pi,col} A_{p,col} \right]$.

- Design the area of the post-tensioning steel, $A_{p,w}$, using Eq.(4.6), which uses the moment equilibrium of forces acting on the base of the wall panel (see Figure 3.4).

$$M_{design,wall} = \left(P_D + f_{py}A_{p,w}\right)*\left(\frac{L_w}{2} - \frac{P_{D,w} + f_{py}A_{p,w} + n_{con}(F_{con1} - F_{con2})}{2*(\alpha.f_{cc}^{'})t_w}\right) + 0.5L_w n_{con}(F_{con1} + F_{con2}) \quad (4.7)$$

where P_D, the summation of the wall self weight and superimposed live load, and is equated to ($\gamma_c L_w t_w H_w$ + W_{floor} L_w), γ_c is the unit weight of concrete, W_{floor} is the distributed superimposed live load at the base of wall from all floors, and $\alpha.f_{cc}^{'}$ approximates the expected confined concrete strength of the equivalent rectangular stress block with $f_{cc}^{'}$ representing the strength of the confined concrete. Based on the minimum confinement reinforcement requirement of ACI as detailed in *Step 8*, it is suggested that the value of $f_{cc}^{'}$ is taken as $1.35f_c^{'}$ with a suitable value for α from Eq. 4.8. A more accurate value for $f_{cc}^{'}$ may be used after completing *Step 8*, which will optimize the amount of prestressing steel in the walls.

$$\alpha = \frac{2*r*\left(0.98 - 0.0022*f_c^{'}\right)}{r - 1 + 2^r} \quad (4.8a)$$

where $$r = 1.24 + 0.01*\left(\frac{f_c^{'} - 4.0}{0.25}\right) \quad (4.8b)$$

It is noted that the effects of cover concrete were not separately accounted for in Eq. (4.7). Instead, the entire compression region is treated as a confined region to simplify the design procedure. A similar approach should be followed in conjunction with the recommended design procedure. When substituting for all known variables, Eq. 4.7 will lead to a quadratic equation in A_p and the small positive root should be used as the design value for A_p.

- Once the area of the post-tensioning tendons ($A_{p,w}$) is estimated, the connector forces (F_{con1} and F_{con2}) should be revised, using a better estimate for the connector deformations (Δ_{con1} and Δ_{con2}) from Eq. (4.9). With a revised values for connector

forces a new value for $M_{design,wall}$ and the corresponding $A_{p,w}$ should be obtained from Eqs. 4.6 – 4.8.

$$\Delta_{con1} = \theta_{des}\left(L_w - \frac{P_D + f_{py}A_{p,w} + n_{con}(F_{con1} - F_{con2})}{\beta(\alpha.f_{cc}^{'})t_w} \right) \tag{4.9a}$$

$$\Delta_{con2} = \theta_{des}\left(0.5l_{col} + \frac{P_D + f_{py}A_{p,w} + n_{con}(F_{con1} - F_{con2})}{\beta(\alpha.f_{cc}^{'})t_w} \right) \tag{4.9b}$$

Step 6: Design the initial stress for the post-tensioning steel in the wall panel

- Using Eq.(4.9), estimate the neutral axis depth at the base of the wall at the design drift.

$$c_{design,wall} = \frac{P_D + f_{py}A_{p,w} + n_{con}(F_{con1} - F_{con2})}{\beta*(\alpha.f_{cc}^{'})t_w} \tag{4.10}$$

  where the value of β can be approximated to 0.96, which is derived from examining equivalent stress blocks for confined concrete Sritharan et al. (2007)

- Assuming that the post-tensioning tendons reach to yield limit state in the wall at the design drift, the initial stress in the post-tensioning steel is established from Eq. (4.11).

$$f_{pi} = f_{py} - \frac{\left(0.5L_w - c_{design,wall}\right)\theta_{design}E_p}{H_w} \tag{4.11}$$

Step 7: Estimate the moment capacity

Using the analysis procedure presented in Section 3.2.2, estimate the total base moment resistance of the PreWEC wall system and ensure that Eq. (4.1) is satisfied. Based on the examples investigated to date by the authors, the proposed design method appears to adequately satisfy Eq. (4.1) and no further iteration was found necessary. However, if Eq. (4.1) is not satisfied in a design problem, it is recommended that wall dimensions be altered to improve the design.

Step 8: Design of confinement reinforcement

With the connection between the wall and foundation, strain concentrations are expected at the compressive regions of the wall toes. A realistic maximum strain demand has not been successfully established from experiments or analyses. However, using the data from the PRESSS test building and the PreWEC test results in Chapter 2 and recognizing that the wall would experience the largest resultant compressive force at the base for all values of θ, Eq. (4.12) has been suggested for estimating the maximum concrete strain demand in the compressive regions of the wall toes (Sritharan et al. 2007) and a validation of this equation may be seen in Figure 3.9.

$$\varepsilon_{conc} = c_{\max,wall}\left(\frac{M_{\max,wall}}{E_c I_{gross}} + \frac{\theta_{\max}}{0.06H_w}\right) \tag{4.12}$$

where $M_{max,wall}$ is the base moment resistance of the wall panel at the maximum expected drift, the corresponding base rotation is θ_{max}, which may be taken as $1.5*\theta_{design}$, I_{gross} is the gross moment of inertia of the wall and is equal to $\frac{t_w L_w^3}{12}$, and $c_{max,wall}$ is the neutral axis depth at the base of the wall at θ_{max}. The value of $c_{max,wall}$ may be established as part of the analysis of the wall system in Step 7. Following an estimate for ε_{conc} from Eq. (4.12), quantify the required amount of confinement reinforcement in the wall toes using an appropriate confinement model. If the model proposed by Mander et al. (1988) is selected, then Eq. (4.13) will be used to determine the required amount of confinement reinforcement.

$$\rho_s = \frac{(\varepsilon_{conc} - 0.004) f_{cc}^{'}}{1.4 f_{yh} \varepsilon_{su}} \tag{4.13}$$

where ρ_s is the volumetric ratio of the required confinement steel, f_{yh} and ε_{su} are, respectively, the yield strength and ultimate strain capacity of the confinement reinforcement, and $f_{cc}^{'}$ is the ultimate strength of the confined concrete. Since $f_{cc}^{'}$ is dependent on the value of ρ_s, an iterative approach would be necessary to solve Eq. (4.13). For the first step in the iteration, $f_{cc}^{'}$ may be approximated to $1.35 f_c^{'}$. This is because the selected confinement reinforcement

should also satisfy all seismic design provisions prescribed in the current building standard for the design of transverse reinforcement in the plastic hinge region of a concrete wall. This includes the minimum hoop reinforcement requirement of ACI Eq. 21-4 (2008), which can be interpreted as demanding minimum confinement reinforcement of $0.09 f_c^{'} / f_y$ in both major and minor axis directions of the wall sections. The corresponding effective confinement pressure is $0.09 k_e f_c^{'}$, where k_e is the effective confinement coefficient. With a value of 0.6 for k_e, this minimum confinement pressure will provide a $f_{cc}^{'}$ value of about $1.35 f_C^{'}$.

The confinement reinforcement should extend over a length, l_{cr}, and height, h_{cr}, near both ends of the wall at the base where the concrete strains are greater than the crushing strain of the unconfined concrete, $\varepsilon_{\text{unconfine}}$. Assuming a linear strain distribution in the compression region at the base, the boundary element length can be determined using Eq.(4.14).

$$l_{cr} = c_{\max, lead}\left(1 - \frac{\varepsilon_{unconfine}}{\varepsilon_{conc}}\right) \tag{4.14}$$

The boundary element height, h_{cr}, which depends on the bending moment diagram along the height of the wall, can be arrived at in similar fashion as in traditional reinforced concrete shear walls.

Step 9: Shear design

Shear design of the wall system includes designing for the shear forces, preventing diagonal tension failure, similar to traditional reinforced concrete walls. ACI 318 (ACI 318-08, 2008) requirements for special concrete walls can be used for the shear design of the wall panel in a PreWEC system. Shear design should also eliminate potential shear slip failure along the horizontal joints between the wall panel and at the wall-foundation interface, which requires

$$\varphi_s V_{slip} \geq V_{design} \tag{4.15}$$

where ϕ_s = shear strength reduction factor, V_{slip} = shear slip resistance of the PreWEC system, and V_{design} = design base shear at wall base.

The shear slip resistance of a PreWEC system can be determined as:

$$V_{slip} = \mu \left(A_{p,w} f_p + P_D \right) \tag{4.16}$$

where, μ = friction coefficient, A_p = area of post-tensioning steel in wall, f_p = stress in the post-tensioning steel, and P_D = the summation of the wall self weight and superimposed live load.

The value of the friction coefficient depends on the interface material placed between the precast walls and foundation. Typically, if a fiber grout is used as an interface material, a value of 0.6 can be used for μ (ACI ITG 5.2-09, 2009, Soudki et al., 1995 and Hutchinson et al., 1993). Since the stress in the post-tensioning steel and the connector force increase with drift, it will be necessary to perform this check at both θ_{design} and θ_{max}.

4.3 Design Example

The following example demonstrates the design of a PreWEC wall system using the proposed seismic design approach.

The following assumptions and simplifications are made for the design:

1. The floor diaphragms are assumed to be rigid.
2. Seismic loads out of the plane of the walls are ignored (only loads in the direction of the walls are considered).
3. Torsional effects on the building (including accidental torsion effects) are ignored.
4. Vertical ground acceleration effects are ignored.
5. No capacity reduction factors are used in the design of the walls (i.e., ϕ=1).
6. The distribution of the equivalent lateral forces over the height of the walls is assumed to be equal to the linear elastic first mode distribution of inertia forces.
7. The wall foundations are assumed to be rigid.

Step 1:

- **Design Material Properties**

Unconfined concrete compressive strength, f_c' = 6 ksi (41.4 MPa).

Spiral steel yield strength, f_{spy} = 60 ksi (414 MPa)

Spiral steel strain at peak strength, εs_{pm} = 0.08

Post-tensioning steel yield (i.e., linear limit) strength, f_{py} = 245 ksi (1688.5 MPa).

Post-tensioning steel ultimate (i.e., peak) strength, f_{pu} = 270 ksi (1860 MPa)

Post-tensioning steel Young's modulus, E_p = 29,000 ksi (200000 MPa)

Assuming that a high strength fiber grout is placed along the interface between the wall and the foundation, frication coefficient μ can be taken as equal to 0.6.

For this design example, the connectors along the vertical joint between the wall panel and column are assumed to be O-connectors, whose force-displacement behavior (see Figure 3.2) is presented in chapter 3 of this report.

- **Wall system details**

Wall length, l_w = 20 ft (6.10 m).

Column length, l_{col} = 2 ft (0.61 m)

Wall system length, l_{sys} = 20 ft +2 (2 ft) = 24 ft (7.315 m)

Wall system height, h_w = 81 ft (24.7 m).

Wall aspect ratio, h_w/l_w = 4.05.

Wall thickness, t_w = column thickness, t_{col} = 12 in. (305 mm).

Unbonded length of strands = 84 ft (25.6 m)

Dead load on the wall system = 995 kips (given)

Step 2: design moment resistance and base shear

Based on the force-based design procedure, it was given that, the design base shear (V_{design}) for each wall is equal to 852 kips at the design roof drift of 2.3%. The details about the procedure for calculating the design base shear, design drift etc. are not presented here and can be found in a design example by Kurama (2005). The wall base moment demand, M_{design} is determined using the first mode distribution of inertia forces over the wall height as: M_{design} = (852) (62.8) = 53, 517 kip-ft.

V_{design} = 852 kips

M_{design} = 53,517 kip-ft

θ_{design} = 2.3%

Step 3: Estimating the forces resisted by the connector

The initial connector forces to estimate the number of connectors needed to provide required hysteretic damping is calculated using the force-displacement curve for the O-connector (Figure 3.2) and assumed connector deformations of 4.968 in. and 1.104 in.

Assumed hysteretic damping for the PreWEC system = 14%

Using Eqn. 4.3, number of O-connectors per vertical joint = 59; therefore, provide 60 O-connectors (30 pairs) per joint along the vertical joint between the wall and the column. The distance between each connector pair = 81ft /30 = 32.4 in.

Step 4: Estimating the area of post-tensioning steel and initial stress in columns

Assuming the safety factor against column uplift, Γ, is equal to 1.15 and the initial stress in the post-tensioning steel of the column is $0.75f_{py}$ = 183.75 ksi;

Using Eqn. 4.4, the area of post-tensioning steel needed = 3.127 in^2

= 14.41 - (0.6 in. diameter strands)

Therefore, use 15- 0.6 in. diameter strands to anchor the columns to the foundation.

Steps 5 and 6: Estimating the area of post-tensioning steel and initial stress in wall

Assuming that the post-tensioning steel in the wall yields at the design drift,

The design moment for the wall panel ($M_{design,\ wall}$) = 51523.27 kip-ft (using Eqn. 4.6) (note that the ϕ factor is assumed to be equal to 1 instead of 0.9)

The area of the post-tensioning steel needed = 17.2 in^2 (using Eqs 4.7-4.9)

= 79.27 – 0.6 in. diameter strands

Therefore, provide 80 – 0.6 in. diameter strands at the center of the wall panel.

The neutral axis depth in the wall panel = 50.05 in. (using Eqn. 4.10)

The initial stress in the post-tensioning steel = 198.71 ksi (= 0.81 f_{py})

Step 7: Estimating the moment capacity of the PreWEC wall system

Using the analysis procedure proposed in chapter 3, the moment capacity of the PreWEC system at the design drift is estimated.

The nominal moment capacity of the PreWEC system (M_n) = 54681.67 kip-ft > 53,517 kip-ft (M_{design}) (OK).

Step 8: Design of confinement reinforcement

Concrete confinement is needed at the wall boundaries to prevent premature crushing and failure of the concrete before the wall roof drift demand is reached. As described in Section 4.2, this requires an iterative procedure. Only the final step of the iteration is provided herein. A confinement model developed by Mander et al. is used to develop the stress-strain relationship of the confined concrete.

Using the Eqs 4.12-4.13, the required confinement ratio = 0.0377

The confined concrete strength = 1.63 (6 ksi) = 9.78 ksi

Maximum expected concrete strain in the toe regions of the wall panel at 3% drift = 0.0301 in./in. (using Eqn. 4.12)

The boundary element length = 46.72 in. (using Eqn. 4.14)

Step 9: Shear Design

Shear design of the wall system includes designing for the shear forces, preventing diagonal tension failure, similar to traditional reinforced concrete walls. Therefore, it is not provided herein. Using Eqs 4.15-4.16, it is clear that the shear slip condition is satisfied and thus no slip is expected.

$$\varphi_s V_{slip} = 0.75 V_{slip} = 0.75\mu\left(A_{p,w} f_p + P_D\right) = 0.75(0.6)(80 * 0.217\,\text{in}^2 * 245\,\text{ksi} + 829\,\text{kips})$$
$$= 2287\,\text{kips} \quad \geq 852\,\text{kips}\ (= V_{design}) \quad (\therefore \text{OK})$$

Stability of Wall Panels

Design to prevent out-of-plane buckling of the wall panels between lateral restraints (usually at the floor and roof levels) and to prevent buckling of the compression zone in the base panel is not within the scope of this example.

Summary of Design:

Wall panel:

No. of 0.6-dia strands in the wall panel: 80
Initial prestress in the strands: 198.71 ksi
Boundary element length: 46.72 in.
Required confinement steel ratio = 3.77%

End Columns:
No. of 0.6-dia strands in the wall panel: 15
Initial prestress in the strands: 183.75 ksi

Number of O-connectors: 60 per vertical joint (total of 120 connectors for the system)

Chapter 5
Conclusions

5.1 Summary

A 1/2-scale post-tensioned precast wall system was tested at the National Center for Research on Earthquake Engineering (NCREE), Taiwan as part of an international collaboration. The unbonded post-tensioned precast wall, referred to as PreWEC-1, was designed to mimic the observed experimental behavior of monolithic cast-in-place wall (RWN) in #6 and #5 bars in tension direction. PreWEC-1 consisted of a precast wall and two CFT columns connected together using an economical steel O-connector. PreWEC-1 performed superbly under applied cyclic lateral loads with stable response up to 3.5% lateral drift. The O-connectors experienced large inelastic strains providing good energy dissipation capability to PreWEC-1. PreWEC-1 experienced only minor damage limited to the spalling of cover concrete in the wall toe regions. Overall, PreWEC-1 surpassed all requirements of the performance validation document for precast wall systems. The analysis of the PreWEC-1 requires addressing the issue of non-existence of compatibility between the unbonded post-tensioning steel and concrete. This was addressed by incorporating an assumed trilinear variation for the wall contact length into a simplified analysis procedure. The analytical procedure predicted wall response with reasonable accuracy. More details about the PreWEC-1 performance and validation of the analytical procedure are presented in sections 3.7 and 3.8. A simplified design procedure was developed by realizing the facts that post-tensioning force in end columns does not vary significantly under later loading and by idealizing the cyclic force-displacement response with an multi-linear curve. More details of the design procedure are presented in Chapter 4.

5.2 Conclusions

The following conclusions are drawn from the research presented in this report:

- The lateral load behavior of a new precast wall system, which combines an unbonded post-tensioned precast wall with end columns using special connectors, was validated experimentally.
- The lateral load behavior of the PreWEC-1 under cyclic loading was excellent and its performance superseded the comparable performance of the cast-in-place reinforced concrete wall. The load carrying capacity of PreWEC-1 was 15% more than that of the reference wall, RWN. No strength degradation was observed up to a lateral drift of 3.5%, nearly 40% more than the comparable cast-in-place concrete wall.
- The precast wall in PreWEC-1 experienced only minor damage limited to the spalling of cover concrete in the wall toe regions at the base. The end columns did not experience any damage.
- The economical O-connectors performed exceptionally well during the component tests and during the PreWEC-1 testing. They produced a dependable stable hysteretic response during the test, contributing towards the energy dissipation capability of the PreWEC-1 system. The O-connectors produced nearly 17% viscous damping during PreWEC-1 test. The O-connectors experienced progressive fracture starting at 3% lateral drift and ultimately experiencing failure during 3.5% drift cycles. However, they continued to transfer forces when the fracture faces came in contact with each other.
- The proposed simplified method comparable to the conventional section analysis method accurately predicts the monotonic response of PreWEC-1 as a function of lateral drift. The comparisons between the experimental and analytical results are satisfactory at both small and large drifts as well as at 2% drift which is commonly used as the design drift for this wall type. At all drifts, the analytical lateral resistance is within 5% of the experimental value.
- The proposed simplified method captured the wall contact length and the displacement demand on the connectors accurately. Comparison with experimental data confirms that the trilinear approximation used for the neutral axis depth variation at the critical wall section is adequate.

- The compression end of the wall contributes significantly towards the relative displacement between the leading column and wall. Thus, it should not be neglected while estimating the connector displacement at the vertical joint.
- The proposed equation for the concrete strain demand in the wall toe regions seems adequate to estimate the expected compression strain demand, thereby allowing a realistic estimate of the confinement reinforcement needed in the walls.
- The proposed equation for the equivalent viscous damping provided by the O-connectors seems to adequately predict the damping capability of PreWEC-1. This allows the designers to arrive at the number of special connectors based on the required damping.

5.3 Future research

- One more experimental testing of PreWEC specimen for the code acceptance of the PreWEC system for seismic applications.
- Develop suitable connections between rocking walls (PreWEC) and floors;
- Further investigation into the true dynamic response behavior of the PreWEC system is warranted to develop seismic resilient structures;
- Improve analytical simulation of rocking walls and seismic resilient buildings designed with rocking walls;

References

1. Aaleti, S. 2009. “Behavior of rectangular concrete walls subjected to simulated seismic loading”, PhD thesis, Department of Civil, Construction and Environmental Engineering, Iowa State University, Ames, IA, USA.
2. Aaleti, S., and Sritharan, S. (2007). “A Precast Wall with End Columns (PreWEC) for Seismic Applications”, Proc., 8th Pacific Conference on Earthquake Engineering, Singapore, Paper 157.
3. Aaleti, S, and Sritharan S., "A simplified analysis method for characterizing unbonded post-tensioned precast wall systems," Engineering Structures, Elsevier, 2009 (in press).
4. Abrams, D.P., “Laboratory Definitions of Behavior for Structural Components and Building Systems,” ACI Special Publication 127, Vol. 127, No. 4, pp. 91-152, April 1991.
5. ACI Committee 318, (2005) “Building Code Requirements for Structural Concrete,” American Concrete Institute, Farmington Hills, Michigan, 2005.
6. ACI Committee 318, (2008) “Building Code Requirements for Structural Concrete,” American Concrete Institute, Farmington Hills, Michigan, 2008.
7. ACI Innovation Task Group 5, “Acceptance Criteria for Special Unbonded Post-Tensioned Precast Structural Walls Based on Validation Testing (ACI ITG 5.1-07) and Commentary,” American concrete Institute, Farmington Hills, MI, 2007.
8. ACI Innovation Task Group 5, “ITG-5.2-09 Requirements for Design of a Special Unbonded Post-Tensioned Precast Shear Wall Satisfying ACI ITG-5.1 & Commentary,” American Concrete Institute, Farmington Hills, MI, 2009.
9. Englekirk, R. E., *Seismic Design of Reinforced and Precast Concrete Buildings*, John Wiley & Sons, Hoboken, NJ, 2003.
10. Felipe J. Perez, Stephen Pessiki, Richard Sause. “Seismic Design of Unbonded Post-Tensioned Precast Concrete Walls With Vertical Joint Connectors”. PCI Journal, Vol. 49, No. 1, Jan-Feb 2004.
11. Fintel, M., “Performance of Buildings with Shear Walls in Earthquakes of the Last Thirty Years”, *PCI Journal*, 2002, Vol. 40, No. 3, pp. 62-80.
12. Henry, R. S, Aaleti, S., Sritharan, S., and Ingham, J. M., "Concept and finite element modeling of new steel shear connectors for self-centering wall systems," ASCE Journal of Engineering Mechanics,2010
13. Kurama, C., Y. “Seismic Design of Partially Post-Tensioned Precast Concrete Walls” PCI Journal, V. 50, No. 4, July-Aug., 2005, pp. 100-125.
14. Priestley, M. J. N., Sritharan, S., Conley, J. R., Pampanin, S., “Preliminary Results and Conclusions From the PRESSS Five-Story Precast Concrete Test Building”, PCI Journal, 1999, Vol. 44, No. 6, pp. 42-67.

15. Rahman, A. and Restrepo, J.I., “Earthquake Resistant Precast Concrete Buildings: Seismic Performance of Cantilever Walls Prestressed using Unbonded Tendons”, Research Report 2000-5, Department of Civil Engineering, University of Canterbury, Christchurch, New Zealand, 2000.
16. Smith J. Brian, Kurama C.Y (2009) “Design of Hybrid Precast Concrete Walls for Seismic Regions”, Proceedings, 2009 Structures Congress, ASCE, Austin, TX.
17. Soudki, K. A., S. H. Rizkalla, and R. W. and Daikiw. "Horizontal Connections for Precast Concrete Shear Walls Subjected to Cyclic Deformations Part 2: Prestressed Concrete." PCI Journal, V. 40, No. 5, July-Aug., 1995b, pp. 82-96.
18. Sritharan, S., Aaleti, S. and Thomas, D. (2007). “Seismic Analysis and Design of Precast Concrete Jointed Wall Systems”, ISU-ERI-Ames Report, Department of Civil and Construction and Environmental Engineering, Iowa State University, Ames, Iowa.
19. Stanton, J. F. and Nakaki, S. D., Design Guidelines For Precast Concrete Seismic Structural Systems, PRESSS Report No. 01/03-09, UW Report No. SM 02-02, The University of Washington and The Nakaki Bashaw Group, Inc., 2002.
20. Thomas, D. J. “Analysis and Validation of a Seismic Design Method Proposed for Precast Jointed Wall Systems”. M.S. thesis, Department of Civil, Construction and Environmental Engineering, Iowa State University, 2003.
21. Tony Holden, Jose Restrepo, and John B. Mander. “Seismic Performance of Precast Reinforced and Prestressed Concrete Walls”. ASCE structural Journal, 2003.
22. Zhao, J., and Sritharan, S. (2007) “Modeling of Strain Penetration Effects in Fiber-Based Analysis of Reinforced Concrete Structures,” *ACI Structural Journal*, Vol. 104, No. 2, pp. 133-141.
23. Waugh, J., Aaleti, S., Sritharan, S., and Zhao, J., 2009. “Nonlinear Analysis of Rectangular and T-shaped Concrete Walls,” ISU-ERI-Ames Report ERI-09327, Iowa State University, Ames, IA.

Intentionally blank